INFLUENCE OF WELDING PROCESSES AND TECHNIQUES ON WELDING OF DISSIMILAR ULTRA HIGH STRENGTH STEELS

Submitted in partial fulfillment of the requirement

for the award of the degree of

DOCTOR OF PHILOSOPHY

by

Jaiteerth. R. Joshi
ROLL NO: 701348

Under the supervision of

Dr. Adepu Kumar

Associate Professor

and

Dr. K. Ramesh Kumar

Scientist G, DRDL,Hyderabad

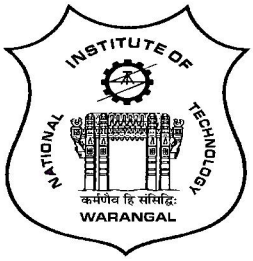

DEPARTMENT OF MECHANICAL ENGINEERING

NATIONAL INSTITUTE OF TECHNOLOGY

WARANGAL (Telangana) INDIA 506 004

Oct. 2017

NATIONAL INSTITUTE OF TECHNOLOGY
WARANGAL (T.S.) INDIA 506 004

CERTIFICATE

This is to certify that the thesis entitled "**Influence of welding processes and techniques on welding of dissimilar ultra high strength steels**", being submitted by **Mr. Jaiteerth. R. Joshi** for the award of the degree of Doctor of Philosophy in Mechanical Engineering is the record of bonafide research work carried out under our supervision. **Mr. Jaiteerth. R. Joshi** fulfills the requirement of regulations laid down by the **National Institute of Technology, Warangal**, **Telangana**. This work has not been submitted elsewhere for the award of any degree.

Dr. ADEPU KUMAR
Research Supervisor
Department of Mechanical Engineering

Dr. K. Ramesh Kumar
Scientist G, DRDL, Hyderabad
External Supervisor

Date: -2017

NATIONAL INSTITUTE OF TECHNOLOGY

WARANGAL (T.S.) INDIA 506 004

DECLARATION

This is to certify that the work presented in the thesis entitled "**Influence of welding processes and techniques on welding of dissimilar ultra high strength steels** ", is a bonafide work done by me under the supervision of Dr. Adepu Kumar and Dr. K. Ramesh Kumar and was not submitted elsewhere for the award of any degree.

I declare that this written submission represents my idea in my own words and where other's ideas or words have not been included. I have adequately cited and referenced the original sources. I also declare that I have adhered to all principles of academic honesty and integrity and have not misinterpreted or fabricated or falsified any idea/data/fact/source in my submission. I understand that any violation of the above will be a cause for disciplinary action by the Institute and can also evoke penal action from the sources which have thus not been properly cited or from whom proper permission has not taken when needed.

Date: **(Jaiteerth. R. Joshi)**

Place: Warangal Research Scholar, Roll No.701348

ACKNOWLEDGEMENT

I shall ever remain extremely grateful to the mentor, guide, and supervisor of my thesis, **Dr. ADEPU KUMAR, Associate Professor,** Department of Mechanical Engineering, National Institute of Technology, Warangal. I thank him profusely for his remarkable guidance, sustained interest, explicit instructions, incomparable counsel and unending benevolence in during my research, without which the completion of the present work would not have been possible. He has always been a source of inspiration, warmth, and affection during the entire course of my research.

I am also thankful to the co-supervisor of the present thesis, **Dr. K. RAMESH KUMAR**, Scientist G, DRDL-Hyderabad for his help and support in completion of the thesis and Director, DRDL, Hyderabad for providing me an opportunity to carry out the work.

I am thankful to the **DIRECTOR, Prof. G.R.C. REDDY**, National Institute of Technology, Warangal, the **Head**, **Prof. P. BANGARUBABU**, Department of Mechanical Engineering, for his continuous support towards carrying out research work.

I would like to express my sincere thanks to **Prof. C.S.P RAO**, former Head, Mechanical Engineering Department, National Institute of Technology, Warangal, for his timely suggestions, support and for providing necessary department facilities and services during successful completion of research work.

I wish to express my sincere and whole-hearted thanks and gratitude to **Prof. K. V. SAI SRINADH**, **Dr. R. N. RAO** and **Dr. N. NARASAIAH** (DSC members) for their kind help, encouragement and valuable suggestions for successful completion of research work.

I would like to express my sincere thanks to Dr. G. M. Reddy, Outstanding Scientist, DMRL, Hyderabad, Mr. P. Mastanaiah, Scientist E, Mr. M. Venkata Reddy, Scientist E, DRDL, Hyderabad, Mr. P. Naveen Kumar, SRF and Project LRSAM Team for their support and encouragement to carry out my research work. I gratefully acknowledge the contributions of Ms. R. Madhavi & Mr. R. Hari Babu in documentation & reprography support.

Words seem to be inadequate to express my deep sense of indebtedness to my parents and other family members, especially my wife and daughters**,** who rendered their active support and constant encouragement to pursue my studies. I extend my thanks for their valuable support during the work. I wish to thank all my friends, well-wishers and others, who have directly or indirectly helped me in the completion of this research work. I gratefully acknowledge and appreciate their contribution.

Place: Warangal **Jaiteerth. R Joshi**

Date:

Dedicated

to

My Mother

Late Smt. Shanta Joshi

ABSTRACT

In many engineering applications, welding is often performed between dissimilar metals in order to meet the end functional requirements. Numerous methods such as mechanical fastening, adhesive bonding, soldering, brazing, and welding are possible in joining dissimilar metals, each one with its own advantage, drawbacks and problems. Normally none of them can produce joints, which are fully satisfactory from all the considerations, and the designer has to choose the method, which will give adequate result for the intended application though it may have many deficiencies, the strength of these dissimilar welds to some extent dictated by welding process, techniques and filler metal selection. The differences in thermal conductivity between dissimilar materials should not lead to any difficulty, but the differences in thermal coefficients of expansion can set up stresses in restraint joints, both during welding and in service entailing cycling over wide temperature range.

The dissimilar joining of metallic materials by fusion-related processes frequently encounters the problems like metallurgical compatibility, chemical interaction among the elements involved in the dissimilar combination to form the brittle intermetallic compounds, differences in the thermal and physical properties(like thermal conductivity, coefficient of thermal expansion), type of heat treatment applicable to the dissimilar joint, galvanic corrosion etc. One should understand the metallurgy of both the materials and should devise a suitable post weld heat treatment for the dissimilar joint. However, the other major issues to be considered in fusion welding are, solidification and liquation cracking, porosity, segregation of alloying elements and loss of volatile solute elements.

Ultra high strength steels are extensively used in aerospace and defense applications because of their exceptional characteristics i.e., high strength to weight ratio. 18% Ni Maraging steels are a class of very low-carbon high alloy steels exhibiting a unique combination of ultra-high strength, excellent fracture toughness, and good weldability. The alloy gains its strength from the precipitation hardening of its soft iron-nickel martensite microstructure. As a consequence, it possesses a combination of strength and toughness superior to other high strength steels by employing a relatively simple heat treatment. AISI 4130 steels come in the category of high

strength medium carbon low alloy steels. It is one of the most widely used steels in aircraft construction because of its combination of moderate strength and reasonable ductility in the quenched and tempered conditions. AISI 4130 steels are strengthened by quenching to form martensite and tempered to the desired strength levels. Another important feature of these two steels is that they exhibit good weldability. These steels are therefore important candidate materials for critical applications such as rocket motor casings, submarine hulls, connecting rods, landing gears and bridge layer tanks. These materials are used extensively individually, but not much is reported about the dissimilar combination. For many of these applications, welding is a major route adopted for fabrication of the components made of these steels. Maraging steels are highly weldable steels as compared to high strength low alloy medium carbon steels of AISI 4130, AISI 4140, AISI 4340, AISI 4330 class.

Although the maraging steel and medium carbon high strength low alloy steel have been used extensively and individually, however, little work has been published concerning the applicability or use of maraging steel in dissimilar metal joints. These two materials are dissimilar with respect to the factors such as main alloying elements, thermal conductivity, strengthening mechanism and heat treatment processes. The primary objective of the dissimilar welding of these two steels is producing weld joint with maximum joint efficiency by employing different welding processes like gas tungsten arc welding (GTAW) and laser beam welding (LBW) processes. Another aim of the research work is to improve the joint efficiency or joint strength of the gas tungsten arc dissimilar weld joint by adapting suitable heat extraction methods.

In the first phase of the present work, the test rings of two dissimilar high strength steels AISI 4130 steel and maraging steel are welded by gas tungsten arc welding (GTAW) process in continuous current mode and in pulsed current mode. The continuous current GTA welds have demonstrated lesser tensile strength as compared to that of pulsed GTA weld joints with a fracture in heat affected zone of AISI 4130 steel.

In the second phase, the effect of pulse frequency on weld joint strength was studied by varying the frequency from 4Hz to 10Hz with an interval of 2Hz. It was observed that the pulsed GTA

weld joints produced with 4Hz have possessed higher joint strength as compared to the welds made with other pulse frequencies. The joint strength was noticed to be reducing with increase in the pulse frequency from 4 Hz to 10Hz. All the weld joints have shown a fracture in heat affected zone of AISI 4130 steel during tensile testing. The fracture in HAZ of AISI 4130 steel was correlated to the lower mechanical properties of AISI 4130 steel as compared to that of maraging steel.

With a goal to improve the weld joint efficiency, in the third phase of the work, the influence of external cooling methods on continuous current and pulsed current GTA welds was studied. The study has clearly revealed that the external cooling applied in HAZ of AISI 4130 steel has drastically reduced the HAZ softening due to welding heat input thereby improving the weld joint strength and efficiency. The pulsed current GTA welds in combination with external cooling have resulted in improved joint strength as compared to that of the welds with continuous current and cooling.

In the final phase of the work, the laser beam welding process was adapted to join the two high strength steels, which imparts minimum welding heat input. The laser beam welded joints have shown the highest joint strength as compared to the all the GTA welds (continuous current and pulsed current) both with cooling and without cooling. The tensile strength of laser beam welds is found to be very close to that of the parent metal strength of AISI 4130 steel. It is concluded that the dissimilar steel weld joint strength is predominantly affected by the extent of HAZ softening in the AISI 4130 steel and highest possible joint efficiency of 97% is possible by the laser beam welding process, as the process imparts minimum most welding heat input compared to GTA welding process conditions.

TABLE OF CONTENTS

LIST OF FIGURES

LIST OF TABLES

LIST OF ABBREVIATIONS

AST	Annealing+solution+tempering
AWST	Annealing+welding+solution+tempering
BCC	Body centered cubic
BCT	Body centered tetragonal
CC	Continuous current
CCGTA	Continuous current gas tungsten arc welding
CE	Carbon equivalent
CGHAZ	Coarse grain heat affected zone
DBTT	Ductile brittle transition temperature
EBW	Electron beam welding
EPP	Electrolytic plasma process
FZ	Fusion zone
GGHAZ	Grain growth heat affected zone
GMAW	Gas metal arc welding
GTAW	Gas tungsten arc welding
HAZ	Heat affected zone
ICHAZ	Inter critical heat affected zone
LBW	Laser beam welding
MIG	Metal inert gas
PC	Pulsed current
PCGTA	Pulsed current gas tungsten arc welding
PWHT	Post weld heat treatment
SMAW	Shielded metal arc welding
TIG welding	Tungsten inert gas welding
UTS	Ultimate tensile strength
YS	Yield strength

LIST OF SYMBOLS

H_m	Maximum Vickers hardness for the full martensite
H_b	Minimum Vickers hardness for the nil martensite

CHAPTER - I

INTRODUCTION

1.1 Importance

For joining of materials, welding is the most widely used technique by manufacturers as it is highly reliable & cost effective process. Welding is the process of joining two materials. There are various types of welding process used to join materials. Arc welding (MMAW, TIG, MIG, SAW, Plasma welding) is the most common and extensively used welding processes for fabrication. Arc welding is a group of welding process, wherein coalescence is produced by heating with a electric arc or arcs, mostly without application of pressure and with or without the use of filler material depending upon the plate thickness. Welding is having a distinct advantage over other forms of joining like fastening with nut and bolt, riveting, casting and machining.

Welding offers many advantages over other metal joining processes like riveting, bolting and it enables:

- The transfer of stresses between the members directly.
- The fabrication cost is reduced compared to other fabrication methods.
- It offers leak tight joints therefore, it is used for pressure vessels, missiles, airframe structures, automobile, railways, ships etc.
- The structures related to welding are more stiff compared to other fabrication methods.
- The effect of stress concentration is significantly lower in welded structure.
- Welding requires skilled manpower for getting a defect free structures or components.

Welding is extensively used in manufacturing & construction industries as the process is highly cost effective and efficient. It plays a major role in nuclear, marine, aerospace & defense application.

Ultra-high-strength steels are extensively used in aerospace and defense applications because of their exceptional characteristics i.e., high strength to weight ratio. 18% Ni Maraging steels are a class of very low-carbon high alloy steels exhibiting a unique combination of ultra-

high strength, excellent fracture toughness, and good weldability. The alloy gains its strength from the precipitation hardening of its soft iron-nickel martensite microstructure. As a consequence, it possesses a combination of strength and toughness superior to other high strength steels by employing a relatively simple heat treatment [1]. AISI 4130 steels come in the category of high strength medium carbon low alloy steels. It is one of the most widely used steels in aircraft construction because of its combination of moderate strength and reasonable ductility in the quenched and tempered conditions. AISI 4130 steels are strengthened by quenching to form martensite and tempered to the desired strength levels [2]. Maraging steel and AISI 4130 are having good weldability properties and which leads to usage in aerospace applications such as landing gears, connecting rods and rocket motors [3 - 6].

Maraging steel (MDN-250 grade) and AISI 4130 steel are used widely in aerospace applications such as landing gears, connecting rods, and rocket motor casing. Hence these materials are important materials for such important applications and welding is the main fabrication method for components manufactured by the above materials.

Weldability of maraging steel is excellent compared to low alloy steels such as AISI 4130, 4140, 4340 etc. There are enough publications individually on maraging steel and low alloy steels of medium carbon and high strength, however, publications on the usage of maraging steel with low alloy steels i.e. dissimilar welding are very limited. Maraging steel, AISI 4130 are different with respect to alloying elements heat treatments and strengthening mechanism.

By using different materials for fabrication of component, we can achieve different properties at different locations as per their functional requirements.

The characterization of the dissimilar joints related to microstructural changes.

Joints manufactured with a dissimilar combination of welds will have different tensile, hardness properties etc. as there will be changes in the microstructure of the joint and metallurgical inaptness. Welding of a dissimilar combination of materials is complex as compared to similar materials. [7, 8]. The dissimilar material welding is relatively a challenging issue due to the difference in chemical, physical properties and metallurgical incompatibility of base material and filler wire.

For joining of similar materials and also dissimilar materials by using low energy heat input processes such as Electron beam welding and LASER beam welding shall be used. [9,10]. Even though the processes like CCGTAW and PCGTAW is extensively used in various important applications for economy operation and high-quality joints [11, 12]. As per the research carried out, PCGTAW produced quality joints with adequate penetration with lower heat input to the joint. The joints produced by the above process gave fine refined grain structure with better mechanical properties [13]. Use of pulsed current mode instead of the continuous current mode in gas tungsten arc welding process can drastically reduce the welding heat input thereby improving the mechanical properties [14, 15]. Unimportant elements dilution is a major issue as large heat input will increase the chances of elemental migration. The strength of the weld joint depends on the welding process and selection of filler material. [16].

Mechanical properties and corrosion resistance of the joints will deteriorate because of the segregation within the dendritic structure which can be minimized by proper selection of filler wire. [17].

As limited data is available on dissimilar metal welding of maraging steel and AISI 4130, a detailed analysis was carried out on microstructure in relation to its mechanical properties and microhardness variation across the weld was attempted in this present study.

1.2 Need for advanced joining process

Design engineers prefer to use dissimilar combination of materials for critical structural application based on requirements. Sometimes the component needs high corrosion and high thermal resistance in one segment and excellent mechanical properties in another segment. As such it is difficult to get these properties in single material. Hence, dissimilar material combination is used.

Welding of dissimilar materials is not easy as that of similar materials or alloys. To the extent possible this challenge has been overcome be development of suitable welding processes and specialized techniques.

1.3 Continuous TIG, Pulsed TIG, Laser Beam Welding process

1.3.1 TIG Welding Process

Tungsten inter gas (TIG) welding process has been popular since 1943 and widely employed in aerospace industries as the process produces high-quality weld joints which meets the high-performance functional requirements involving various materials like aluminum alloys, high strength steels, magnesium alloys, titanium alloys etc. The heat for GTAW is produced by an electric arc between the non-consumable electrode and the part to be welded. The heated weld zone, the molten metal, and the tungsten electrode are shielded from the atmosphere by an inert gas. The electric arc is produced by the passage of current through the ionized inert shielding gas. The tungsten electrode is a non-consumable and filler wire is added to the base material during welding either manually or automatically. The great advantage of TIG welding process is that it can weld a wide variety of materials with ease.

1.3.2 Pulsed TIG welding

In pulsed TIG welding mode, the current is varied from peak current to background current. The major advantages of Pulsed TIG welding are:

- Better penetration with less heat input
- Low distortion
- Better control of the weld pool
- Easy to weld with thin walled components
- Easy to weld dissimilar materials of different thicknesses.

The main advantage of the pulsed current TIG welding arc is that the process produces low heat input with the better quality welds compared to continuous TIG welding. The pulsed current arc reduces the need to adjust the current while welding advances. This gives the welder a major comfort while welding dissimilar thick joints as well as out-of-position joints. The waveform of the current versus time is shown in **Fig. 1.1** given below.

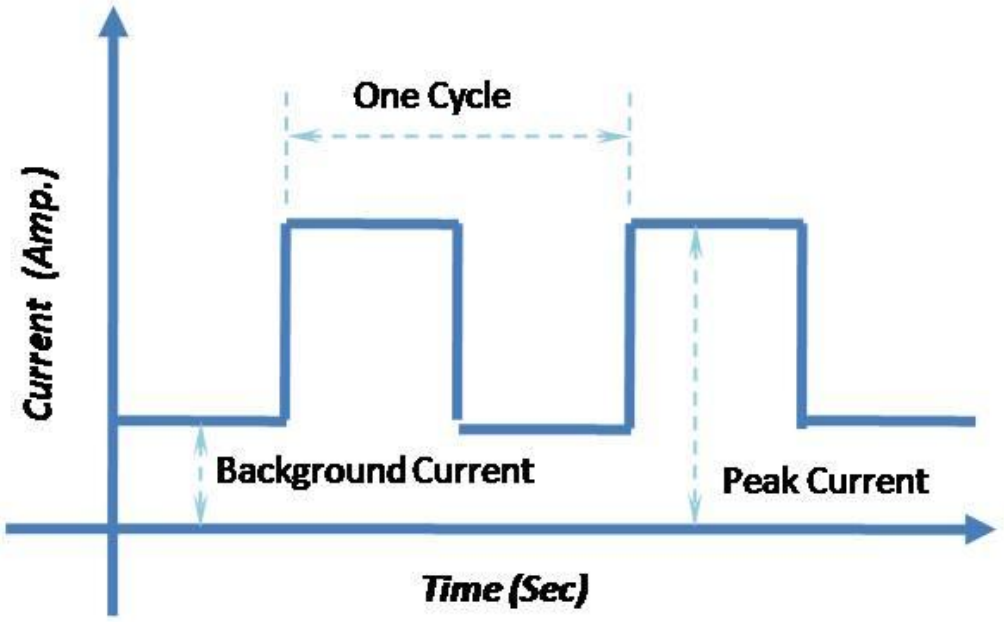

Fig.1.1 Waveform of current versus time during pulsed TIG welding process.

1.3.3 Laser Beam Welding Process (LBW)

Laser beam welding is a technique whereby materials are joined through the use of the laser beam (light amplification by stimulated emission of radiation). The laser beam is transported from source to the work center through a series of optical mirrors/lenses then focused into a small diameter spot (to increase the power density) by employing focusing lens. In this power beam welding process, requires inert gas shielding close to the weld pool and filler metal.

Numerous types of laser sources are available in the manufacturing industries namely gas lasers, solid state Nd: YAG lasers, diode lasers, fiber lasers. These lasers are categorized based on the type of lasing material used for generation of lasers. Fiber lasers are the latest class of lasers with better beam quality and ease of transport through optical fibers, unlike CO_2 lasers.

The major advantages of laser beam welding process are:

- Low Heat input during welding
- Reduced HAZ and distortion
- High penetrations are possible
- No filler wire is required as the weld joints are made with square edge preparation
- Welding in inaccessible areas are also possible
- No vacuum is required, as required in electron beam welding process
- High aspect ratios are possible (depth to width ratio of 10:1)

1.4 Problem definition

Joining of dissimilar high strength steels is essential in certain applications where the designer looks for the varied level of strengths in the different zones of an aerospace subsystem. In particular, certain airframe structures involve joining of two high strength steels such as maraging steel and AISI 4130 steel in a single airframe itself depending on the functional requirements. The end application calls for welding of these two high strength steels thereby ensuring minimum yield strength of 900MPa for the dissimilar weld joint. The aim of present study is to investigate the influence of gas tungsten arc welding techniques (continuous current and pulse current mode) with and without external cooling, Laser beam welding on microstructure and its correlation with degree of HAZ softening and mechanical properties.

1.5 Objectives and scope of research

The main aim of the work is to minimize the degree of HAZ softening thereby improving the mechanical properties of dissimilar welds of 18% Maraging steel and AISI 4130 steel using different welding processes such as continuous welding, pulsed TIG welding with and without external cooling methods and laser beam welding.

The scope of the present work is

1. Weldability study of dissimilar welds of 18% Maraging steel and AISI 4130 steel using continuous current mode, a pulsed current mode with and without external cooling.
2. To observe the various zones on either side of the weld portion and measure the width of the dark band and white band region.
3. To study the temperature history in various zones in AISI 4130 steel and correlate the microstructure in the same zone.
4. Optimization of pulse frequency in PCGTAW to improve the strength.
5. To study the weldability characteristics of dissimilar welds of 18% Maraging steel and AISI 4130 steel using Laser beam welding.
6. To study the structure-property correlation.
7. To compare the mechanical properties of dissimilar welds with different welding processes such as continuous TIG, pulsed TIG, and Laser beam welding.

1.6 Methodology

The total work is divided into three subsections, namely continuous TIG welding, pulsed TIG welding and laser beam welding. The experiments were conducted on steels MDN-250 and AISI 4130 grades to study the effect on the width of the degree of softening, metallurgical, tensile, & hardness properties. Development of experimental set-ups and procurement of various materials such as Maraging steel, AISI 4130 steel and filler wire etc. and conduct of pilot/preliminary experiments and decision of experimental region (working range) of process parameters. Conduct the experiments by varying the pulse frequency in pulsed TIG welding process and keeping other parameters to be constant. And also study of welded microstructure in optical, scanning electron microscopy (SEM) and properties of LBW joints and compare the results with a pulse and continuous TIG welding process.

1.7 Significant contributions from the investigation

The influence of external cooling methods on continuous current and pulsed current GTA welds was studied. The study has clearly revealed that the external cooling applied in HAZ of AISI 4130 steel has drastically reduced the HAZ softening due to welding heat input thereby improving the weld joint strength and efficiency. It is concluded that the dissimilar steel weld joint strength is predominantly affected by the extent of HAZ softening in the AISI 4130 steel and highest possible joint efficiency of 97% is possible by the laser beam welding process, as the process imparts minimum most welding heat input compared to GTA welding process conditions.

1.8 Structure of the Thesis

The entire thesis is subdivided into five chapters. The detailed chapters and the contents are shown below.

- **Chapter 1** - It consists of the importance of advanced materials and welding process, needs for advanced welding processes, application of a similar and dissimilar combination of welds. Also, it is subdivided into problem definition, objectives and scope of the present investigation.

- **Chapter 2** - It highlights the gaps in the published literature associated with Maraging steel and AISI 4130 steel, dissimilar weld combination of these materials, various welding processes.

- **Chapter 3** - It presents the information of the experimental setup and procedure of the present investigation including a selection of base materials, welding techniques, selection of filler materials and selection of cooling techniques and measurement of temperature during the welding process.

- **Chapter 4** - This chapter highlights the overall results, discussion, and analysis of the Dissimilar combination of Margining steel and AISI 4130 steel by using various welding

processes such as CC, TIG. Pulsed TIG (with and without cooling) Inter Pulse TIG, and LBW with respect to mechanical properties and as well as microstructural properties.

- **Chapter 5** - It deals with summary and conclusions of the work.

- **Chapter 6** - It consists of scope for further work.

CHAPTER - II

LITERATURE REVIEW

2.1 Introduction

The fabrication of engineering assemblies quite often calls for joining of certain components and parts. In general, three types of joining methods are widely popular such as mechanical joining (nuts & bolts, clamps, rivets), adhesive joining (epoxy resins, fevicol), welding (welding, brazing, and soldering) for manufacturing variety of engineering subsystems. Each type of joint offers different load carrying capacity, reliability, compatibility in joining of similar or dissimilar materials besides their fitness for use in different environments and cost.

Welding is most widely used technique by manufacturers as it is highly reliable & cost effective process. Welding is the process of joining two materials. There are various types of welding methods. The commonly used welding processes include MMAW, SAW, TIG, MIG and Plasma arc welding. However, for aerospace applications, GTAW & Pulsed GTAW are extensively used for their low cost, reliable & consistent weld quality. In addition to the above LBW & EBW arc also used depending upon the requirements and criticality.

2.2 Physical metallurgy aspects of steels

2.2.1 Maraging Steels

Maraging steels are different from the conventional steels. They contain high nickel and very low carbon content. Hence their strength is not derived from a metallurgical reaction involving carbon. Instead, steels are strengthened by the precipitation of intermetallic compounds [18-19]. The heat treatment of these steels involves Solutionizing in the austenitic region which is followed by cooling. The composition of these steels is such that in as cooled condition body-centered cubic (BCC) martensitic microstructure is obtained (Fig 2.1a).

Unlike in the medium carbon alloy steels, the martensite formation in these steels is not cooling rate sensitive. Since the martensite in the maraging steels is BCC as against BCT structure in low alloy carbon steels, distortion is not observed in these steels. However, it may be noted that if these maraging steels are exposed to high temperatures, martensite would revert back to austenite+ ferrite/austenite (Fig.2.1a, b). The as cooled martensite microstructure is soft in nature. Aging of this martensite subsequent to cooling leads to increased strength. The increase in hardness is dictated by the temperature- time history of aging (Fig.2.2).

At low temperatures, the time taken for the attainment of peak hardness is more than that in high-temperature aging. The aging reaction is similar to other age hardenable alloy and that after peak aging further extension of aging leads to a reduction in hardness as a consequence of over aging of precipitates leading to their coarsening and leaner distribution.

The strength of MDN-250 depends on the quantum of alloying elements has a bearing on the strength attainable in these maraging steels. They do exhibit synergic effects. Compositions of maraging steels and their strengths are presented in Tables 2.1 & 2.2 respectively**.** Increasing Mo content results in enhancing the hardness of annealed martensite and also increased response to aging (Fig 2.3a, and Fig.2.3b).The addition of Co in combination with Mo increases the annealed martensite hardness and also the hardness of the aged martensite.

This is governed by the product of Mo and Co (Fig2.3b).Since the strength of this class of steels is obtained through aging treatment they are named as maraging steels. The strength increment during aging is due to the precipitation of Ni_3Mo, Ni_3Ti, Ni_3 (TiMo) and Fe_2(Mo, Ti). Over-aging leads to the equilibrium phase Fe_2Mo formation. During reversion of martensite to austenite at higher aging temperature, enrichment if Ni occurs in the areas where the intermetallic precipitates decompose. This nickel enrichment results in retained austenite.

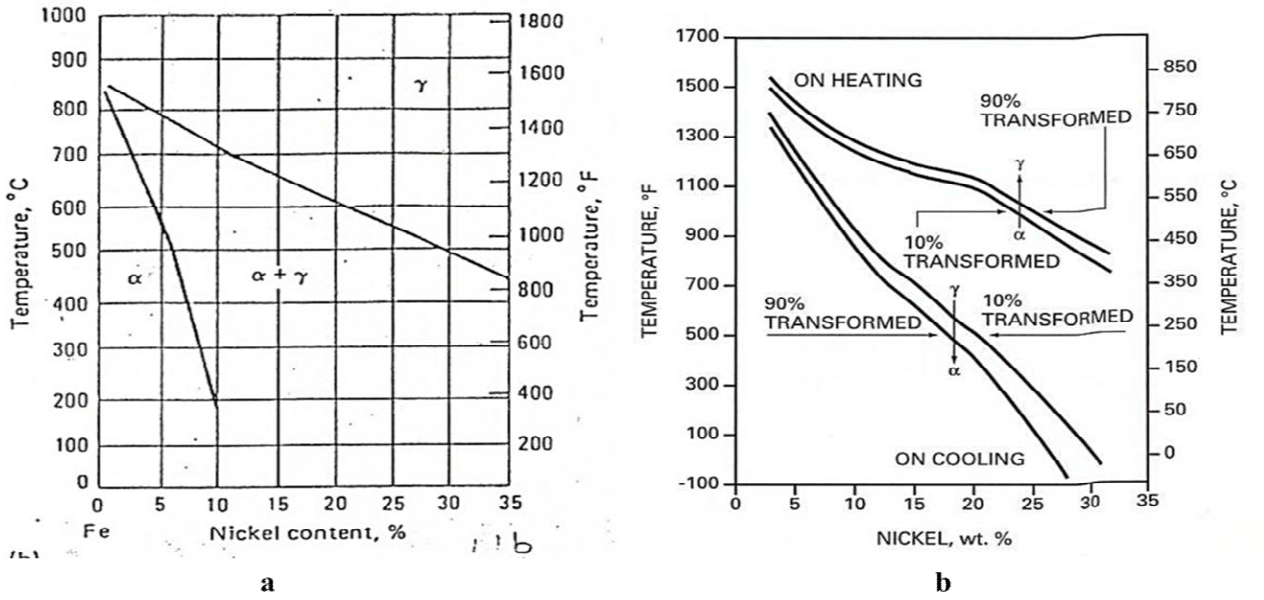

a b

Fig. 2.1 Effect of Ni on Phase stability in Iron-Nickel system: a) Metastable equilibrium; b) Stable equilibrium diagram.

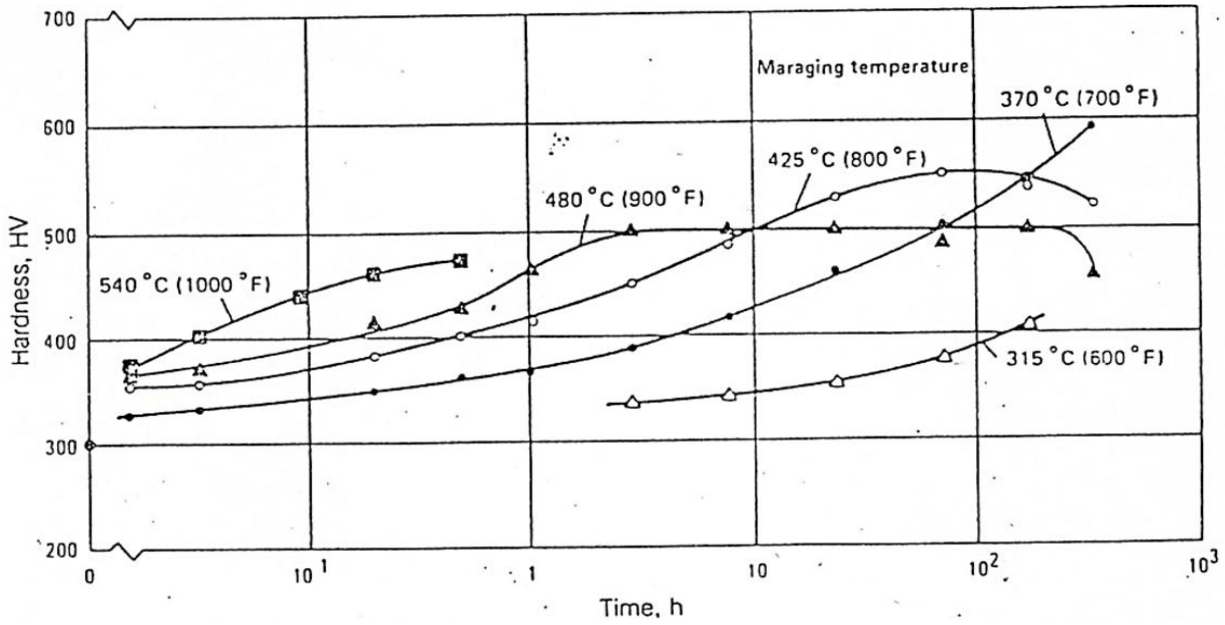

Fig. 2.2 Effect of time and temperature on the ageing behavior of 18 % Ni maraging steel.

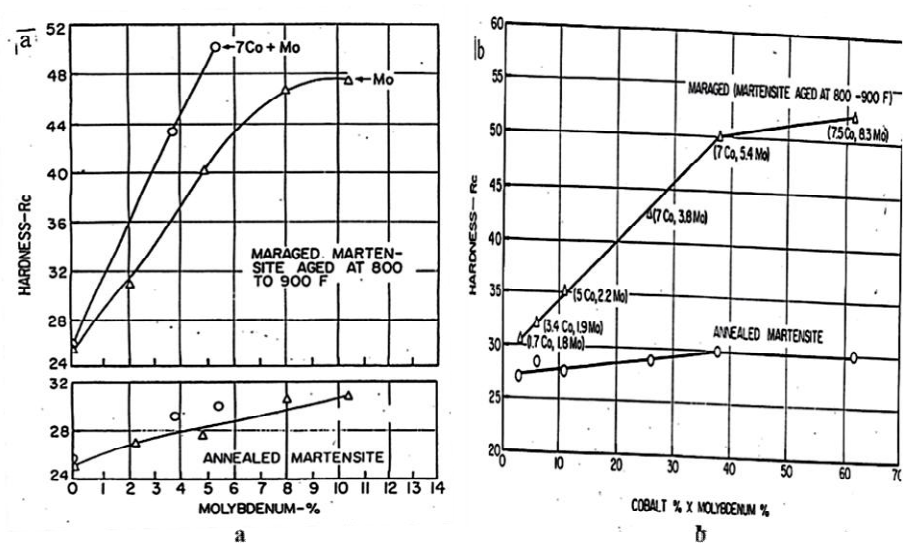

Fig. 2.3 Effect of Mo and Co on the hardness of annealed and aged martensite: a) Influence of Mo, Mo + Co; b) Effect of the product of Co and Mo.

Table.2.1 Composition of maraging steels (ref.18)

Grade	Ni	Mo	Co	Ti	Al	Nb
Standard grade						
18Ni(200)	18	3.3	8.5	0.2	0	----
18%Ni(200)	18	5.0	8.5	0.4	0.1	----
18%(200)	18	5.0	9.0	0.7	0.1	----
18%(200)	18	4.2b	12.5	1.6	0.1	----
18%(200)	17	4.6	10.0	0.3	0.1	----
12-5-3(180)	12	3	----	0.2	0.3	----
Cobalt- free and low-cobalt bearing grades						
Cobalt-free 18%Ni(200)	18.5	3.0	----	0.7	0.1	----
Cobalt-free 18%Ni(250)	18.5	3.0	-----	1.4	0.1	----
Low-Cobalt 18Ni(250)	18.5	2.6	2.0	1.2	0.1	0.1
Cobalt-free 18Ni(300)	18.5	----	----	1.85	0.1	----

a) All grades contain no more that 0.03%C.

b) some procedures use a combination of 4.8% Mo and 1.4% Ti, nominal.

c) contains 5% Cr.

Table 2.2 Tensile strength data on maraging steels (ref. 18)

Grade	Heat treatment(a)	Tensile strength(MPa)	Yield strength(MPa)	El. (50mm G.L)	Reduction In area %	Fracture toughness (MPa√m)
18Ni(200)	A	1500	1400	10	60	155-240
18Ni(250)	A	1800	1700	08	55	120
18Ni(300)	A	2050	2000	07	40	80
18Ni(350)	B	2450	2400	06	25	35-50
18Ni(cast)	C	1750	1650	08	35	105

a) Treatment A: solution treat 1 h at 820^0C (1500^0 F), then age 3 h at 480^0C (900^0 F).

b) Treatment B: solution treat 1 h at 820^0C (1500^0 F), then age 12 h at 480^0C (900^0 F).

c) Treatment C: anneal 1 h at 1150^0C (2100^0 F), then age 1 h 595^0C (1150^0 F). Solution treat 1 h at 820^0C (1500^0 F), then age 3 h at 480^0C (900^0 F).

2.2.2 Low alloy ultra-high strength steels

The composition of some of the ultra high strength steels of this category is listed in Table 2.3 Ni-Cr-Mo steels and Cr-Mo steels [20] fall in the category of medium carbon low alloy steels. They are quenched and tempered class of steels i.e. the steels are austenitic at temperatures of around 900^0c and then quenched in either water or oil and subjected to tempering treatment. The tempering temperature should be indicated by the toughness and strength requirements. Tempering is carried out at below the certain temperature resulted in low toughness and high strength and with increasing the temperature, an increase in toughness at the cost of strength (Table 2.4-2.6). The low toughness observed in the temperature range 260-315^0C is due to temper embrittlement. The high strength of these steels in the as-quenched condition is due to body-centered tetragonal (BCT) martensite microstructure. The strength of this martensite is dictated by the carbon content and other alloying elements that influence hardenability. The martensite transformation is cooling rate sensitive (Fig.2.4 a and b) and is dictated by the amount of carbon and other elements that influence the transformation of austenite at high temperature to

low temperature products such as pearlite, bainite, and martensite. Of this Martensite is the hardest structure.

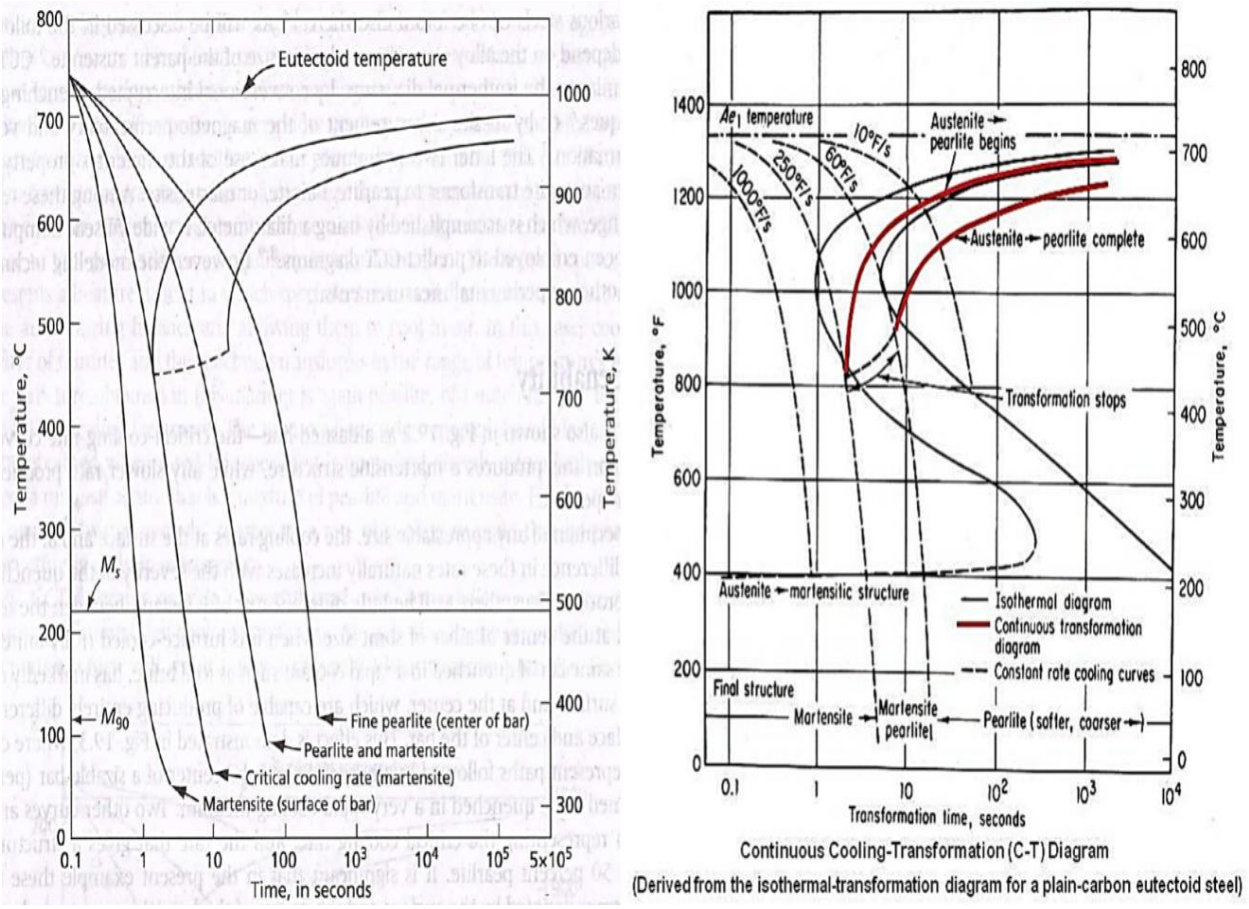

a **b**

Fig.2.4 Effect of cooling rate on phase transformation in steels (a) Temperature vs Time (b) Temperature vs transformation

Table 2.3 composition of ultra-high strength steels(Ref.18)

Designation or Trade name	C	Mn	Si	Cr	Ni	Mo	V	Co
Medium carbon low-alloy steels								
4130	0.28-0.33	0.4-0.6	0.2-0.35	0.8-1.1	---	0.15-0.3	---	---
4140	0.38-0.43	0.7-1.0	0.2-0.35	0.8-1.1	---	0.15-0.3	---	---
4340	0.38-0.43	0.6-0.8	0.2-0.35	0.7-0.9	1.65-2.0	0.2-0.3	---	---
ASM6434	0.31-0.38	0.6-0.8	0.2-0.35	0.65-0.9	1.65-2.0	0.3-0.4	0.17-0.2	---
300M	0.40-0.46	0.65-0.9	1.45-1.8	0.7-0.95	1.65-2.0	0.3-0.45	0.5min	---
D-6a	0.42-0.48	0.6-0.9	0.15-0.3	0.9-1.2	0.4-0.7	0.9-1.1	0.05-0.1	---
6150	0.48-0.53	0.7-0.9	0.2-0.35	0.8-1.1	---	---	0.15-	---
8640	0.38-0.43	0.75-1.0	0.2-0.35	0.4-0.60	0.4-0.7	0.15-0.3	0.25	---
Medium-alloy air-hardening steels								
H11	0.37-0.43	0.2-0.4	0.8-1.0	4.75-5.3	----	1.2-1.4	0.4-0.6	----
H13	0.32-0.45	0.2-0.5	0.8-1.2	4.75-5.5	----	1.1-1.75	0.8-1.2	----
High-frequency toughness steels								
AF1410(b)	0.13-0.17	0.1max	0.1max	1.8-2.2	9.5-10.5	0.9-1.1	0.06-	13.5-14.5
HP9-4-30(9)	0.29-0.34	0.1-0.35	0.2max	0.9-1.1	7.0-8.0	0.9-1.1	0.12	4.25-4.75

a) P and S contents may vary with steel making practice. Usually, these steels contain no more than 0.035 P and 0.040 S.

b) AF1410 is specified to have 0.008P and 0.0055S composition. Ranges utilized by some producers are narrower.

c) HP 9-4-30 is specified to have 0.10max P and 0.1 Max S. Ranges utilized by some producers are narrower.

Table 2.4 Influence of tempering temperature on the strength of 4130 steel (after ref.18)

Tempering temperature ^{0}C	Tensile strength MPa	Yield strength MPa	%El.,in 50mm (2 in.)	Reduction in area%	Hardness, HB	Izod impact Energy J
Water quenched and tempered (a)						
205	1765	1520	10.	33.0	475	**18**
260	1670	1430	11.5	37.0	455	**14**
315	1570	1340	13.0	41.0	425	**14**
370	1475	1250	15.0	45.0	400	**20**
425	1380	1170	16.5	49.0	375	**34**
540	1170	1000	20.0	56.0	325	**81**
650	965	830	22.0	63.0	325	**135**
Oil quenched and tempered (b)						
205	1550	1340	11.0	38.0	450	---
260	1500	1275	11.5	40.0	440	---
315	1420	1210	12.5	43.0	418	---
370	1320	1120	14.5	48.0	385	---
425	1230	1.30	16.5	54.0	360	---
540	1030	840	20.0	60.0	305	---
650	830	670	24.0	67.0	250	---
a) 25mm (1 in,) diam round bars quenched from 845 to 870 ^{0}C (1550 to 1600^{0}F). b) 25mm (1 in.) diam round bars quenched from 860^{0}C (1575^{0}C=F)						

Table 2.5 Influence of tempering temperature on the strength of 4140 steel (ref.18).

Tempering temperature ^{0}C	Tensile strength MPa	Yield strength MPa	%El.,in 50mm (2 in.)	Reduction in area%	Hardness, HB	Izod impact energy J
205	1965	1740	11.0	42	578	15
260	1860	1650	11.0	44	534	11
315	1720	1570	11.5	46	495	9
370	1590	1460	12.5	48	461	15
425	1450	1340	15.0	50	429	28
480	1300	1210	16.0	52	388	46
540	1150	1050	17.5	55	341	65
595	1020	910	19.0	58	311	93
650	900	790	21.0	61	277	112
705	810	690	23.0	65	235	136

Table 2.6 Influence of tempering temperature on the strength of 4340 steel (after ref.18).

Tempering temperature ^{0}C	Tensile strength MPa	Yield strength MPa	%El.,in 50mm (2 in.)	Reduction in area%	Hardness, HB	HRC	Izod impact energy J
205	1980	1860	11	39	520	53	20
315	1760	1620	12	44	490	49.5	14
425	1500	1365	14	48	440	46	16
540	1240	1160	17	53	360	39	47
650	1020	860	20	60	290	31	100
705	860	740	23	63	250	24	102

2.3 Welding metallurgy of steels

2.3.1 Maraging steels

Maraging steels are extremely weldable steels as compared to high strength low alloy medium carbon steels of 4130, 4140, 4340, 4330 class [21]. As welded hardness of low alloy medium carbon steels whose strength is attained by high carbon content and ductile-brittle transition temperature (DBTT) is also influenced by the carbon content, in that, higher the carbon content higher is the DBTT (Fig 2.5a) [22]. From this point of view, maraging steels have an advantage in that the welds of these steels exhibit low hardness in the as-welded condition (Fig.2.5b) [23]. Arc welding and electron beam welding studies by other researchers reveal that maraging steels are highly weldable [21] [24-27].

Studies by Kenyon [21] revealed that 18 Ni maraging steels exhibit good weldability. This study showed that heavy sections can be welded without the risk of embrittlement or cracking. Original strength is restored by simple aging treatment at 485^0C. The same study showed that the welds of these steels exhibit compressive residual stress (Fig.2.6a) as against tensile residual stress (Fig. 2.6b) in heat treatable low alloy steels. It is also reported that these steels are less prone to hydrogen embrittlement. It is reported that these steels exhibit a critical stress of the order of 1000MPa (145 ksi) as against 172MPa (25 ksi) for low alloy steels of AISI 4340 class under similar hydrogen levels in these steels [28][29]. The high susceptibility to hydrogen embrittlement of heat treatable low alloy steels is evident form reduction in strength in matching filler metals has been attributed to the presence of reverted austenite(Fig. 2.7) [30].

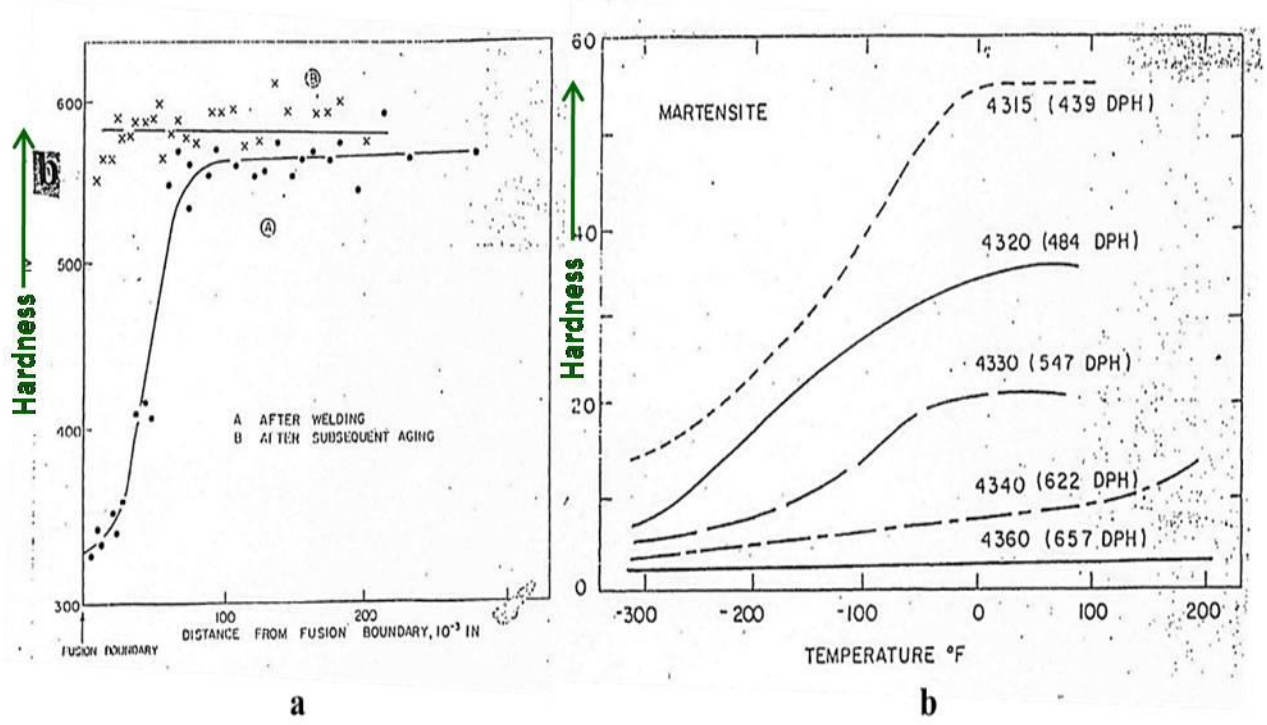

Fig. 2.5 A comparison of the hardness of martensite in a) Medium carbon low alloy steels; b) maraging steels.

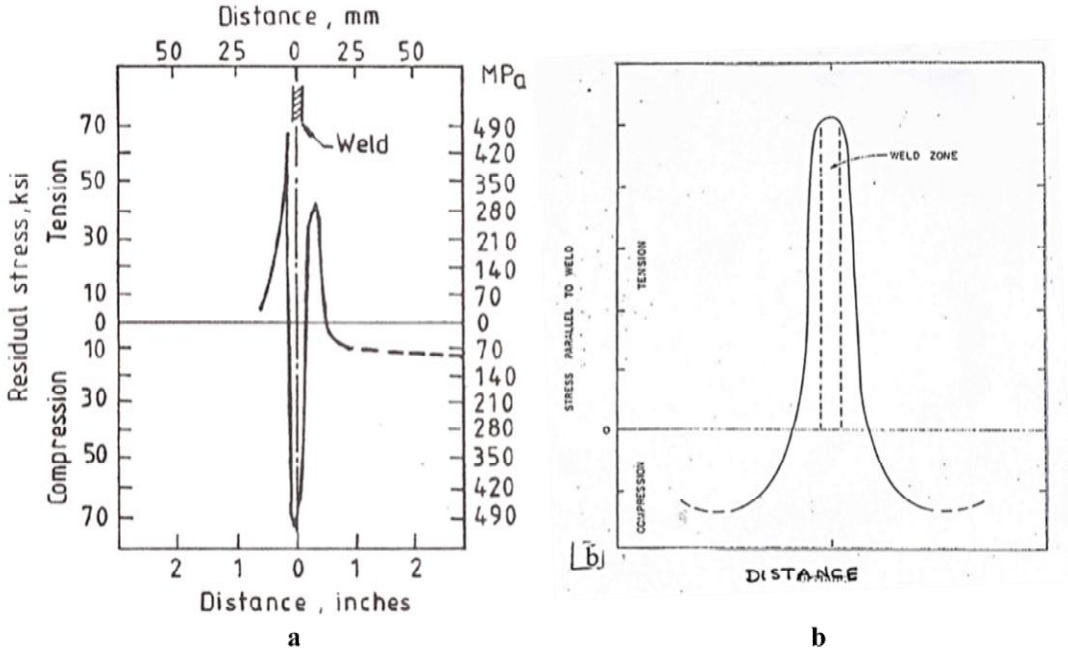

Fig. 2.6 Residual stress distribution in welds: a) maraging steels; b) low alloy medium carbon steels.

Many of these studies indicated that maraging steels are not prone to cracking and joint efficient as high as 90% are reported in the transverse tensile strength of these welds. These studies reported failure in the weld region due to its lower strength, due to loss of Ti [25] and formation of Ti carbon- nitride inclusions [24]. Although the majority of studies reported no cracking in 18 Ni maraging steel weldments studies by Pepe and savage [31] indicated that the steels are prone to cracking in the HAZ and is related to grain boundary film formation due to constitution liquation.

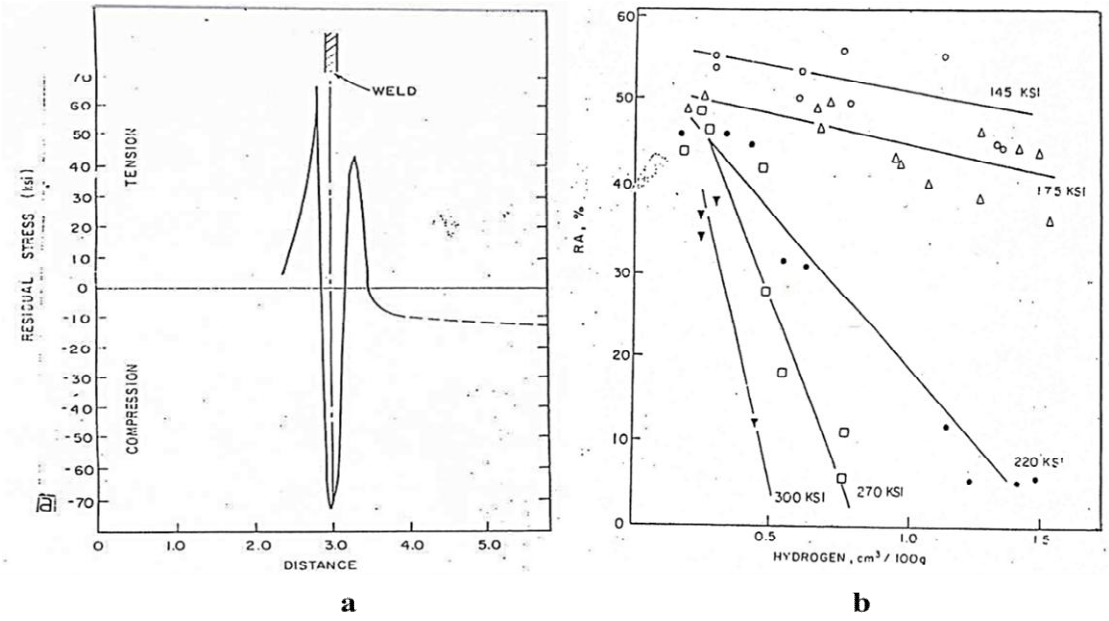

Fig. 2.7 Relation between strength to hydrogen tolerance in low alloy medium carbon steels.

The study by pepe and savage [31] showed that the exposure of HAZ to a temperature in excess of 2300F (1260^0C) leads to liquation cracking phenomena and therefore low ductility. Early studies by Knoth and Lang [32] showed that 18 Ni maraging steels exhibit low hardness in the as-welded condition. Strength could be improved by a more aging treatment. The study showed that GMAW, GTAW and short arc welds exhibit nearly similar strength (Table 2.7). However, the ductility of TIG and SMAW welds are low as compared to GMAW. In GTAW, filler metals containing higher Ni, Co and Mo exhibit higher strength and lower ductility than low Ni, Co and Mo filler welds (Table 2.8). Recent studies on fracture toughness of 18 Ni (250) MDN-250 weldments showed that welds aged at 480^0C exhibit toughness close to that of parent

metal [32]. Some deterioration in toughness has been reported when aged at higher temperature due to segregation effects.

The same study reported that use of matching filler metal resulted in lower strength and higher ductility that the filler metal welds containing high Co and Mo. The reduction in strength in matching filler metals has been attributed to the presence of reverted austenite [33] [32]. Very limited data are reported on dissimilar welding aspects of maraging steels-low alloy steels. Studies by Knoth and Land [32] observed in general, these welds possess low strength. The weld strength is decided by the suitable welding process and filler metal combination (Table 2.9). In general, covered electrode welds with Ni, Cr, Fr, Co, Mo filler exhibit low strength, high ductility, and toughness while MIG welds with maraging filler exhibited high strength and low ductility. It is important to have an understanding of the influence of various elements on strength and cracking tendency while welding dissimilar material combination envisaged in this study. The effect of major alloying elements and residual elements on strength and cracking tendency are presented in (Table 2.10) [32]

Table 2.7 Weld properties obtained in 18% Ni maraging steel (ref 33).

Weld (aged 900F, 3hr)	Weld thickness (mm)	0.2 YS (MPa)	UYS (MPa)	Elongation (%)
TIG	1.57	1622	1697	3.5
MIG	12.7	1518	1622	7
Short Arc	12.7	1573	1691	4

Table 2.8 Effect of filler composition on properties of 18% Ni maraging steel (ref. 33).

Ni	Co	Mo	Ti	Al	Weld thickness (mm)	Welding process	YS (MPa)	UTS (MPa)	EL. (%)	R.A. (%)
17	7.3	2.0	0.7	0.05	12.7	TIG	1387	1470	10	47
18	8	4.5	0.5	0.2	1.57	TIG	1622	1689	3.5	18
18	9.5	4.5	0.7	0.2	1.57	TIG	1870	1904	2.5	10

* aged 900^0F/3hr

Table 2.9 Properties of the weld joint between 18% Ni 250 maraging steel and various dissimilar metals (ref. 33).

Metal joined	Filler metal	Process Used	As welded YS (MPa)	YS (MPa)	Maraged 900^0F/3hr UTS (MPa)	El. (%)	BK.***
Mild steel	Al purpose*	Cov. Elect.	393	324	469	16	B
4340	Al purpose*	Cov. Elect	386	421	690	12	W
Type304	Al purpose*	Cov. Elect.	352	373	628	36	B
Mild steel	18% Ni**	MIG	435	345	462	5	B
4340	18%Ni	MIG	1014	1173	1242	4	B
Type 304	18% Ni	MIG	428	421	621	32	B

73% Ni, 14% Cr, 5% Fe, Cb, Mo, Mn

** 18% Ni, 8% Co, 4.5% Mo, 0.50 Ti, 0.10 Al, bal FE

***Bk= break, W=weld, B=base plate

Table 2.10 Effect of alloying elements on 18% Ni maraging steel (ref 33).

Elements	Amount present	In parent material	In welds
Nickel	Too low	Low strength	lower strength and resistance to cracking
	Too high	Promotes austenite lowering strength and toughness	Segregated austenite pools reduce strength and toughness
Cobalt or molybdenum	Too low	Lower strength	Lower strength and resistance to hot cracking.
	Too high	Raises strength, lowers notch properties	lowers both yield and notch strength
Titanium	Too low	Lowers strength	Increases porosity
	Too high	Lowers notch properties	Promotes segregated stable austenite forms low melting point sulphides.

K.SREE KUMAR et. al. Studied the microstructure of MDN-250 (1800 MPa) 7.8 mm thick welded plates which are used in large aerospace pressure vessels. The defects during the welding were repaired which are subjected to thermal cycles because of repair procedures. The microstructure in the repair weld zone is refined due to additional heat input in the martensite – austenite (α+υ) two –phase region. Microstructure revealed low austenite (υ) content. Heat extraction from the parent material was effective even though weld pool was heavily constrained. These two factors gave rise to a sound microstructure in the weld pool, which exhibited improved mechanical properties including fracture toughness [34].

P.P. SINHA et. al. investigated the effect of ageing on properties of MDN-250 grade (cobalt free). The properties (tensile & fracture toughness) achieved are similar to that of MDN-250 by modifying the ageing cycle. By way of pipe diffusion mechanism, precipitation reaction on dislocation occurs. The strengthening precipitate is a rod-shaped hexagonal η-Ni3Ti has good resistance to coarsening. The decreased strength and toughness in the overage condition are found to be caused by the combined effects of coarse precipitates and the presence of reverted austenite on the inter-lath boundaries. Strengthening owing to precipitates has been found to obey the modified orowan equation [35].

2.3.2 Low alloy ultra-high strength steels

Ni-Cr-Mo, Cr-Mo, and silicon steels contain carbon in the range of 0.25-0.45 by wt% and therefore they exhibit high hardenability. Hence it is recommended that these steels be given a reheat to overcome the problems of hydrogen embrittlement. Desired properties are achieved by heat treating after welding (post weld heat treatment) hence, these steels are classified as heat treatable low alloy steels. To achieve different strengths, these steels [36] welds are tempered at different temperatures.

The levels of sulphur and phosphorous in these steels are to be controlled for resulting in better weldability [36, 37]. The excess of sulphur and phosphorus leads to sensitivity in hot cracking and reduction of phosphorus resulting in an increase in cold cracking tendency and reducing the toughness and ductility due to interdendritic segregation of elements [37] (Table 2.11). It may be observed from this Table 2.11 that elements such as phosphorous and sulphur exhibit maximum damage. The higher content of silicon and nickel are prone to porosity in micro-level and cracking which related to segregation tendency in the weldments [37]. Weld thermal cycle has a profound influence on the microstructure developed in the welds of this class of steels. The microstructure obtained in the as-welded condition is generally martensite if the imposed cooling rates in the weld thermal cycle are too high.

Cooling rates more than 100^0C/s would lead to complete martensite transformation and therefore would be if very high strength and exhibit low toughness. This, therefore, calls for PWHTs dictated by the strength and toughness requirement. The effect of cooling rates on transformation in one of the ultrahigh strength steels (AISI 4340) given in **(Fig.2.8)**. For welding of the above materials, filler wires of similar compositions are available **(Table 2.12)**. These filler wires are available in various forms such as covered electrodes, bare wires, and flux coated electrodes. The properties of some of the arc welds of this class of steels are given in (**Table.2.13).** The effect of tempering temperature on mechanical properties of the welds is depicted **(Fig 2.9)**. It may be noted from this figure that the as welded strength of steels is very high and the ductility is low. With the increase in tempering temperature, ductility improvements occur with a sacrifice of strength.

Table 2.11 Interdendritic segregation of elements in steels (ref 24).

Elements	Segregation Coefficient
sulphur	0.95
Phosphorus	0.93
Oxygen	0.90
Carbon	0.87
Silicon	0.34
Molybdenum	0.30
Nickel	0.20
Manganese	0.16
Vanadium	0.10
Aluminium	0.08
Chromium	0.05

Welding studies on high silicon, High nickel ultrahigh strength steels similar to 300M steels are limited. Some available studies indicate that maraging filler metal gives less strength in the as-welded condition [38]. To enhance the strength of the weld and parent material post weld heat treatment is essential.

It was found that maraging steel filler containing high Co, Mo, and low Ti gives better weld properties in both as welded as well as in post weld heat treatment conditions. Other studies include the use of austenite containing filler that gives very low strength [39]. It may be noted that strength improvement in these austenite welds cannot be obtained by resorting to post weld heat treatment. Matching fillers are reported to give better strength in this class of steels [40] **(Table.2.14)**. The strength of the weld is also dependent on Groove angle. [41]. Low groove angle results in higher strength. A comparative evaluation conventional and pulse current welds showed that pulse current technique results in high strength and ductility [42]. A comparative evaluation of welding processes showed that electron beam welds exhibit better properties [43].

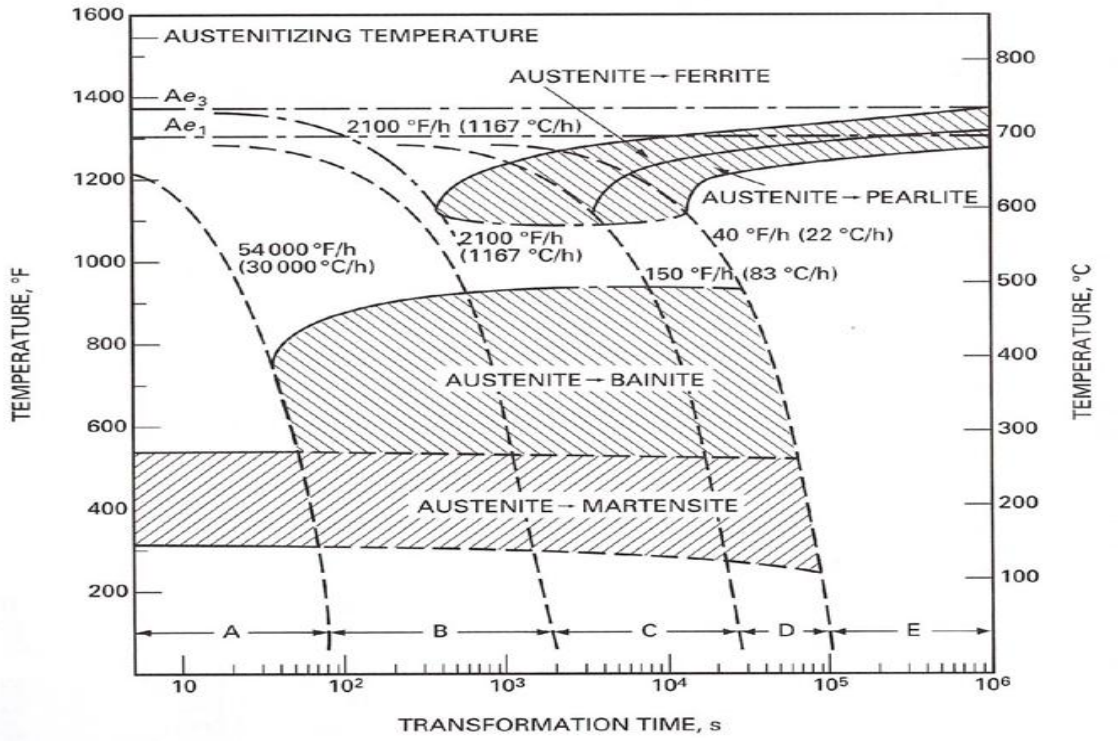

Fig 2.8 Transformation behavior of 4340 steel in continues cooling.

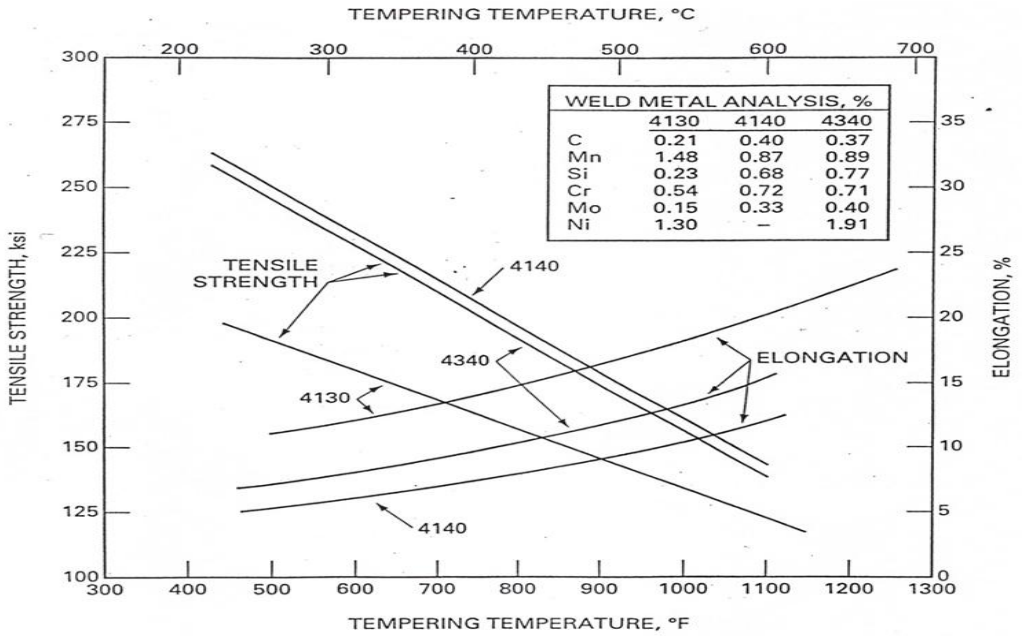

Fig 2.9 Influence of tempering temperature on tensile properties of low alloy medium carbon steel

Table 2.12 Typical mechanical properties of heat treatable electrodes (ref.27)

Electrode types	Ultimate tensile Strength	Minimum Yield Strength MPa	Minimum Elongation %	Charpy impact value, at 0^0C
4130	862-1000	689	11.0	64
	1034-1172	827	8.0	38
	1241-1379	1000	6.0	20
4140	862-1000	689	11.0	64
	1034-1172	827	8.0	38
	1241-1379	1000	6.0	20
	1379-1516	1103	5.0	11
4340	1034-1172	827	8.0	34
	1241-1379	965	6.0	16
	1379-1516	1103	5.0	11
4340	1793-1931	827	8.0	34

Table 2.13 Typical transverse tensile properties of arc welded joints in low steels after quenching and tempering (ref 33)

Steel Designation	Thickness of base metal (mm)	Welding process	Filler metal	Tempering temperature ^{0}C	Tensile strength MPa	yield strength MPa	El. (in 50mm G.L)	Approx base metal Tensile strength MPa
4130	6.35	GMAW	note a1	510	1172	1144	7	1172
4140	12.7	GMAW	4140	482	1303	1227	8b	1310
4340	25.4	GMAW	4340	510	1307	1251	11	1310
4340	25.4	GMAW	note a.2	510	1320	1224	8	1310
4335V	6.35	GMAW	4340	204	1758	1531	9	1786
D6	2.38	GMAW	note a.3	316	1861	1634	6b	1869
D6	2.38	GMAW	D6	316	1779	1503	6	1827
D6	12.7	GMAW	note a.4	538	1544	1427	7	1586

Note : Filler metal compositions are as follows:

a1 : 0.18% C, 1.5% Mn, 0.44% Si, 1.2% Ni, 0.34% Mo, 0.65% Cr

a2 : 0.25% C, 1.17 % Mn, 0.65% Si, 1.8% Ni, 0.8% Mo, 1.17% Cr, 0.21% V

a3 : 0.25% C, 0.28% Mn, 0.03% Si, 1.29% Mo, 0.98% Cr, 0.56% V

a4 : 0.25% C, 0.55% Mn, 0.65% Si, 0.5% Mo, 1.25% Cr, 0.3% V

Table 2.14 Tensile properties of weldments of silicon steels (ref.31)

Prior condition	**Yield strength MPa**	**UTS (MPa)**	**Elongation (50mm G.L), %**
Weld +heat treated			
Maraging filler	1555	1847	3.2
Silicon steel filler	1644	2002	4.4
Heat treated +welded			
silicon steel filler	1458	1576	1.3
silicon base steel	1622	2013	9.5

2.4 Metallurgy of Heat Affected Zone

2.4.1 The Heat-Affected Zone [44]

During fusion welding the material which is welded is heated thereby it reaches its melting point. Under conditions of restraint because of design (geometry) of the joint and cooled rapidly. Due to thermal gradient, the mechanical properties and microstructure of the weld area and adjoining areas are affected. The adjoining area is generally noted as heat affected zone. The HAZ is again divided into a number of zones depending on the welded material. These zones are identified based on the type of microstructure. The properties of HAZ are dependent on the base metal composition, thermal cycling, exposure to the temperature during welding and degree of cooling.

H. G. Pisarski et.al. [45], have investigated the significance of HAZ softening in a 550MPa QT steel has been determined by using fracture toughness and surface notched mini-wide plate test. It is reported that flaws are observed very near to the HAZ boundary showing softening of HAZ, the strain will be concentrated in local regions of lower yield strength, which are affected by the differential strength between the weld zone and base material.

Wei Meng et.al. [46], characterized the microstructure of LASER welded 960 MPa grade high strength steel joint. Strip- like microstructure is produced by rolling and it consists of fine lath martensite, a small quantity of granular bainitic (Bg) and tempered martensite in the base material. Coarse lath martensite and bainitic ferrite are formed in fusion zone (FZ) due to high peak temperatures. The tempered zone (TZ) and base material (BM) are strip-like and fine grained zone (FGZ) and coarse grained zone (CGZ) are uniform lath martensite without strip like characteristics, mixed grained zone (MGZ) is composed of original martensite small block martensite and when the temperature is above the Acl the retained austenite is formed. In TEM it is observed the width of lath martensite in HAZ and FZ are about 100nm. Microhardness distribution is BM>FZ>HAZ, Whereas from TZ to MGZ drops firstly and increases subsequently the zone is located as lower hardness zone (or) softer zone.

Reisuke et.al. [47], have metallurgically characterized Ultrafine grained steels in heat affected zone. Steel A has ferrite and cementite microstructure (grain size <1μm) and Steel B Ferrite and pearlite microstructure (3μm) and SM490 with ferrite grains (10μm). Three conditions were welded and hardness is distributed, where heat input of steel A is 9kJ/cm, HAZ softening width is about 2mm and the most softening level is about Hv 180. On the other hand heat input is 40 kJ/cm, HAZ softening width about 6mm and softening level is about Hv 170 in the both the cases the ferrite grains didn't grow up but, SM490 ferrite grains become 2.7-3.8μm upper than the Ac3 temperature. An alloying of small amount Nb and Ti which suppresses the growth of ferrite grains also reduce of softening zone in HAZ.

F. hochhauser et.al. [48], have examined the influence of HAZ softening on the strength of welded modern HSLA steels with three different levels of energy input to establish soft zones with the various extension was carried out a) 0.42 kJ/mm b) 0.53 kJ/mm c) 0.76 kJ/mm. However, weld metal hardness is more susceptible to increased heat input than the minimum hardness of the soft zone. The width of the soft zone increased linearly with the cooling time.

therefore welding processes with high energy input per pass are recommended for high strength steels.

L. Zhang et.al. [49], have studied the influence of rate of cooling on mechanical properties and microstructure of micro-alloyed HSLA steel weld metals at fusion zone slow cooling rate predominantly interlocked acicular ferrite AF is observed. The heat input is about 10.26 kJ/cm gives much finer ferrite with large aspect ratio where cooling rate is relatively higher the microstructure which is comprising of bainite and AF. The presence of bainite at rapid cooling shows much less tough than tough ferrite, interlocking and AF with fine. Where the presence of bainite at fast cooling shows much less tough than AF with fine, interlocking and tough ferrite. Relatively high Mo, Nb, and Al are contained in weld metal WM due to high dilution from base metal and difference is happened significantly by the addition of Ti in the microstructure, hardness, and toughness.

2.4.1.1 Microstructural Changes in the HAZ

In fusion welding, the heat-affected zone is subjected to the full weld thermal cycle and the solidified weld metal is exposed to the cooling part of the cycle. Heating and cooling rates are usually high, and the heated metal is subject to plastic tensile strain during cooling. The metallurgical effects of the weld thermal cycle are complex and may in some instances result in unfavorable changes in the properties of the material [50]. The thermal cycle associated with welding produces significant changes in the microstructure of the adjacent base metal. The welding heat input combined with geometric factors control the peak temperature, the residence time at that temperature, and the cooling rate at any given location in HAZ. This affects the composition of the austenite, the austenite grain size, and the temperature where the austenite begins to decompose.

Austenite grain size prior to transformation is controlled by the high temperature and residence time. Grain growth is restricted depending on the cooling rate. Depending on steel composition, Nb (C, N) precipitates can restrict grain growth to temperatures in the 1200-1250° C range, whereas V(C, N) is only effective at temperatures up to 900° C. Small additions of Ti to the steel reduce both the grain size and width of the HAZ [51]. Ti forms TiN precipitates, which are stable to higher temperatures than Nb (C, N). However, the temperature is above 1300^0C, the precipitates dissolve and coarsen. The chemical composition of the HAZ region is

essentially same as the base metal. However, the effective austenite composition varies with the local peak temperature. In the coarse-grained HAZ, all precipitates are generally dissolved and the region has the austenite composition predicted from phase diagrams and thus, transformation characteristics similar to the base composition. When the precipitates do not dissolve, they are very effective in limiting the growth of the grain, but the effective austenite composition is lower in precipitate forming elements, and therefore lower the local hardenability. At the peak temperatures in the inter-critical range, [(ϒ + α) Region], the austenite present is rich in carbon. The welding heat input and the thickness of the plate decide the temperature gradient and the cooling rate. The rate of cooling is uniform across the HAZ is essential. However, the cooling rate from 800-500 ºC, $t_{8/5}$, is most critical because most of the austenite transformation occurs in this temperature range [51]. The heat-affected zone (HAZ) of single pass welds can be divided into five distinct zones, depending on the peak temperature. In order of decreasing peak temperature (Tp), these are (a) partially molten region: Tp close to the melting point (b) coarse-grained HAZ adjacent to fusion zone: 100 ºC <Tp< 1450 ºC (c) fine-grained HAZ: Ac_3<Tp< 100 ºC (d) intercritical HAZ: Ac1 <Tp< Ac3 (e) subcritical HAZ: Tp below Ac1 but high enough to cause some tempering (3). All these different regions of HAZ are schematically shown in Fig. 2.10.

When the peak temperature of the weld thermal cycle exceeds than the required one, the grain coarsening occurs and below this particular temperature will produce smaller grain size than that of the parent metal.

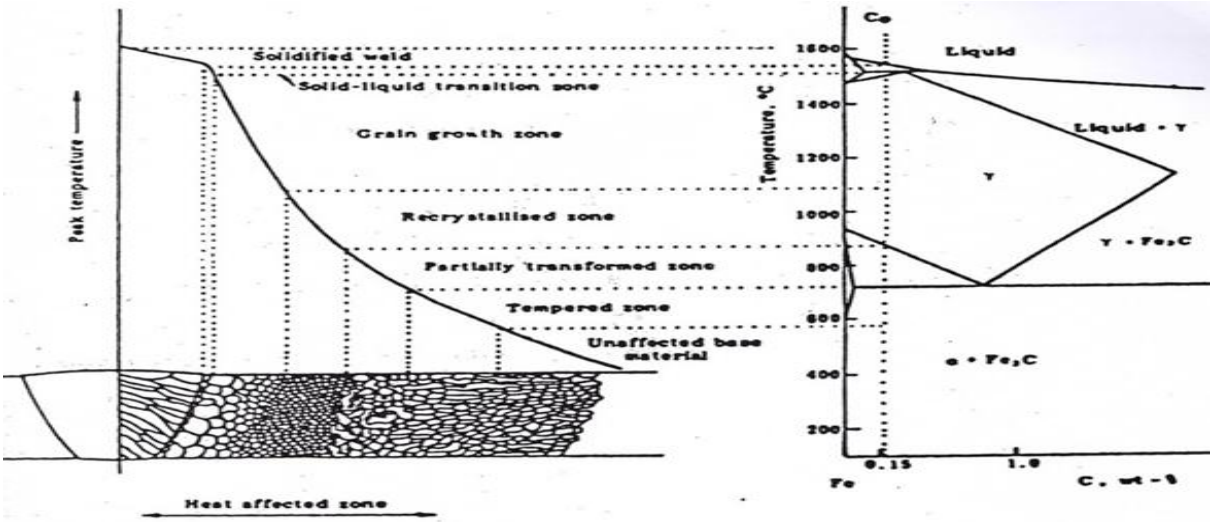

Fig. 2.10 Schematic diagram of various zones of HAZ corresponding to 0.15% C steel [18]

The transformation structure with the austenite grains and grain size are the two features dictated by the grain growth in the microstructure. The average grain size is dictated by two factors such as grain coarsening temperature of the steels, and the nature of the weld thermal cycle. For any steel, above the grain coarsening is the function of heat input, and time of exposure. In any weld thermal cycle, the grain growth time is reduced with higher grain coarsening temperature. In aluminum treated carbon steel which contains Al_3N precipitates which reduce the austenite grain growth up to a temperature above 1250^0C. Above this temperature Al_3N precipitates gets dissolved and growth of the grain is faster such that grain size at the fusion boundary is similar to that of the steels containing aluminum [50].

The microstructure resulted in the region of coarse-grain mainly rely on three factors i.e. % of carbon content and alloy content of the steel, cooling rate, and grain size. The proeutectoid ferrite in the low carbon steel separates initially at the grain boundaries of prior to austenite grain boundaries and within the grains a ferrite-bainite and/or ferrite-pearlite structure occurs. The small globular cementite particles in parallel arrays are seen in the pearlitic constituent. With increasing carbon and alloy content and /or increasing cooling rates, the austenite grains transform completely to the acicular structure: e.g.: upper bainite, lower bainite or martensite; or a mixture of these components and the proeutectoid ferrite disappears.

The spacing between martensite laths is wider resulting coarser austenite grain size and transgranular microstructure and also it promotes the formation of coarse microstructure would result from the transformation of a fine grain material [50]. The peak temperature and cooling rate decreases with increasing the distance from the weld centerline Consequently, the microstructure region is refined that is similar to normalized steels [50]. In the portion of HAZ where the Ac3 exceeded (850-950 ºC), and a sufficient number of precipitates are present to restrict grain growth, the austenite grain size is small and equiaxed. The Υ - - > α transformation on cooling tends to produce a fine-grained microstructure depending on welding heat input, plate thickness and chemical composition of the base metal. The large grain boundary area tends to promote ferrite nucleation and the austenite that remains in the grain centers may transform to pearlite or ferrite and carbide aggregates depending on the carbon content of the alloy. This zone

tends to be particularly wide in micro alloyed steels because of the effectiveness of carbonitride in preventing grain growth at these temperatures [51].

The partial transformation may happen in the intercritical zone which is small. In a carbon steel having a ferrite-pearlite structure prior to welding, the pearlite islands, which are of eutectoid carbon content, transform to austenite on heating and to martensite or bainite on cooling. In this as-welded, condition, the region may, therefore, consist of hard grains embedded in a relatively soft untransformed ferritic matrix.In the subcritical region, no significant microstructural changes take place. Optically, the microstructure is identical to the parent metal because the temperature is insufficient to cause a phase change of the ferrite or recrystallization. Only micro microstructural changes can be observed by electron microscopy. However, hardness survey in many steels of hardenable variety shows a dip hardness at the base metal and HAZ boundary interface. This may be attributed to ejection of carbon from martensite leading to carbide nucleation and growth which can be observed only in transmission electron microscope.

2.4.2 Effect of Parent Metal Chemistry and Prior Processing History on HAZ Softening

The hardness of the HAZ is directly related to the carbon equivalent of the material and the prior properties of the material. All steels do not show the softening phenomena and are generally found in HSLA steels. Thermo mechanically controlled processed steels, quenched and tempered steels, precipitation strengthened steels, and some ferritic steels are prone to HAZ softening.

2.4.3 Carbon Equivalent

The tensile strength of the steel is the function of hardness in the heat-affected zone (HAZ) and the hardness of the HAZ dictates the ductility of the weldment. The HAZ hardness depends on cooling rate, time of exposure, and hardenability of the steels. The hardness of the steels is generally correlated with the carbon equivalent (CE). The effect of hardening with respect to each element is compared with that of carbon content, and respective content in the alloy in mass percentage divided by a factor that implies carbon equivalent of the element. Carbon equivalent provides an indication of the type of microstructure to be expected in the weld heat-affected zone as a function of cooling rate from peak temperature. More specifically, it is

supposed to give an indication of whether or not martensite is able to form, i.e. of the hardness of the weld. Carbon equivalent formulae used in the present study are given a blow.

1. C.E. (IIW) = C + Mn/6 + (Cu + Ni)/15 + (Cr + Mo +V)/5.

2. C.E. (Graville) = C+ Mn/16 – Ni/50 + Cr/23 + Mo/7 + Nb/8 + V/9

2.4.4 Softening in the Heat-affected zone:

2.4.4.1 **Cr-Mo-steels [52]**

Hardness generally decreases through the HAZ with a definite decrease in hardness in the region which experienced temperatures just above the Ac_1 temperature at the outer boundary of the HAZ. Numerous instances of HAZ softening have been revealed in different steels and the concern over the occurrence of the softened regions is related to a reduction in transverse weld tensile and creep strength.Softening in the outer reaches of the HAZ is common in the Cr-Mo steels and has been related to 'over-tempering' of the region just below the lower critical temperatures Ac_1. Although the majority of investigators have related the hardness dip to the over tempering effect (carbide coarsening) and another possibility is that the softened region lies 'just above' the Ac_1 temperature rather than 'just below' the Ac_1 and evidence for this has been gained by weld HAZ hardness characterization and Gleeble studies isolating the peak temperature for maximum softening [33,53]. Typical softening behavior in 3Cr-1.5Mo pressure vessel steel is schematically shown in Fig. 2.11.

The mechanism for softening above Ac_1 temperature involves the formation of high carbon austenite and ferrite in the intercritical HAZ region (A+F). At temperatures above the Ac_1 austenite will begin to form at grain boundaries and subgrain boundaries while carbides, primarily concentrated in the same locations, will undergo dissolution. The higher solubility of alloying elements, particular carbon, leads to the rapid partitioning of alloying elements which stabilize the austenite. The equilibrium solubility of carbon in the first austenite to form just above the Ac_1 is approximately 0.8% and therefore the driving force for partitioning of carbon is high. Further, carbon can easily diffuse over the inter-carbide distance during relatively short times permitted by the welding thermal cycle. With carbon and the austenitizing elements concentrated in the low-temperature austenite (Ac_1 + T); the carbon concentration is lower in the

ferrite. Upon cooling of the microstructural constituents so formed, the austenite transforms to high carbon martensite and the ferrite remains unchanged.

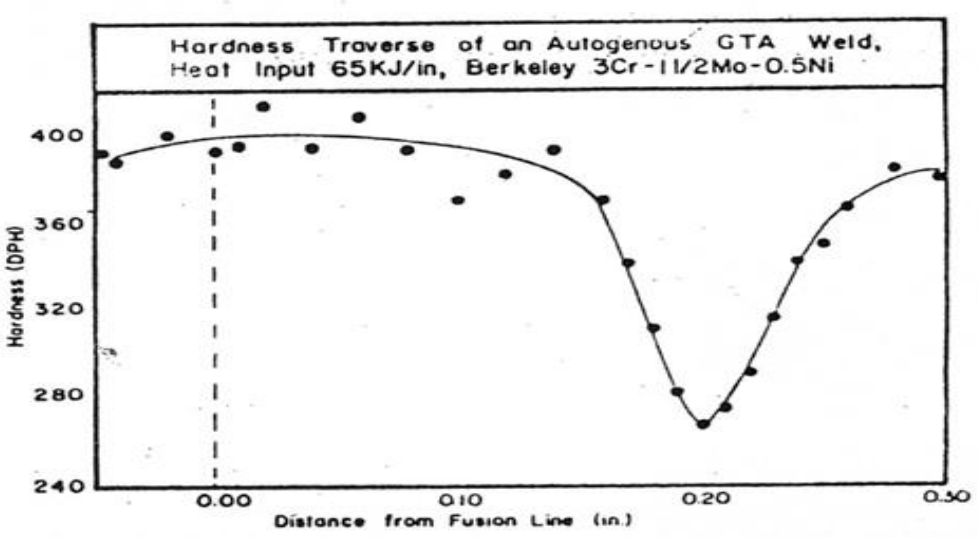

Fig. 2.11 Illustration of the occurrence of the soft zone in 3Cr- 1.5 Mo Pressure Vessel steel [52].

The possibility of retained austenite, a soft phase, also exists due to the high carbon content of the initial austenite. Upon post-weld heat treatment (PWHT) at temperatures below Ac_1 the low carbon ferrite would not experience a change but the high carbon martensite would temper rapidly. Thus a decrease in hardness would be anticipated due to the presence of low carbon ferrite and softer temper products derived from the high carbon martensite as opposed to the constituents present in a normalized and tempered base metal structure [52].

At higher temperatures in the inner critical region of the HAZ, the carbon content of the austenite would be less and the amount of free ferrite would decrease. Further, just above the Ac_3, the austenite will be of the same carbon content as the base material and no ferrite will be present. After cooling, the tempering of transformed structures during PWHT would be less dramatic than for the high carbon transformed austenite regions just above the Ac_1 and a harder region would exist after PWHT below Ac_1. Thus, a softened zone would result at the outer boundaries of the HAZ. Gleeble testing of Cr-Mo samples tends to show this effect and permits an evaluation of the temperature regime which results in maximum softening. A softened zone has occasionally been revealed adjacent to the fusion line in Cr-Mo materials. This softened zone is a reflection of carbon migration during heat treatment. The driving force for the carbon migration is primarily a difference in chromium content of the base material versus the weld

metal. The carbon migration is towards the higher chromium weld material where the carbon activity is the lowest (other alloying elements may also affect carbon activity but chromium is the most commonly encountered). This is applicable in the case of high Cr-containing austenitic welding filler metals and those containing higher Cr than the base metal.

2.4.5 Effect of welding process

Heat input rate will have a bearing on the HAZ microstructural transformations. The heat input characteristics and efficiency of heat utilization will be different for different welding processes. Heat efficiency characteristics of different welding processes are given in Table 2.15. For a given condition of cooling, the HAZ microstructural transformations and kinetics are dependent on the welding process.

If 'V' represents arc voltage 'I' arc current and 'ϰ' is the proportion of arc energy that is transformed into heat to the workpiece, then the heat input rate 'q' per length of weld is,

$$Q = \varkappa \times (VI/S) \text{ ---------} \rightarrow (2.1) \text{ [50]}$$

Where 'S' is the welding speed. The heat input rate is one of the most important variables in fusion welding since it governs heating rates, cooling rates, and weld pool size. In general, higher the heat input rate lower would be the cooling rate and larger is the weld pool. Grain size will get affected by the amount of heat input. Grains in the solidifying weld metal grow coherently with grains in the solid metal at the fusion boundary. Therefore, the longer time spent above the grain coarsening temperature of the alloy, the coarser the grain structure in the heat-affected zone and in the weld metal. Thus a high heat input rate process will, in general, gives a longer thermal cycle and tend to generate a coarse grain structure.

In quenched and tempered steels, the high heat input rate results in the wider soft zone. The effect of heat input is to alter the weld thermal cycle. This would lead to changes in $t_{8/5}$ (cooling time between 800 to 500° c). This influences the widths of different HAZ regions. A higher heat input which results in higher $t_{8/5}$ leads to wider soft zone. It was indicated that the soft zone was not observed with low heat input rate [54]. The maximum and minimum hardness of the HAZ is related to the heat input rate. Thus the degree of softening depends on the weld heat input. In some TMCP steels, it was noted that the location of minimum hardness value in HAZ gradually shifted towards the base metal with increasing heat input [54]. It has also been

reported that the tensile strength of an accelerated controlled cooled steel weldment decreases significantly with welding heat input [54]. The variations of hardness profiles in HAZ of accelerated controlled cooled steel welded with different heat inputs are shown in Fig. 2.12. The variations of minimum hardness in HAZ of accelerated controlled cooled steel as a function of welding heat input is shown in Fig. 2.13.

Table 2.15 Heat source efficiencies of different welding processes [50]

Welding process	Heat source efficiencies
Electro slag welding	0.85 – 0.82
Submerged arc welding SAW	0.8 – 0.99
Gas metal arc welding (GMAW)	0.65 – 0.85
Shielded metal arc welding (SMAW)	0.65 – 0.85
Gas tungsten arc welding (GTAW)	0.5 – 0.8 (DCSP), 0.2 – 0.5 (AC)
Electron beam welding	0.8 – 0.95
Laser beam welding	0.005 – 0.7

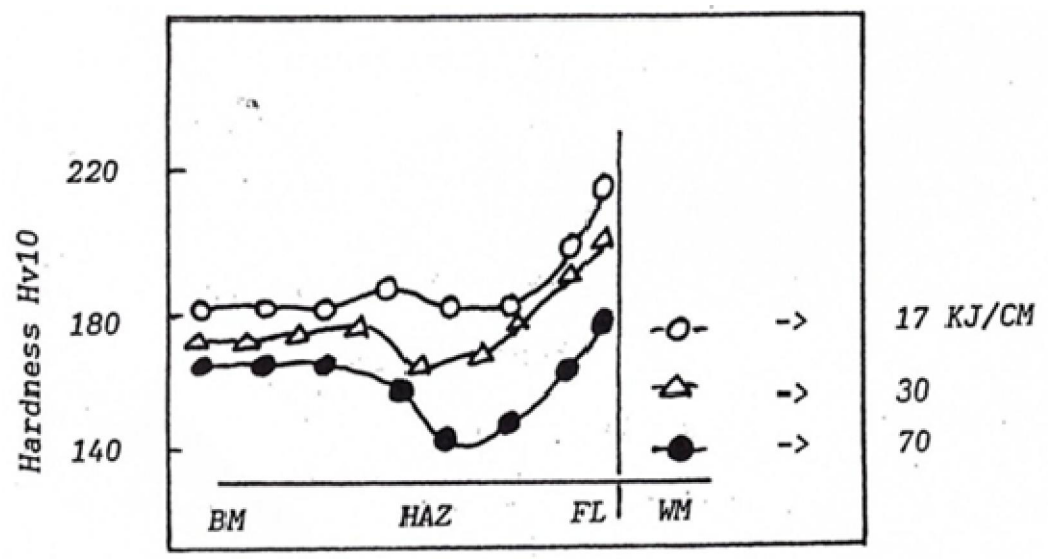

Fig. 2.12 Variation of minimum hardness in HAZ of ACC steel weld as a function of welding heat input [54].

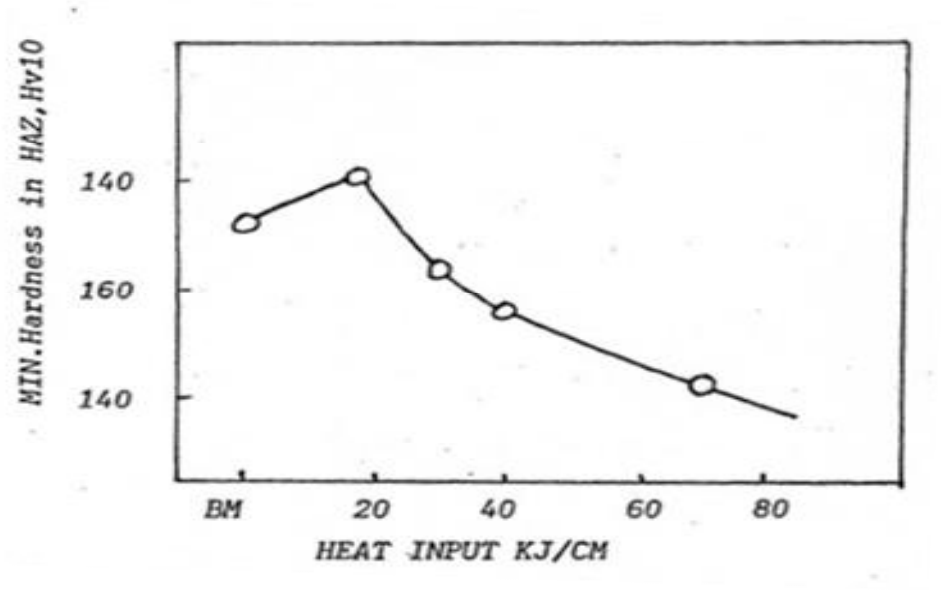

Fig. 2.13. Variation of hardness profiles in the HAZ of an ACC steel welded with heat inputs of 17, 30, 70 KJ/CM [54].

2.4.6 Effect of External Jigs & Fixtures

External Jigs & Fixtures will provide the necessary cooling for the weldment and base metal. Generally, an inert gas is supplied for the cooling purpose. One can control the cooling rates by controlling the flow rate of the gas. The cooling rate will impact on the microstructural changes and mechanical strength of the base plate. Controlled cooling can get the desired properties. Backing plates of materials of high thermal conductivity can also be used for the extraction of heat to enhance cooling rate.

2.4.7 Effects of cooling after welding:

The weld metal and the heat – affected base metal may receive from surrounding cold base metal a quench that ranges from that of relatively slow air cooling to fast water quenching. Therefore, parent metal and HAZ may contain soft, almost fully hardened, or mixed soft and hard structures. The cooling rate associated with the weld nugget depends on the total heat of the molten pool and the mass and temperature of the weld deposit. For any process, the volume of molten metal will depend upon the heat input and the efficiency of utilizing this heat in producing molten metal. For a specific section being welded, the cooling rate depends upon the heat of the molten metal in the weld bead much of which is transmitted to the parent metal

immediately after the welding. The cooling rate will have a bearing on the extent of hardness in the HAZ of the hardenable steels. In this maximum hardness is measured by some method such as knoop method. It is possible to determine the changes in hardness due to variation in cooling rate based on the size of the nuggets. The cooling rate depends mainly on three variables i.e. rate of heat input, parent material temperature, joint geometry & thickness of parent material. High heat inputs and preheating favor slow cooling, while heavy sections encourage fast cooling rates. The first two factors can be used in welding to control the cooling whether the process is arc, gas or resistance welding. A comparison of the microstructures in two heat-affected zones, one produced by a high heat input and slow cooling and the other by a slow heat input and fast cooling reveals that the slowly cooled HAZ contains only pearlite and ferrite, while the rapidly cooled HAZ contains considerable amount of light etching martensite in the coarse grains [55].

2.4.8 Effect of heat input, geometry and preheat on cooling rate:

High welding currents and low travel speeds in arc welding have long been known to provide a large amount of heat per inch of the weld and thus encourage slow cooling. In addition, thick plates and low plate temperatures permit rapid dissipation of the welding heat and, hence, rapid cooling. However, the quantitative relationship between welding conditions and cooling rates were not known until the subject was extensively investigated by Hess and Co-workers at Rensselear Polytechnic Institute and by Doan and Co-workers at Le high university [56, 57]

They correlated the actual cooling rate with heat input, plate thickness, and initial plate temperature. The weld cooling rates were determined indirectly by correlating the maximum hardness, in the heat-affected zone of a weld with the cooling rate at a location in an end-quenched bar exhibiting the same hardness [57]. It was indicated that the thermal properties such as conductivity and specific heat, vary so little between carbon steels and a variety of low alloy steels, and the cooling rate is not affected in any significant manner by these factors [57].

2.4.9 Effect of weld size on cooling rate:

It is assumed that energy input is a linear function of arc travel speed. This assumption is reasonably valid for low energy inputs obtained with electrode travel speeds lower than about 12 inches per min. However, for higher rates of travel, the heat transfer efficiency in the welding process is improved. The weld cooling rates will be governed by the cross-sectional area of weld

metal and to a lesser extent by the energy input per unit length of weld. The cooling rates will be slower for those weld beads for which the weld metal area is large and as the weld area decreases, the cooling rates in the HAZ will become more drastic [58].

2.4.10 Effect of cooling rate on HAZ hardness variation:

It has been reported that the difference between the hardness of the base metal and the minimum HAZ hardness, ΔH is a function of cooling rate, i.e. the degree of softening depends on cooling rate [59]. Effect of cooling time $t_{8/5}$ on the decrease in HAZ hardness is shown in Fig. 2.14. In TMCP steels, it was reported that the ΔH increases rapidly at shorter times and tends to approach a saturation value at longer cooling times [59]. It has also been reported that, in TMCP steels, the soft zone width increases linearly with $t_{8/5}$ [59]. The soft zone width increase depends on the material, grain size, chemical composition, amount of inclusion & base metal temperature. Recovery and Recrystallization kinetics also get affected. Variation of soft zone width with a cooling tie is shown in Fig. 2.15.

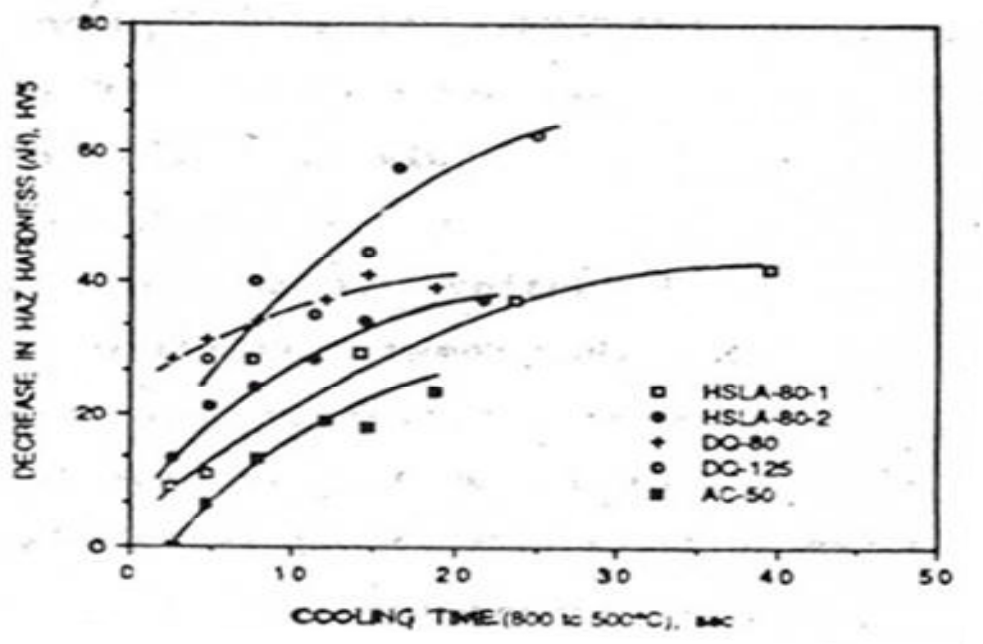

Fig. 2.14 Effect of cooling time, $t_{8/5,}$ on the decrease in HAZ hardness [59].

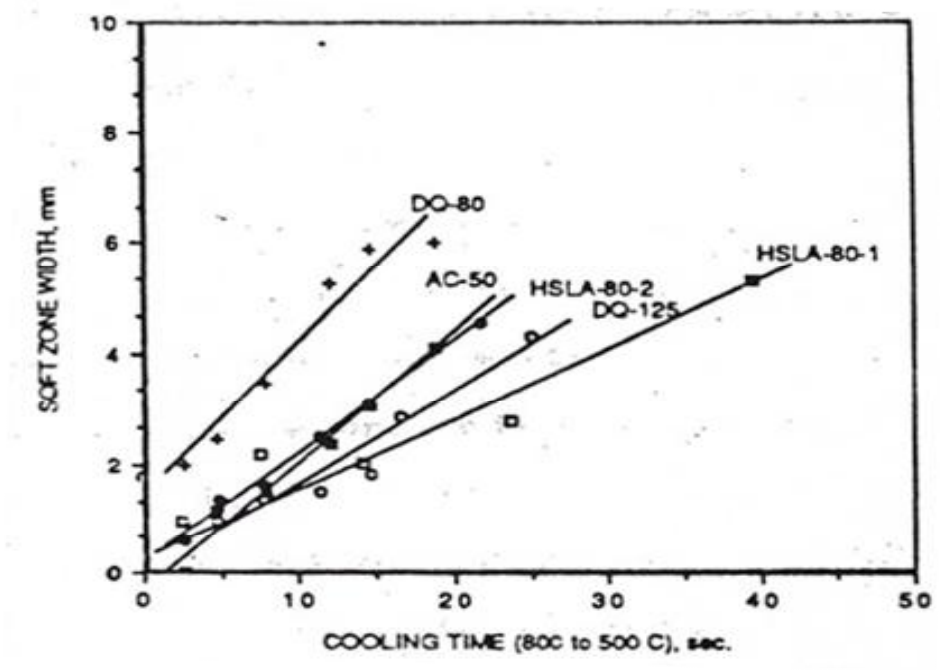

Fig. 2.15 Variation of soft zone width with cooling time ($t_{8/5}$) [38].

2.4.11 Effect of post weld heat treatment

Properties of weldments can be improved by Post weld heat treatment. The parent material can be stress relieved by uniform heating up to the transformation temperature followed by uniform cooling. The beneficial effects of stress-relief heat treatment are not primarily due to residual stresses but rather to the improvement of metallurgical structures by tempering. Tempering is a process by which steels are heated below the lower critical temperature followed by air cooling or at any other desired rate, thereby lowering the hardness and increase the strength and wear resistance marginally. However, this marginal loss is adequately compensated by advantages gained by relieving of internal stresses, restoration of ductility and toughness and transformation of retained austenite. Higher the tempering temperature, more is the restored ductility and tougher the steel.

2.4.12 Structural changes during tempering:

A number of structural changes take place during tempering treatment. These changes include the isothermal transformation of retained austenite, ejection of carbon from a body-centered tetragonal lattice of martensite, growth, and spheroidization of carbide particles and formation of the ferrite-carbide mixture. Depending on the range of tempering temperature, the

treatment proceeds to various stages.The first stage of tempering is referred as low-temperature tempering. Heating of steel restricted to about 250°C at this stage.

This results in the decomposition of high carbon martensite. The decomposition of high carbon martensite proceeds essentially by nucleation and growth. The carbon content of the product martensite is independent of the carbon content of the original martensite. Carbon content decreases with increase in tempering time. It continues till the carbon of product martensite reaches a value equal to 0.3 %C. This amount of carbon in martensite leads to a stable state within this temperature range and this martensite does not decompose further.The carbide precipitated from the high carbon martensite during the first stage of tempering is not cementite. This carbide is known as epsilon carbide which has a hexagonal closed packed structure. The carbon content of epsilon carbide is more than that of cementite (Fe_3C) and the chemical formula is approximately $Fe_{2.4}C$. The carbon atoms are located at octahedral interstices and arrange themselves in such a fashion that each is separated from the other with a maximum possible distance. Epsilon carbide is metastable. Hence, the carbide particles are very fine in size. A marginal decrease in hardness value takes place at this stage. Strength improves considerably. Toughness also improves.

In the second stage, tempering is done between 350 to 500^{o}C. During this stage, retained austenite transforms to bainite. This bainite differs from conventional bainite in the sense that it consists of ferrite and epsilon carbide. Ductility and Toughness increases by this treatment with a corresponding decrease in hardness and strength. The third stage of tempering is known as high-temperature tempering. It consists of heating steel within a temperature range of 500 to 680 ^{o}C. Heating to such temperature results in the formation of the ferrite-cementite mixture. Martensite changes to ferrite by losing its carbon. Carbon thus released combines with epsilon carbide which in turn transforms to cementite. All these changes occur with by diffusion and nucleation phenomena.

During tempering the zone containing martensite undergoes the following changes [60]. (GEORGE et al., 1965) Martensite changes to ferrite with the precipitation of epsilon carbide from the super-saturated tetragonal crystal lattice.

1. Any austenite that has not changed to martensite during quenching changes to ferrite and epsilon carbide.

2. The minute crystals of carbides in the martensite and the larger crystals of carbides in other constituents such as fine pearlite increase in size.

Changes (3) seems to account for the major drop in hardness on tempering, that is, the hardness of martensite steel depends upon a fine dispersion of carbide particles on each crystal plane, which hinders slip and thus raises hardness while reducing ductility. Reheating coarsens the carbide particles and reduces their number thus reducing hardness.

Steels with carbide forming elements, such as chromium, molybdenum, tungsten, vanadium, tantalum, and titanium resist softening considerably because of the formation of respective alloy carbides. In these steels, improvement in hardness values has been observed, which is contrary to the nature of tempering process. Such a behavior is referred to as secondary hardening. This hardening results from the formation of alloy carbides. These alloy carbides are formed at a higher temperature and are harder and more stable than cementite.

2.4.13 Effect of post weld heat treatment on HAZ softening:

It has been reported that post-weld heat treatment (PWHT) causes further softening in TMCP steels. This softening is called secondary softening [54]. The effect of PWHT on softening of TMCP steel weldment is shown in Fig. 2.16. The strength & hardness of TMCP steels is reduced due to the heat of welding, as it erases the effect of TMCP, so further heat treatment still reduces the hardness. It has been reported that in precipitation strengthened steels, PWHT results in an increase of hardness.

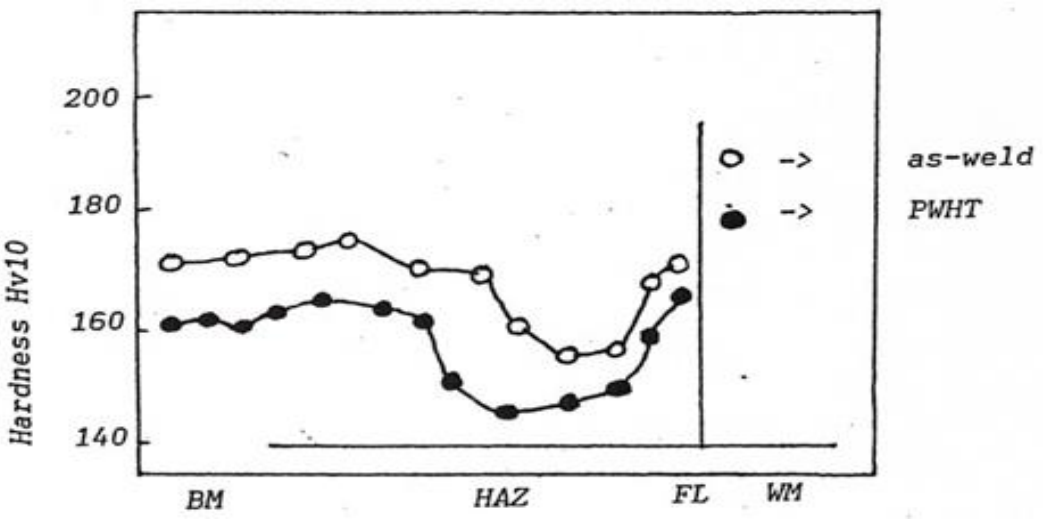

Fig 2.16 Effect of post-weld heat treatment (PWHT) on softening of TMCP steel weldment.

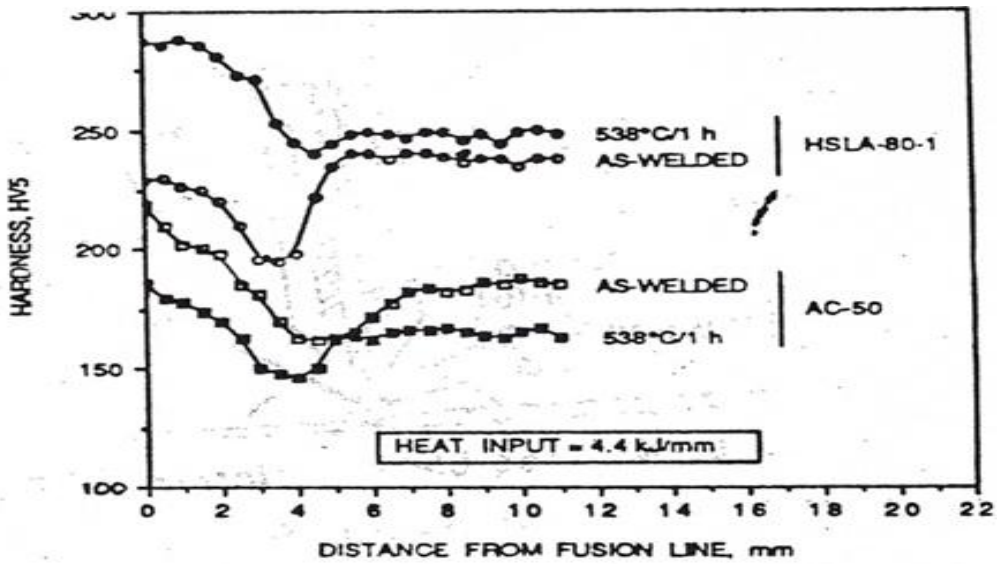

Fig. 2.17 Effect of Post Weld Heat Treatment on the HAZ hardness profile in precipitation strengthened steel [59].

The softening in precipitation strengthened steels is due to the dissolution of precipitation, but due to PWHT, hardness increases and soft zone disappears. This is attributed to the re-precipitation [59]. Effect of post weld heat treatment on the HAZ hardness profile in precipitation strengthened steel is shown in Fig. 2.17.

2.5 Welding

2.5.1 Welding of maraging steel

P.Venkatramana et.al. Studied the dispersion of residual stress in maraging steel welds using X-ray diffraction techniques with Cr kα radiation on filler wire composition. Three types filler materials were used they include maraging steel filler, austenitic stainless steel, and medium alloy medium carbon steel filler metal. They found that the tensile and compressive residual stresses were observed in welds of maraging steel and medium alloy carbon steel respectively. Using austenitic stainless steel filler welds shows lower hardness due to austenite stability but higher hardness is observed in medium alloy and medium carbon steel filler welds because of the martensitic microstructure. They also stated that maraging steel filler welds are responded to PWHT [61].

D.Sivakumar et.al. Studied on the influence of PWHT on the weld zone microstructure and toughness of cobalt-free maraging steel. They found that after PWHT, toughness increases marginally in cobalt free maraging steel. It was observed that toughness of the welded samples is lower than that of the solution heat treated and aged condition. They also noticed that austenite phase is the responsible for changes in the microstructure. They also concluded that, increasing in solution treatment temperature decreases the quantity of austenite phase[62].

Jain et.al. studied the effect of PWHT on the characterization of stainless steel welds. Laser weldments of dimensions 200x100x3mm using a CO_2 laser. The weldments are subjected to post weld-ageing treatment in the range of 420°C to 580°C for 2hrs. Mechanical characterization were evaluate and noticed that hardness in the heat affected zone and fusion zone varied with ageing temperature differently from that of the parent metal. Above 420°c hardness in heat affected zone and weld zone was superior to in base metal. Higher tensile strength was achieved at ageing treatment temperature at 420°C. The untimely and the quantity of reverted austenite were not the main factors influence the difference of the unlike hardness with an ageing temperature between weld zone and the treated parent material zone [63].

C. R Sharma et. Al. Studied the effect of two passes using a GTAW process with argon shielding using CCGTAW and PCGTAW processes with two filler materials , one having the similar composition as the base material & additional with high cobalt and aluminum and inferior molybdenum and titanium contents on 3.5mm thick sheet of 18Ni (250-grade) Maraging steel. Post weld ageing was performed at three different temperatures viz., 425°, 480° and 520°c. Micro-structure revealed marked separation, apparently of Ti and Mo, the length of inter-dendrites and intercellular boundaries in the weld metal formed with the corresponding composition; this lead, decreasing following ageing, to austenite reversion temperatures much lower than in wrought (unwelded) materials. Separation and austenite setback were not observed when lower contents of Ti and Mo in the filler material, not together from at the maximum ageing temperature used [64].

2.5.2 Welding of AISI 4130 steel

I K Lee et.al Studied the influence of PWHT on the mechanical properties of AISI 4130 by multilayer CCGTAW. They found that AW (Annealing + welding) influenced smaller hardness in Grain-Growth Heat Affected Zone (GGHAZ) because of grain growth coarsening. The Very rapid decrease in hardness value in multi-pass welds, however, the hardness values are higher than that of minimum value at HAZ. After heat areatment, the improvement in terms of mechanical properties of the welds after proper heat treatment i.e., Annealing followed by Welding then Solutionizing then Tempering. It is also found that AST had a greater necking than AWST. The results indicated that in the AWST Process, the PWT thermal refinement had a huge influence in fracture toughness [65].

Neto et.al. Studied on the influence of PWHT on different mechanical properties of AISI 4130 steel weldments. In the present study, the LBW technique is an alternative for GTAW process for improving the mechanical properties. They found that in laser welding and GTAW process, the martensite is observed in fusion zone. However, the grain size is found to be different in both the process and also they found that PWHT of weldments pertaining to both the process leads to better mechanical properties compared to as-welded condition. [66].

Mohammad W et. al. Studied the influence of PWHT and electrolytic plasma process on the residual stresses, microhardness, microstructure and tensile properties of GTAW welded AISI 4140 alloy steel with AISI-4130 chromium- molybdenum alloy welding filler wire. They observed that there is an enhancement in ductility and decline in yield strength after PWHT at 650ºC. This may be due to the breakdown of martensite and the grain coarsening of α-phase. In comparison, EDP-treated samples revealed lower residual stresses but the very less important difference on the grain refinement. They also found that the EDP treated specimens displayed superior tensile strength but lesser ductility and toughness for the martensite development due to the quick heating and quenching effects. They stated that the EDP after PWHT at 650ºC did not exhibit significant improvement on the tensile strength [67].

2.5.3 Welding of Dissimilar Metals

P.Venkatramana et.al. studied on the effect microstructure, residual stress variation, and hardness and strength for similar and dissimilar welds. They found that the symmetrical and unsymmetrical fusion zones in similar and dissimilar welds respectively and the width of the HAZ is varied due to the variation in material thermal conductivity. Further, it is also noticed that compressive residual stresses are observed in similar welds of maraging steels whereas tensile residual stresses in similar welds of low-alloy medium carbon steels. In the HAZ of the quenched temper steel shows minimum hardness as compared to the parent material due to coarsening of martensite laths [68].

G.Madhusudhan Reddy and P.Venkata Ramana made an attempt to enhance the mechanical properties of friction stir welding (FSW) of low alloy high strength steel and maraging steel with nickel as an interlayer. The tensile strength, toughness, and hardness are found to be better when nickel used as an interlayer because it is acted as a deficient barrier and also observed mechanical properties of dissimilar friction stir welds are better in PWHT condition. However, it may be added that notch tensile strength and impact toughness is observed to be lower compared to the parent material. They found that the properties like notch tensile strength and toughness are higher in dissimilar combination with Nickel interlayer [69].

G.MADHUSUDHAN REDDY and P.VENKAT RAMANA et. al.(2011) Investigated the influence of filler material composition on the residual stress distribution in similar and dissimilar gas tungsten arc welding of Maraging steel and medium carbon steel. It is noticed that in the fusion zone of maraging steel is found to be compressive in nature whereas tensile stresses in medium-carbon steel. This is confined to different physical and mechanical properties of the materials and type of heat treatment process. The magnitude of residual stresses decreased when the Maraging steel is taken in the soft condition in the dissimilar metal welding post-weld ageing resulted in lowering of residual stresses in medium alloy medium carbon steel [70].

2.6 Pulsed TIG welding

A. KUMAR, et.al Studied the influence of PCTIG welding process variables like peak current, background current, welding speed and pulse frequency (Hz) on mechanical properties of AA5456 250mmx150mmx2.14mm aluminum alloys weldments and the process parameters were optimized using Taguchi method. From their investigating they found that pulsed arc welding process gives fine grain structure materials compared to continuous arc welding because of thermal variations. The optimum combination of peak current ~80amps, base current 40amps, welding speed 230mm/min and pulse frequency of 4Hz is observed in better mechanical properties They also studied the effect of planishing after weld and found that, there is 10-15% improvement in mechanical properties due to the fact that, internal stresses are relieved or redistributed in the weld [71].

MINGXUAN YANG et.al. Investigated the influence of pulse frequency (Hz) on characterization of Ti-6Al-4V, with the dimensions of 200x80x1.5mm by adopting ultrahigh – frequency UHF-PCGTA they observed that in the UHF-PCGTA process, a decrease in the heat input compared to GTAW and the decreasing in heat input with increasing pulse frequency the effect of pulse frequency caused the basket weave & short “acicular” martensite distributed is the f7 only. It was noticed between the parallel long “acicular” martensite in the coarse –grained region at f>30khz better mechanical properties were with an elongation using rate of 68% & Percentage of area 150% with f=30khz. Overall they found that the combined effects of pulsing and heat input are the main problems for the reduction in grain size and in obtaining necessary properties [72].

S. KRISHNAN et.al. Studied in details the suitability of 12mm thick PCGTAW of P91 grade steels in butt weld joint arrangements with filler wire of cored type and observed that both the type of single as well as multi-pass welds resulted with satisfactory weld bead surface morphology, at larger groove angles i.e., of 60° & 75° for the operating range of current and welding speed resulted in better welds. It is observed that mechanical properties of weldments are affected by heat input (J/unit length) and joint angle. The welding speed is enhanced by 20% and 42% rate for filler wire deposition compared to solid wires [73].

G. LOTHONGKUM et.al Studied the effect of welding speed, pulse /bare currents, pulse frequency (Hz) , ON time (%) and Ar+N_2(0 vol% to 4vol%) as a shielding of TIG pulse gas welding parameters on the plate of 3mm thick AISI-316L stainless steel at the welding positions of 6hrs-12hrs. After conducting initial experiments, the base current of 61amp, 5 Hz pulse frequency and ON time (65%) is made constant in respective welding configurations. They found that by increasing the welding speed, pulse current increases. The speed of welding is restricted to 6mm/s at different welding configurations of 6h to 12h. With high welding speed i.e., more than 6mm/s resulted in slag inclusion formation on the welded top. At different welding positions of 8 to 10 hrs in step of 1hr welding speed was limited up to 5mm/s, incomplete filling of the weld material is observed when the speed of welding is above 5 mm/s. It is also observed that the in the weld delta –ferrite content varying from 6 to 10% of volume [74].

K.DEVENDRANATH RAM KUMAR et.al Investigated the welding of different marine grade alloys including Monel 400 and AISI- 904l by PCGTA technique using ernicu-7 and ErNi (Cr) mo-4 filler metals. They revealed that successful dissimilar welds were noticed. Microstructure at the fusion zone (FZ) showed the formation of long and short dendrites of ernicrmo-4 weldments. Tensile studies showed that the fracture occurred at the parent metal of Monel 400 for weldments, as well as fracture was observed at the HAZ of Monel 400. The mean ultimate tensile strength of the welds was observed to be larger than the ernicrmo-4 which is attributed to the presence of unmixed zone in the weldments. Charpy v-notch studies showed that the mean toughness of both the welds is almost equal or slightly greater than one of the base metals, AISI- 904l [75].

N.Arivazhagan,V.Rajkumar et.al studied on different aspects of mechanical properties related to AISI 4340 and maraging steel MDN 250 weldments using gas tungsten continuous current arc (CCGTA) welding and PCGTA welding using an ErNiCrMo-3 grade filler wire and observed that lack of porosity in weld microstructure. And they also studied that optical microscopy of the dissimilar weldments and observed that tempered martensite is more at the

low-alloy weld interface in both the techniques. And it also observed that more elemental migration in CCGTA than that of PCGTA. From the microhardness survey, it is revealed that hardness is very low in the HAZ of maraging steel, high in HAZ of low alloy steels side. Finally, they concluded that better mechanical properties in PCGTA compared to CCGTA [76].

2.7 Laser Beam Welding

Another way of reducing the heat affected zone softening is by employing low heat input welding processes such as EBW or LASER welding processes in place of TIG / Pulsed TIG welding processes. Huang et al [77] have discussed the effect of PWHT on the strength and resulting residual stresses in electron beam welded joints of AISI 4130 steel. Their work has shown that subjecting weld joints to heat treatment results in reduced residual stresses and improved the percentage elongation. The work by Wang and Chang [78] has demonstrated that by applying electron beam and post weld heat treatments on AISI 4130 steel EB welds, it is possible to change the nature of tensile residual stresses into compressive stresses. This reversal of mode of residual stresses has drastically improved the resistance offered by EB welds to fatigue crack growth. Neto et al [79] have compared the mechanical properties of TIG and laser beam weld joints of AISI 4130 steel. Their study revealed that HAZ width of laser beam welds of AISI 4130 steel is ten times lesser than that of gas tungsten arc welds. In the recent past, fiber lasers are invented and introduced into the manufacturing sector. The fiber lasers score better than conventional CO_2 type lasers in terms of high energy density, deeper, narrower and possible high welding speeds especially in thin-walled cross sections [80].

2.8 Summary

A broad literature was conceded out on welding metallurgy of maraging steel and AISI 4130 steel, welding of a similar and dissimilar combination of this steel. A literature survey was also carried out on different welding techniques to reduce the width of the soft zone in both the steels. The joints fabricated by continuous, pulsed TIG and LASER beam welding process with and without external cooling was also studied. And further, the effect of contamination i.e. oil, grease and water on strength of dissimilar combination of weldments was also studied. Based on the literature survey welding processes were improved, which resulted in improving mechanical properties, joint efficiencies, overall quality of welds.

CHAPTER - III

REPORT ON PRESENT INVESTIGATION

3.1 Introduction

A series of experiments have been conducted to study the effect of different welding processes such as Continuous TIG welding and Pulsed TIG welding, and laser beam welding of dissimilar welds of Maraging steel and AISI 4130 steel on metallurgical and Mechanical Properties.

3.2 Experiment layout

The total work is divided into three subsections, namely continuous TIG welding, pulsed TIG welding and laser beam welding. The experiments were conducted to investigate the width of the degree of softening, microstructure and mechanical properties of dissimilar welds of maraging steel and AISI 4130 steel. The experimental layout for the present investigation is shown in Fig.3.1.

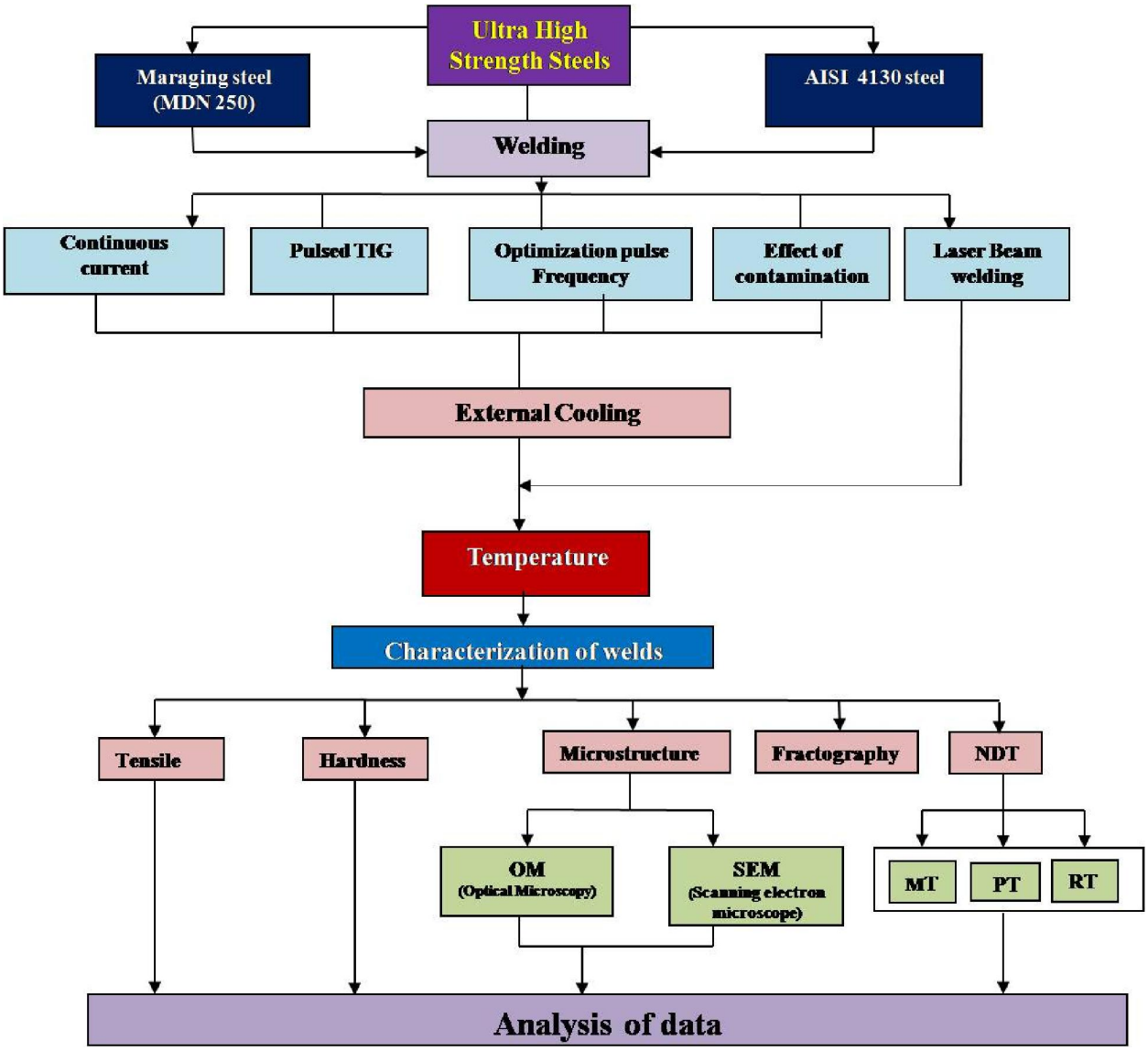

Fig. 3.1 Experiment layout.

3.3 Experimental details

3.3.1 Selection of base material and filler material

The materials under the investigation were 18%Ni (MDN-250 grade) maraging steel and AISI 4130 heat treatable high strength low alloy steel. The pre-form of maraging steel was received in solution annealed condition and subsequently flow formed to a test ring of size 250 mm diameter with a wall thickness of 2mm and length of 125mm.The test ring was subjected to

the ageing treatment by heating to 485°C/3.5hrs followed by air cooling. A forged AISI 4130 steel ring was austenitized at 870°C/1hr with oil quenching and tempered at 260°C/1 hr followed by air cooling. The heat treated AISI 4130 forged ring was machined to match maraging steel test ring in all dimensions. The chemical composition of maraging steel and AISI 4130 steel is presented in Table 3.1 and Table 3.2 respectively. The heat treated condition and mechanical properties of the base materials are presented in Table.3.3. The W2 grade maraging steel filler wire is used for welding trials but had higher cobalt, aluminum and lower molybdenum and titanium contents to compensate the loss of strength due to segregation of vital alloying elements in fusion zone [23]. The chemical composition of W2 grade filler wire is shown in Table.3.4.

Table 3.1 Chemical composition of 18% Ni Maraging steel in wt%.

	C	**Ni**	**Co**	**Mo**	**Ti**	**Al**	**Mn**	**Fe**
18% Ni Maraging steel	0.02	18.9	8.1	4.9	0.4	0.15	0.04	Balance

Table 3.2 Chemical composition of AISI 4130 steel in wt%.

	C	**Cr**	**Mo**	**Si**	**Mn**	**S**	**P**	**Fe**
AISI 4130 steel	0.3	0.86	0.25	0.26	0.48	0.02	0.019	Balance

Table 3.3 The typical tensile properties of base materials in their respective heat-treated conditions.

S.No	**Type of base material**	**UTS(MPa)**	**0.2%YS (MPa)**	**%Elongation**
1	18% Ni Maraging steel (Solution annealed and aged)	1839	1810	2.9
2	AISI 4130 steel (Hardened and tempered)	1530	1215	8.5

Table 3.4 Chemical composition of W2 grade maraging steel filler wire.

	C	**Ni**	**Co**	**Mo**	**Ti**	**Al**	**Fe**
Filler wire W2	0.006	18.2	11.9	2.5	0.16	0.46	Balance

3.3.2 Welding process

Various welding processes such as continuous TIG welding, pulsed TIG welding, and Laser Beam welding were used to welding of dissimilar metals of 18%Ni (MDN-250 grade) maraging steel and AISI 4130 heat treatable high strength low alloy steel. All the experimental conditions for various processes were tabulated in Table 3.5. The welding experimental trials were conducted maintaining fixed dimensions for the test rings and constant welding setup in order to maintain similar heat flow conditions during welding. The welding heat input was reduced by using pulsed mode. The external cooling using a water circulated copper jacket as shown in Fig.3.2 was provided on the heat affected zone of AISI 4130 steel side considering the inferior mechanical properties of AISI 4130 steel compared to maraging steel. The experimental setup for the TIG welding and Laser Beam welding machine is shown in Fig. 3.3 and Fig. 3.4 respectively.

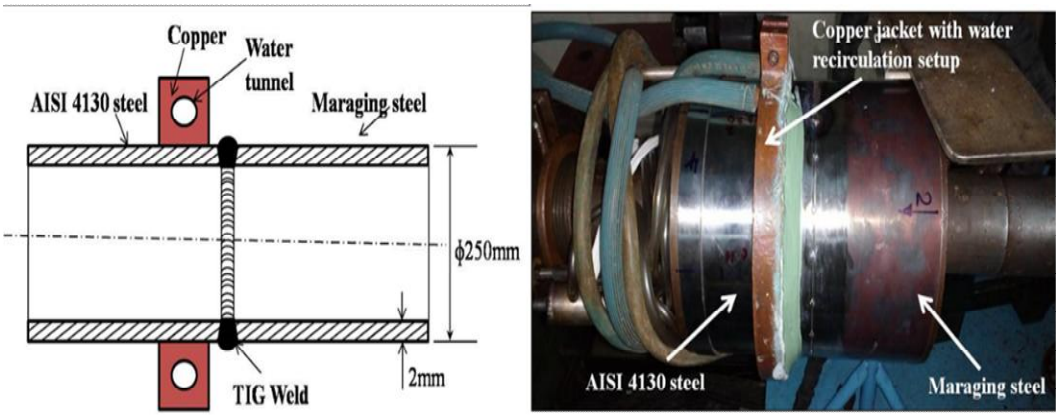

Fig. 3.2 Schematic sketch and actual experimental setup showing the arrangement of weld test rings with the external cooling method.

Fig. 3.3 TIG welding machine.

Fig. 3.4 Laser beam welding machine.

Table.3.5 TIG welding parameters used under different conditions.

Experimental condition		Welding parameters
Without external cooling	Continuous Current	Current =65 Amp, Voltage = 10 V and welding speed = 64 mm/min
	Pulsed Current	Peak Current: I_p= 90 Amps, Back ground current: I_b = 25 Amp, % Pulse on time =50%, Pulse frequency = 4 HZ, voltage = 10 V, welding speed = 64 mm/min
With external cooling	Continuous Current-TIG	Current 65 Amp, Voltage = 10 V and welding speed = 64 mm/min
	Pulsed Current-TIG	Peak Current: I_p= 90 Amps, Back ground current: I_b = 25 Amp, % Pulse on time =50%, Pulse frequency = 4 HZ, voltage = 10 V, welding speed = 64 mm/min
	Laser Beam Welding	Type of laser: Fiber, Laser Beam Power: 3700W, Welding Speed=2000mm/min. Focal Length of welding head=300mm, Dia of optical fiber=100μm.

3.3.3 Temperature profiles in HAZ of AISI 4130 steel

The measurement of temperatures in HAZ of AISI 430 steel was carried out considering the softening behavior of this steel during exposures to welding heat input. The top surface view of welded test ring shown in Fig.3.5 illustrates the positions of the thermocouples bonded next to weld reinforcement using a micro resistance spot welding technique. Five thermocouples are bonded starting from next to fusion line to locations covering various zones in heat affected zone of AISI 4130 steel.

A data logger of GRAPHTECH make (model: GL900) was employed to record temperatures at the rate of 50 readings per second during welding trials. Average of the three temperature measurements are considered in this work.

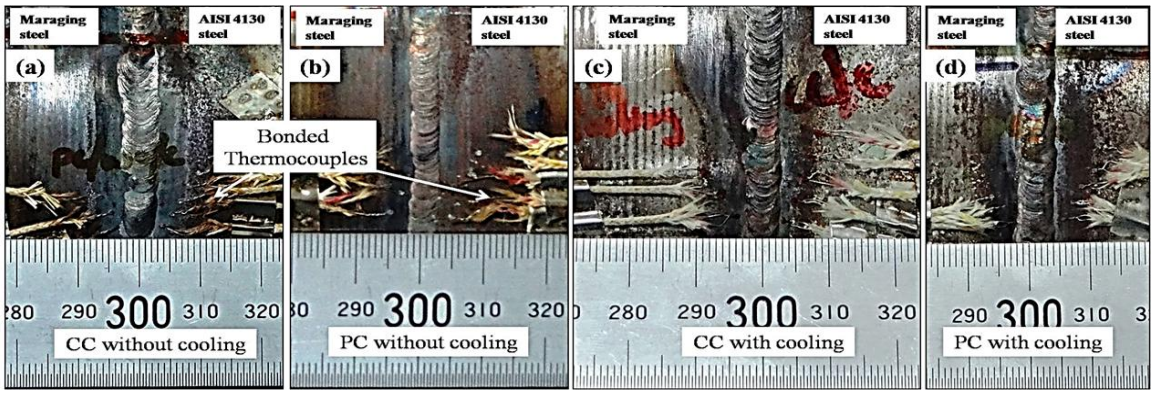

Fig. 3.5 Top surface appearance of weld joints produced (a) continuous current without external cooling (b) pulsed current without external cooling (c) continuous current with external cooling (d) pulsed current without external cooling.

3.4 Characterization of welds

3.4.1 Microstructure

The specimens were suitably sectioned, mounted, mechanically polished according to standard metallographic procedures and are etched selectively with a solution 2% nital (2 ml HNO3 and 98 ml methanol) on AISI 4130 steel side and modified fry's reagent (50 ml HCl, 25 ml HNO3, 1g CuCl2 and 150 ml water) at fusion zone and maraging steel side. The respective etchants were used to etch fusion zone, heat affected zone (HAZ) and base material regions. The microstructures of dissimilar weld joints of various regions were studied by using an optical metallurgical microscope (Make: OLYMPUS) as shown in Fig 3.6.

Fig. 3.6 Inverted optical microscopy.

3.4.2 Non-destructive testing

All the weld joints are subjected to non-destructive examination of X-ray radiography, magnetic particle and dye penetrate test in order to investigate for internal and surface discontinuities respectively.

3.4.3 Destructive testing

3.4.3.1 Tensile test

The transverse tensile specimens are machined from the weld joints (from the zones containing porosities) as per the specimen configuration mentioned in ASTM A370 standard and shown in Fig. 3.7. Tensile testing was carried out on a universal tensile testing machine shown in Fig. 3.8 (make: INSTRON) and evaluated ultimate tensile strength, 0.2% yield strength and % elongation. The fractured surfaces of tensile test samples were observed under scanning electron microscope to understand the mode of failure.

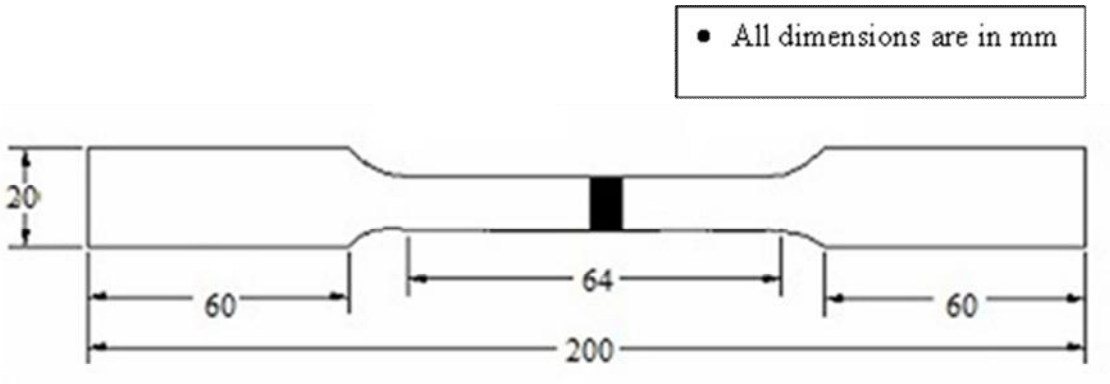

Fig. 3.7 Schematic diagram of the tensile specimen.

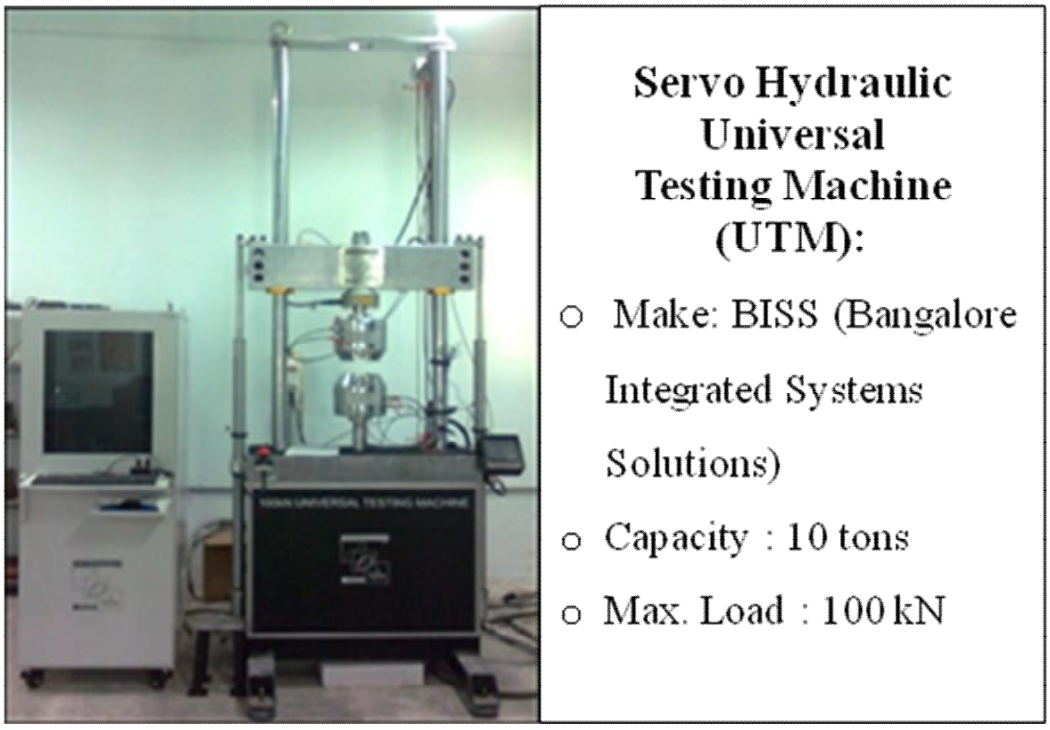

Fig. 3.8 Tensile Testing Machine and Specifications.

3.4.3.2 Microhardness test

Microhardness measurements were carried out across the weld joints at mid thickness with Vickers indenter on a Mitsuzawa make micro hardness tester by applying a load of 300gf

shown in Fig 3.9. A spacing of 0.5mm was maintained between the two microhardness indentations.

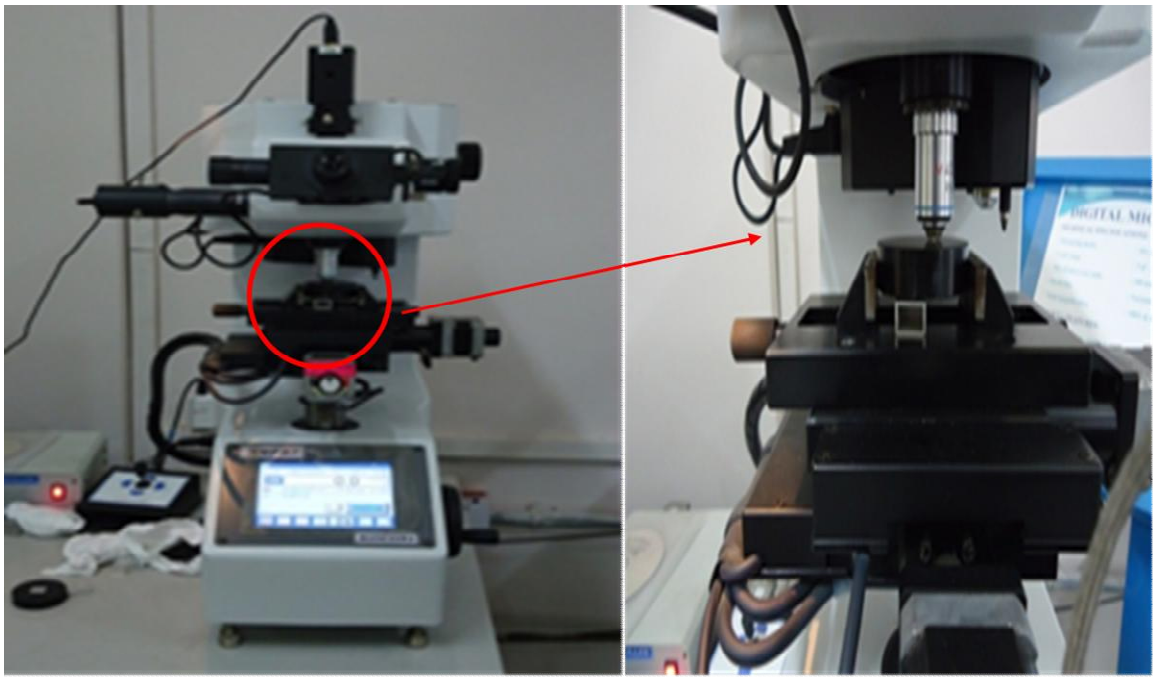

Fig. 3.9 Vickers hardness testing machine (MITSUZAWA).

3.5 Summary:

The experimental procedure followed in the present investigation for characterizing the weldments for understanding the mechanical behavior of the dissimilar combination of maraging steel and AISI 4130 steel. Various external cooling methods are employed for reducing the width of the soft heat affected zone also discussed. The measurement of temperature during welding process using thermocouple and data acquisition system for storing the temperature vs. time is also discussed in this chapter.

CHAPTER - IV

RESULTS AND DISCUSSION

4.1 Introduction

This chapter presents the influence of various welding processes such as continuous TIG, pulsed TIG and laser beam welding of dissimilar welds of Maraging steel and AISI 4130 steel. The experiments have been conducted to investigate the effect of heat input for various welding processes and welding techniques on microstructure, mechanical properties and extend of softening zone. Also, a comparative analysis was made between continuous TIG, pulsed TIG with and without cooling and laser welding without cooling on microstructure, mechanical properties and extend of softening zone.

4.2 Continuous TIG welding of Maraging steel to high strength low alloy steel (AISI 4130) without and with external cooling

4.2.1 Quality of weld joints

The appearance of the top surface and X-ray radiograph of continuous current GTA weld joint condition is shown in Fig.4.1 (a & b). The ripples of weld bead are found to be uniform and the zone adjacent to weld joints is noticed to be darkened due to the exposure of the welding heat input in Fig 4.1(a). The extent of darkening indicates directly with the width of heat affected zone. All the weld joints are found to be defect free as it is noticed from the radiographs.

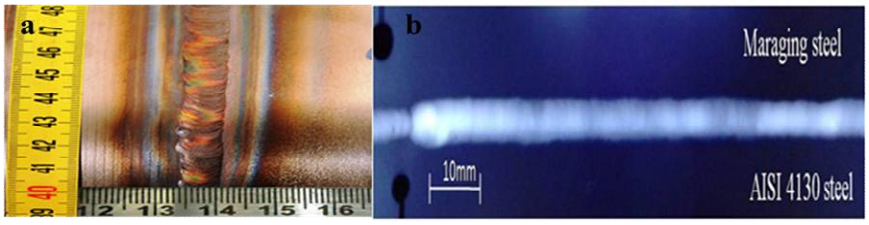

Fig. 4.1(a) Macrograph (top surface) and (b) X-radiograph of continuous current GTAW of the Dissimilar weld of Maraging steel and AISI 4130 steel.

4.2.2 Temperature profiles

The failure of the dissimilar weld is occurred in heat affected zone (HAZ) of AISI 4130 steel side as shown in Fig. 4.2 due to lower hardness experienced in this region. Hence the focus is on towards AISI 4130 steel side for measuring peak temperature in HAZ at different locations i.e. coarse grain heat affected zone (CGHAZ) and inter critical heat affected zone (ICHAZ).

Fig. 4.2 Macrographs of fractured tensile test specimens of dissimilar welds of continuous TIG weld of Maraging steel and AISI 4130 steel.

The peak temperatures measured during welding time at the locations adjacent to the weld joint such as coarse grain heat affected zone (CGHAZ) and inter critical heat affected zone (ICHAZ) of AISI 4130 steel are presented in Table 4.1. The temperature versus time plots corresponding to CGHAZ and ICHAZ are shown in Fig 4.3 and Fig 4.4 respectively. The slope of the temperature profile during heating is found to be higher than that of cooling because of the fact that the sudden heating is experienced from the welding arc heat input. The slope of the plot is less while cooling because it takes more time for the welding heat to dissipate into the base material which generally acts as a heat sink in welding. The CGHAZ has experienced maximum temperature up to 1200^0C, just below the austenite finish temperature. The peak temperature in ICHAZ was noticed to be just below the Ac1 temperature.

Table 4.1 Peak temperatures measured in CG HAZ and IC HAZ's of AISI 4130 steel.

Welding condition		**CGHAZ**	**ICHAZ**
without external cooling	Continuous Current	1200^0C	650^0C
with external cooling	Continuous Current	900^0C	500^0C

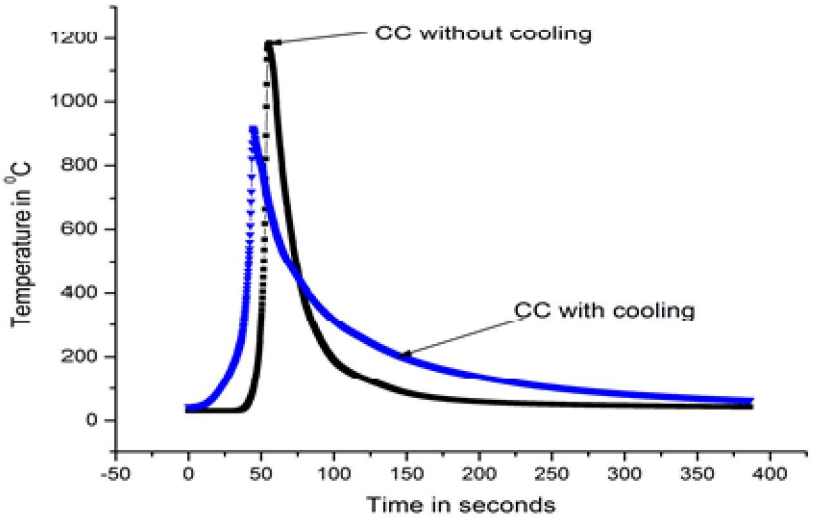

Fig. 4.3 Continuous current (CC) Temperature profiles in CGHAZ of AISI 4130 steel with and without external cooling.

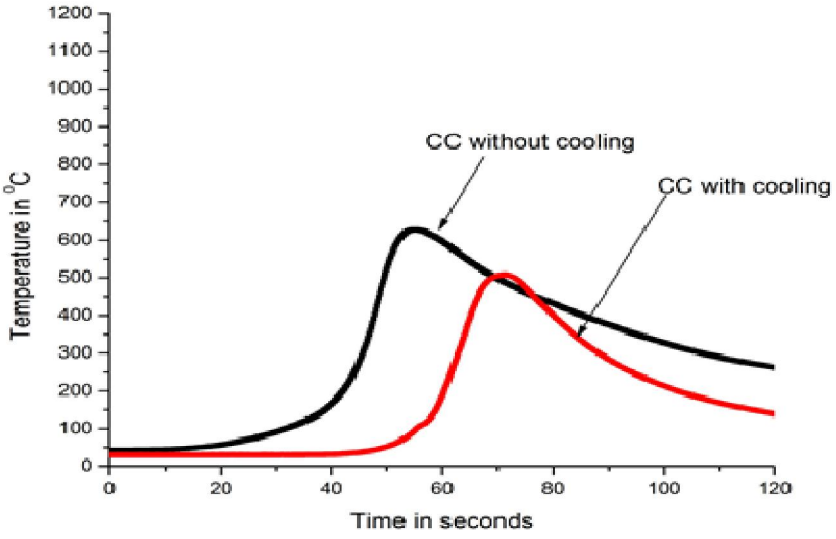

Fig. 4.4 Continuous current (CC) Temperature profiles in ICHAZ of AISI 4130 steel with and without external cooling

4.2.3 Microstructure

The microstructure of the base materials i.e. maraging steel in solutionized condition and AISI 4130 steel in hardened and tempered condition are shown in Fig.4.5. The microstructure of

maraging steel exhibits very fine lath martensite (Fig.4.5 (a)) features elongated along flow forming lines. The AISI 4130 steel contain fine tempered martensite (Fig.4.5 (b)) which could be due to the low temperature (260^0C) in the tempering process. Microstructure details of dissimilar metal weldments of various regions of continuous current GTA weld (without external cooling) are shown in Fig.4.6. The dissimilar weld may be divided into four zones namely, fusion zone, heat affected zone (HAZ) of maraging steel, heat affected zone of AISI 4130 steel and unaffected base material zones of respective materials.

Heat affected zone of maraging steel consists of three regions. Adjoining the weld represents coarse grain martensitic phase (Region-c). During welding, the base material (maraging steel) adjacent to the weld interface is heated to high temperatures in the austenitic phase where considerable grain growth occurs. On cooling, the metal transforms to martensite and inherits the coarse austenitic grain size. Region-b consists of martensite that has been heated due to weld thermal cycle to the austenitic region but not high enough to cause grain growth. Region-a is a dark etching region where martensite phase experiences peak temperatures in the range of 590^0 C to 730^0 C. This dark etching region exhibits two phase microstructures (reverted austenite surrounded by Fe-Ni martensite). The microstructure of weld exhibits a cellular / dendritic structure (Fig. 4.6 (d)).

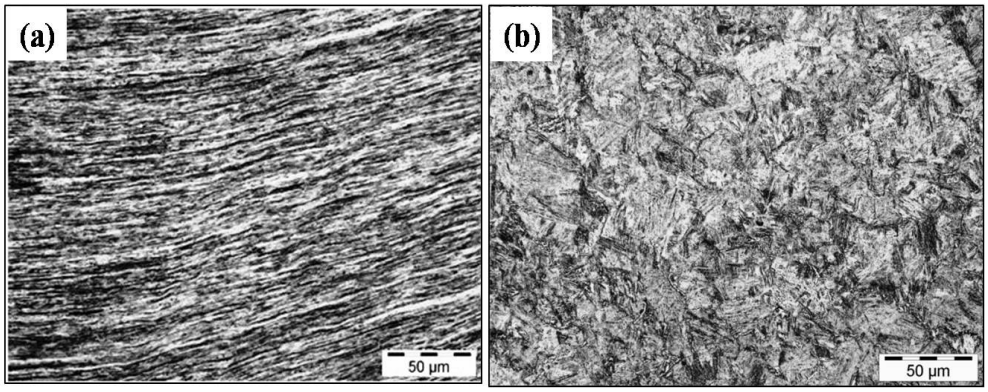

Fig.4.5 Microstructures of base materials (a) Maraging steel (solutionized) (b) AISI 4130 steel (hardened and tempered).

Various regions of heat affected zone of high strength low alloy steel (AISI 4130) of the dissimilar metal weld (continuous current without external cooling) are shown in Fig 4.7. Broadly the heat affected zone of AISI 4130 steel can be divided into three zones, coarse

grained(CG) HAZ, fine grained (FG) HAZ and inter critical(IC) HAZ depending upon the peak temperature that each zone experiences during exposure to weld thermal cycle. The CGHAZ (shown in Fig 4.7(a)) exists very next to the fusion interface and the temperature in this zone reaches peak temperatures of austenitic transformation region and the grain growth occurs. Upon sudden cooling effects caused during weld cooling phase, the zone exhibits coarse martensite inheriting the prior austenite grain size. The FGHAZ (shown in Fig 4.7(b)) experiences the temperatures close to the A_{C3} point and the finer austenite grains are formed during the heating cycle. These finer prior austenite grain size leads to the formation of the fine grained heat affected zone upon cooling. Regions away from the fusion zone on AISI 4130 side experiences lower peak temperatures and probably these regions are heated to within the inter critical zone (temperature between A_{C1} and A_{C3}). The microstructure can be a mixture of ferrite and high carbon austenite which transforms to martensite on cooling (Fig.4.7(c)).

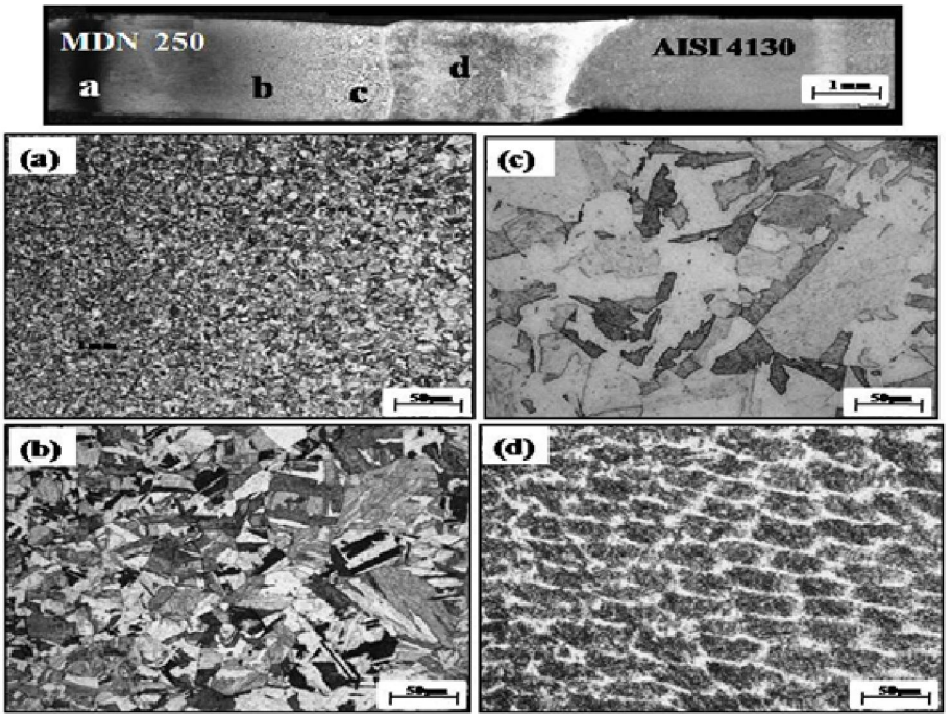

Fig.4.6 The microstructures of various zones of the heat affected zone on maraging steel side of weld produced with continuous current without external cooling (a) Dark band region (b) Fine grained HAZ (c) Coarse grained HAZ (d) Fusion zone.

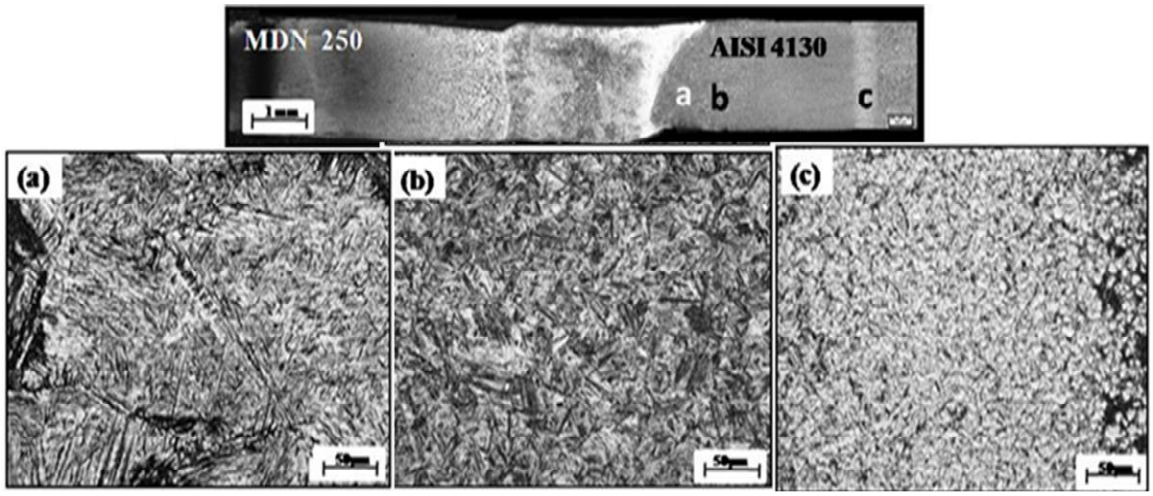

Fig.4.7 The microstructures of various zones of the heat affected zone on AISI 4130 steel side of weld produced with continuous current without external cooling (a) coarse grained HAZ (b) fine grained HAZ (c) inter critical HAZ.

A high magnification microstructures of ICHAZ regions with and without external cooling are shown in Fig.4.8.

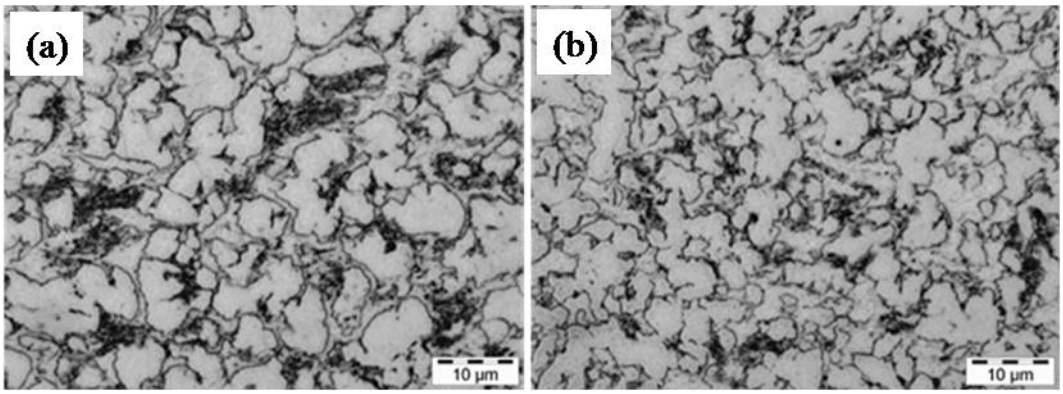

Fig. 4.8 Microstructures of ICHAZ of welds produced with continuous current GTAW (a) without external cooling (b) with cooling.

It is clearly evident from these microstructures that, by coarser ferrite surrounded coarser martensite is observed in the case of welds produced by the continuous current with and without external cooling. More martensite is observed in without cooling compared to with cooling. It could be mainly because of higher peak temperatures (~650^{0}C) experienced by the region ICHAZ in the case of continuous current welds made without external cooling. The

macrostructures depicting varied widths of ICHAZ in weld joints made with and without external cooling conditions are shown in Fig 4.9. The width of ICHAZ of welds made with and without external cooling is measured from the macrostructure and presented in Table 4.2. Weld joints made with continuous current without external cooling were noticed to have higher peak temperature and the HAZ of AISI 4130 steel is found to stay at relatively higher temperatures for a longer time while cooling which might have contributed to increasing the width of ICHAZ.

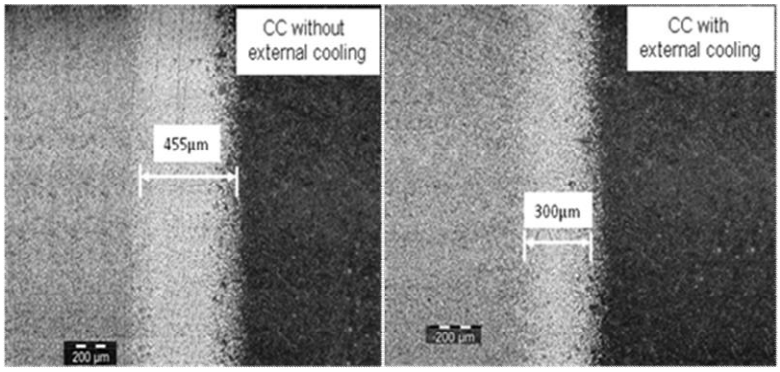

Fig. 4.9 Macrostructures depicting varied widths of ICHAZ in AISI 4130 steel welds produced with continuous current welds made with and without external cooling.

Table 4.2 Width of the ICHAZ in AISI 4130 steel.

Welding condition		**Width of ICHAZ (µm)ICHAZ**
without external cooling	Continuous Current	455
with external cooling	Continuous Current	300

4.2.4 Microhardness

A typical microhardness survey across the weldment of the continuous current dissimilar metal weld without external cooling is shown in Fig.4.10. The hardness in the fusion zone is observed to have an increasing trend from maraging steel to high strength low alloy steel side. It is observed that the hardness of the weld is low compared to that of parent metals. The low hardness of the fusion zone can be attributed to the presence of low carbon soft BCC martensite and the material being in the as-cast condition which is similar to the solutionized condition of maraging steel. Increase in hardness within the fusion zone towards high strength low alloy steel side could be due to dilution fusion zone with low alloy steel.

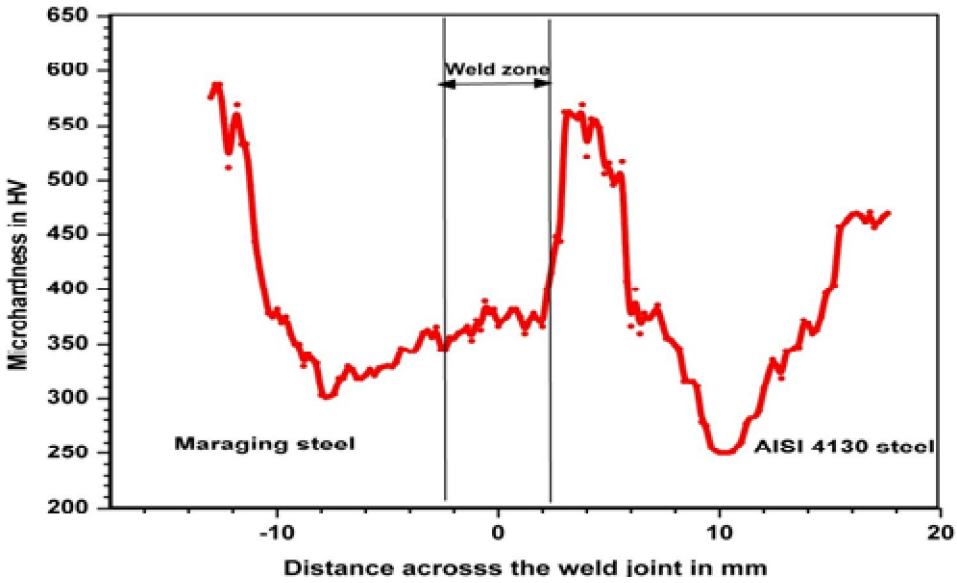

Fig. 4.10 A typical microhardness distribution across the dissimilar weld of maraging steel and AISI 4130 steel produced by continuous current without external cooling.

The reason for low hardness in the heat affected zone of maraging steel close to fusion boundary compared to that of unaffected parent metal (maraging steel) can be explained as follows: though the parent metal is in solution heat treated and aged condition, the region adjacent to the fusion zone during weld thermal cycle, is subjected to temperatures higher than the solutionizing temperature of maraging steel resulting in dissolution strengthening precipitates. This makes the hardness of the heat affected zone close to the fusion boundary lower than that of age hardened maraging steel. A dip in the magnitude of the hardness is observed in the far heat affected zones of maraging steel. This is known as the dark band or dark etched region and this is due to the martensitic phase experiencing a temperature of 590^0C to 730^0C resulting in the formation of reverted austenite in the martensitic phase. The presence of this dual phase structure resulted in lowest hardness in the HAZ of maraging steel. The hardness along the HAZ of AISI 4130 steel side adjacent to the weld interface has shown high hardness. This can be explained as follows: the region of the HAZ near to the fusion zone experiences a high peak temperature exceeding AC_3 line and also subjected to fast cooling rates similar to quenching and tempering treatment for the steel.

Influence of with and without external cooling on microhardness distribution of dissimilar welds of Maraging steel and AISI 4130 steel is shown in Fig.4.11.The softening

tendencies in heat affected zone of AISI 4130 steel due to the exposure of welding heat are presented in Fig 4.12. Location and width of soft zone, hardness in HAZ of AISI 4130 steel of dissimilar welds are shown in Table 4.3. The soft zone in HAZ of AISI 4130 steel can be characterized with respect to the width of the soft zone (considering any hardness less than 350Hv corresponds to soft zone) and distance of minimum hardness from the fusion line of weld towards AISI 4130 steel side. The weld joints produced with continuous current without external cooling have a maximum width of the soft zone and a maximum distance of soft zone from fusion line.

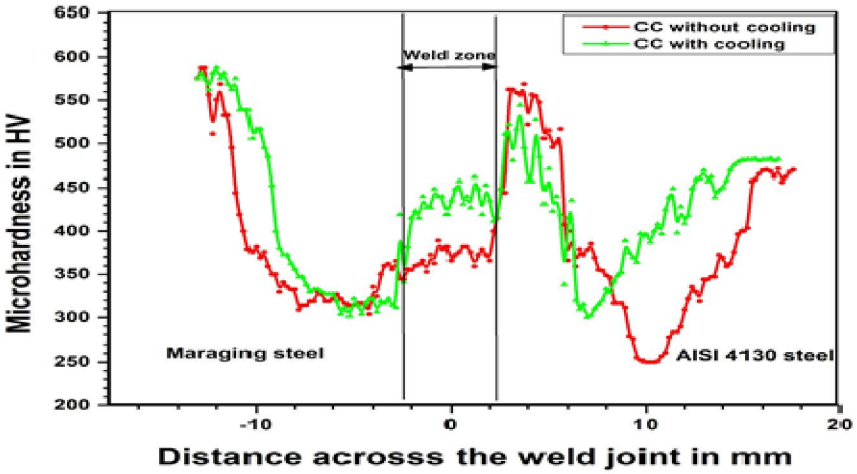

Fig. 4.11 A typical microhardness distribution across the dissimilar weld of maraging steel and AISI 4130 steel produced by the continuous current with and without external cooling.

The microstructure of this part of HAZ was characterized predominantly as martensite. Regions away from the fusion zone experienced lower peak temperatures which are close to AC1 and probably these regions are heated to within the inter-critical zones, exhibiting lower hardness due to the presence of high-temperature transformation products in addition to martensite. This soft region is similar to this reported in quench and tempered steels [59, 81]

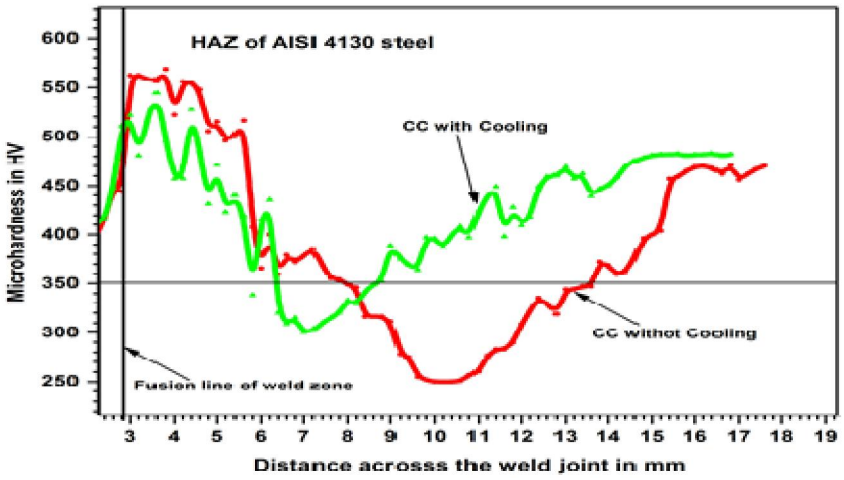

Fig. 4.12 Comparison of microhardness distribution across the softened heat affected zone of AISI 4130 steel in weld joints produced by the continuous current with and without external cooling.

Table.4.3 Location and width of soft zone in HAZ of AISI 4130 steel of different dissimilar weld joints

Welding condition		**Distance of soft zone from the fusion line (mm)**	**Width of soft zone (mm)**	**Min. hardness in HAZ (Hv)**	**Max. hardness in HAZ (Hv)**
Without external cooling	Continuous Current	7.0	5.8	259	556
With external cooling	Continuous Current	4.4	2.4	300	537

4.2.5 Degree of HAZ softening

In order to understand and explain the trend observed in the softening of HAZ in AISI 4130 steel during different welding (heat input) conditions, full martensite hardness(Hm), nil

martensite hardness (Hb), have been calculated using empirical expressions [82] and are presented below.

$$Hm = 884C\ (1\text{-}0.3\ C^2) + 294$$

$$Hb = 145 + 130 \tanh (2.65\ CEII - 0.69)$$

Where, Hm = Maximum Vickers hardness for the full martensite

Hb = Minimum Vickers hardness for the nil martensite

$$CEII = C + \frac{Si}{4} + \frac{Mn}{5} + \frac{Cu}{10} + \frac{Ni}{18} + \frac{Cr}{5} + \frac{Mo}{2.5} + \frac{V}{5} + \frac{Nb}{3}$$

The degree of softening has been estimated based on the difference between the maximum hardness of full martensite and a minimum hardness of nil martensitic structure [17]. The difference between Hm and Hb is considered to be equivalent to 100% softening in HAZ of AISI 4130 steel. The experimental difference between the maximum and minimum hardness derived from the microhardness distribution (Fig.4.12) corresponding to various welding conditions and the same is compared to the hardness difference of 100% softening to estimate the approximate degree of softening in respective welding conditions. The calculated degree of softening in HAZ of AISI 4130 steel in different welding conditions is presented in Table 4.4. The maximum softening has been observed in the case of weld joint produced with continuous current without external cooling compared to that of external cooling.

Degree of softening = (ΔHexpt /ΔHth) *100

Table.4.4 Degree of softening in HAZ of AISI 4130 steel of different dissimilar weld joints.

Hm	**Hb**	**ΔHth = Hm-Hb (Hv)**	**ΔHexpt = Hmax-Hmin (Hv)**		**Degree of softening (%) in HAZ**	
			Without external cooling	***With external cooling***	***Without external cooling***	***With external cooling***
			CC	CC	CC	CC
572	261	311	297	237	95.49	76.21

4.2.6 Tensile properties

The tensile properties of welded joint made with different welding conditions are mentioned in Table 4.5. The comparison of tensile stress versus strain plots of different dissimilar weld joints is given in Fig 4.13. The macrographs of fractured transverse tensile specimens of all dissimilar welds are shown in Fig.4.14 and observed that fracture location is in the inter critical heat affected zone (ICHAZ) of AISI 4130 steel. The fracture location is correlated to the minimum hardness zone on the microhardness profile of weld joint.

Table.4.5 Tensile properties of weld joint made with different welding conditions.

Welding condition		**0.2% YS in (MPa)**	**UTS in (MPa)**	**(%) Elongation**	**Weld joint efficiency based on 0.2%YS**	**Failure location from the fusion zone (mm)**
Without external cooling	Continuous Current	826	960	3.8	67.98	6.8
With external cooling		1014	1041	2.7	83.45	4.9

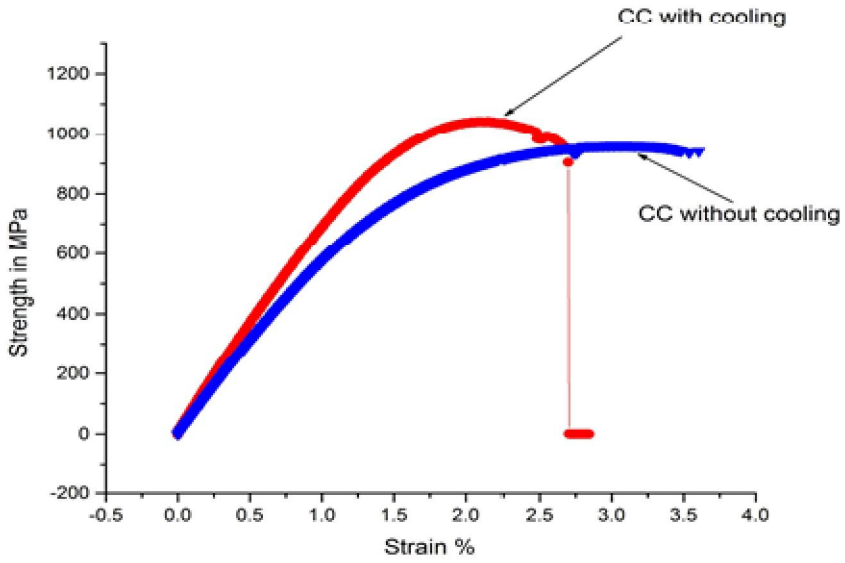

Fig 4.13 Comparison of strength versus strain plots of specimens pertaining to dissimilar welds of maraging steel AISI 4130 steel produced by the continuous current with and without external cooling.

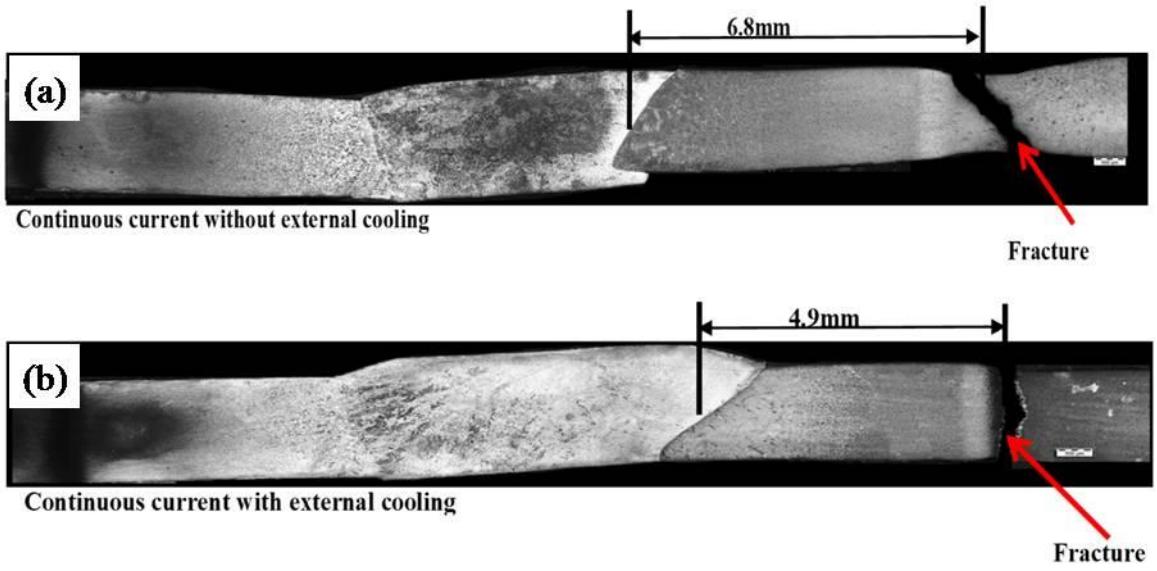

Fig 4.14 Macrographs of fractured tensile test specimens of dissimilar welds of (a) continuous current with and (b) without external cooling.

4.2.7 Fractography

Scanning electron micrographs of fracture surfaces of tensile test specimens of dissimilar metal welds produced with different welding conditions are shown in Fig 4.15 It is observed that the fracture surfaces of tensile specimens corresponding to joints made with continuous current without external cooling have revealed shallow dimpled features while those of continuous and pulsed current with external cooling has shown deep and finer dimples.

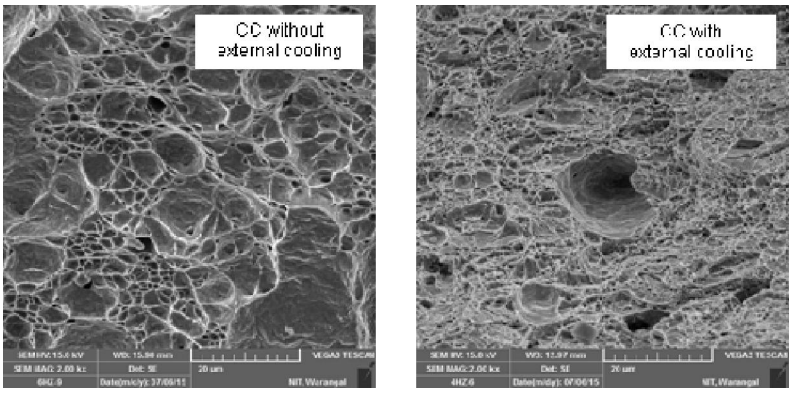

Fig 4.15 Scanning electron micrographs of fracture surfaces of tensile test specimens of dissimilar welds of continuous current with and without external cooling.

4.3 Pulsed TIG welding of Dissimilar Metals (Maraging steel to high strength low alloy steel {AISI 4130})

4.3.1 Effect of pulse frequency in Pulsed TIG welding of Maraging steel to high strength low alloy steel (AISI 4130)

4.3.1.1 Quality of weld joints

The appearance of the top surface of X-ray radiography of pulsed current GTAW weld joint condition is shown in Fig. 4.16(a) and corresponding macrograph is shown in Fig. 4.16(b). The ripples of the weld bead are found to be uniform and the zone adjacent to the weld joint is noticed to be less darkened due to the exposure of the welding heat input is low compared to continuous current welding. The width of the weld bead and reinforcement is observed to be less compared to continuous welds.

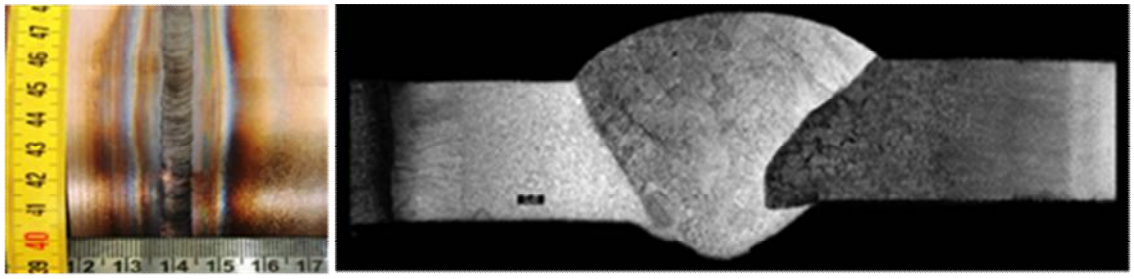

a b

Fig.4.16 (a)Macrograph (Top surface) (b) Macrograph of a cross section of Pulsed current GTAW of the Dissimilar weld of Maraging steel and AISI 4130 steel.

4.3.1.2 Macrostructure

Macrographs of dissimilar material pulsed GTA welds at different pulse frequencies and continuous weld are shown in Fig. 4.17. It is observed that, as the frequency increases, the width of ICHAZ and weld fusion line to the width of ICHAZ end line is also increasing due to increase in heat input.

The dark band region in MDN 250 steel is also observed at different pulse frequencies and is presented in Fig. 4.18. It is revealed that as the pulse frequency increases, dark band width also increases. The dark band appears because at that area the temperature is exposed to nearly 600-800^0 C. There will be two phases present in this region which are ferrite and austenitic phases. In these phases, austenite is more stable even at room temperature. This phase is softer as compared to the base material of MDN-250. So the hardness decreases rapidly. As the frequency increases the heat input increases because of which temperature increases. So the austenite formation is more and the width of the dark band increases. It appears so dark because during etching when we use vilella's reagent the austenite zone reacts first and etches more. So it appears dark black in color.[reference is to be added].

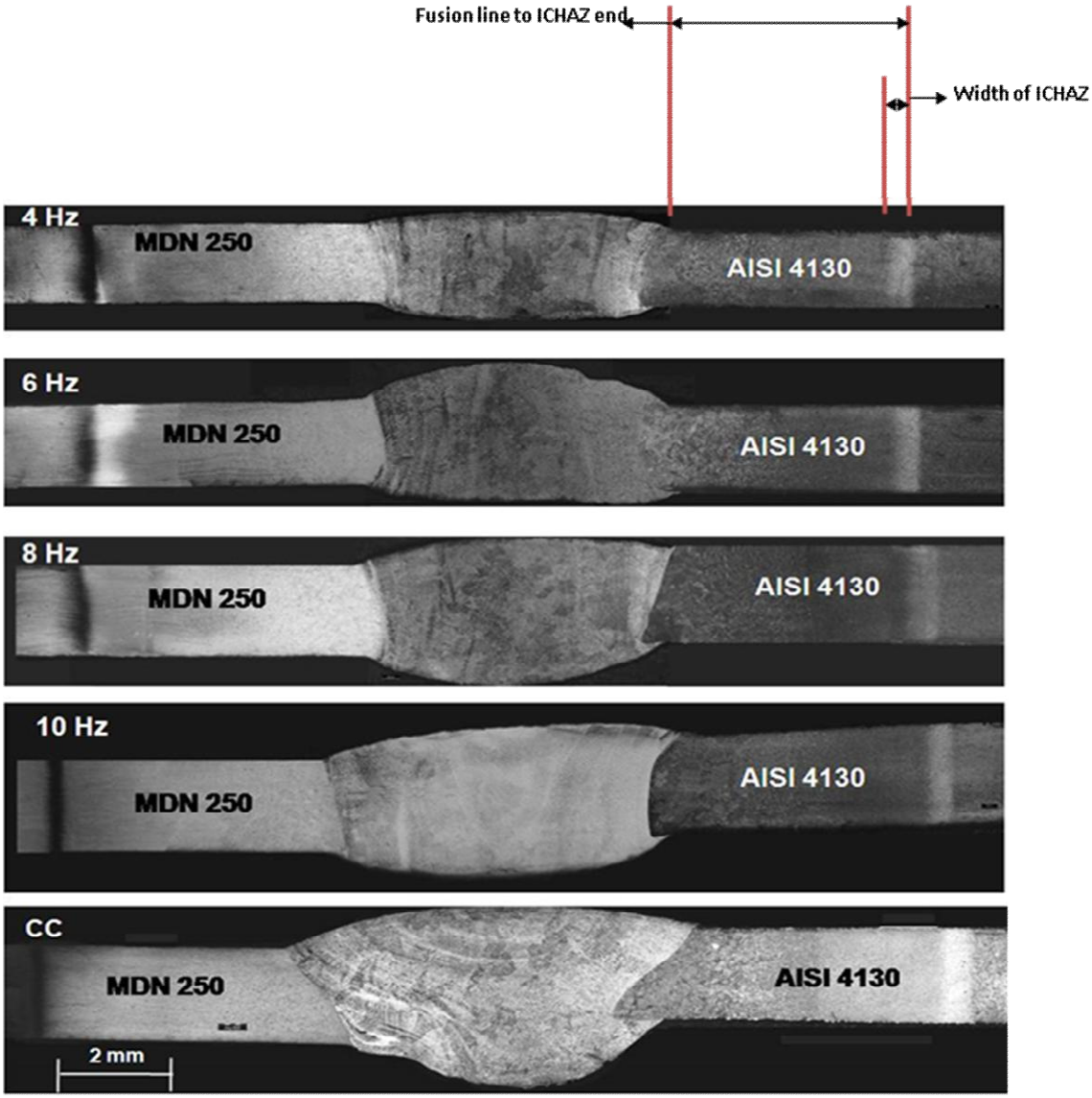

Fig. 4. 17 Macrostructure of pulsed TIG and Continuous current (CC) dissimilar weld of Maraging steel and AISI 4130 Steel.

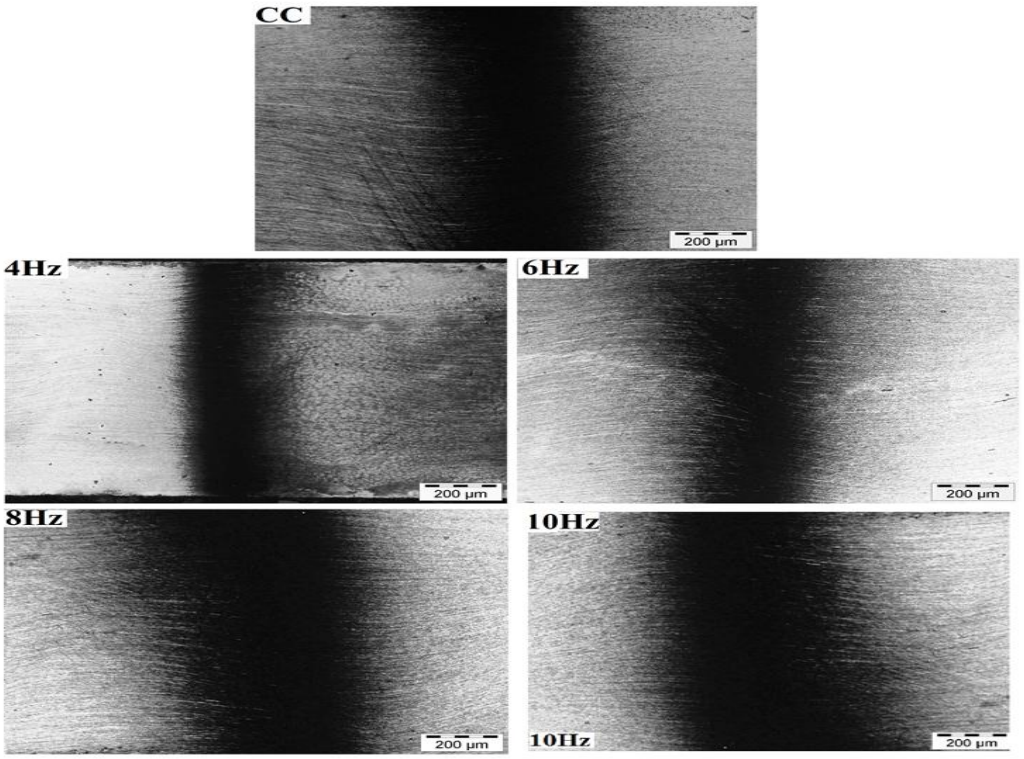

Fig. 4.18 Effect of pulse frequency in pulsed TIG on the dark band width in MDN 250 side.

4.3.1.3 Microstructure

Fine grain HAZ in Maraging steel is observed at different frequencies and are presented in Fig. 4.19. It is observed that, as the frequency increases from 4Hz to 10Hz, the HAZ region is more coarsen due to a large amount of heat input during the welding process.

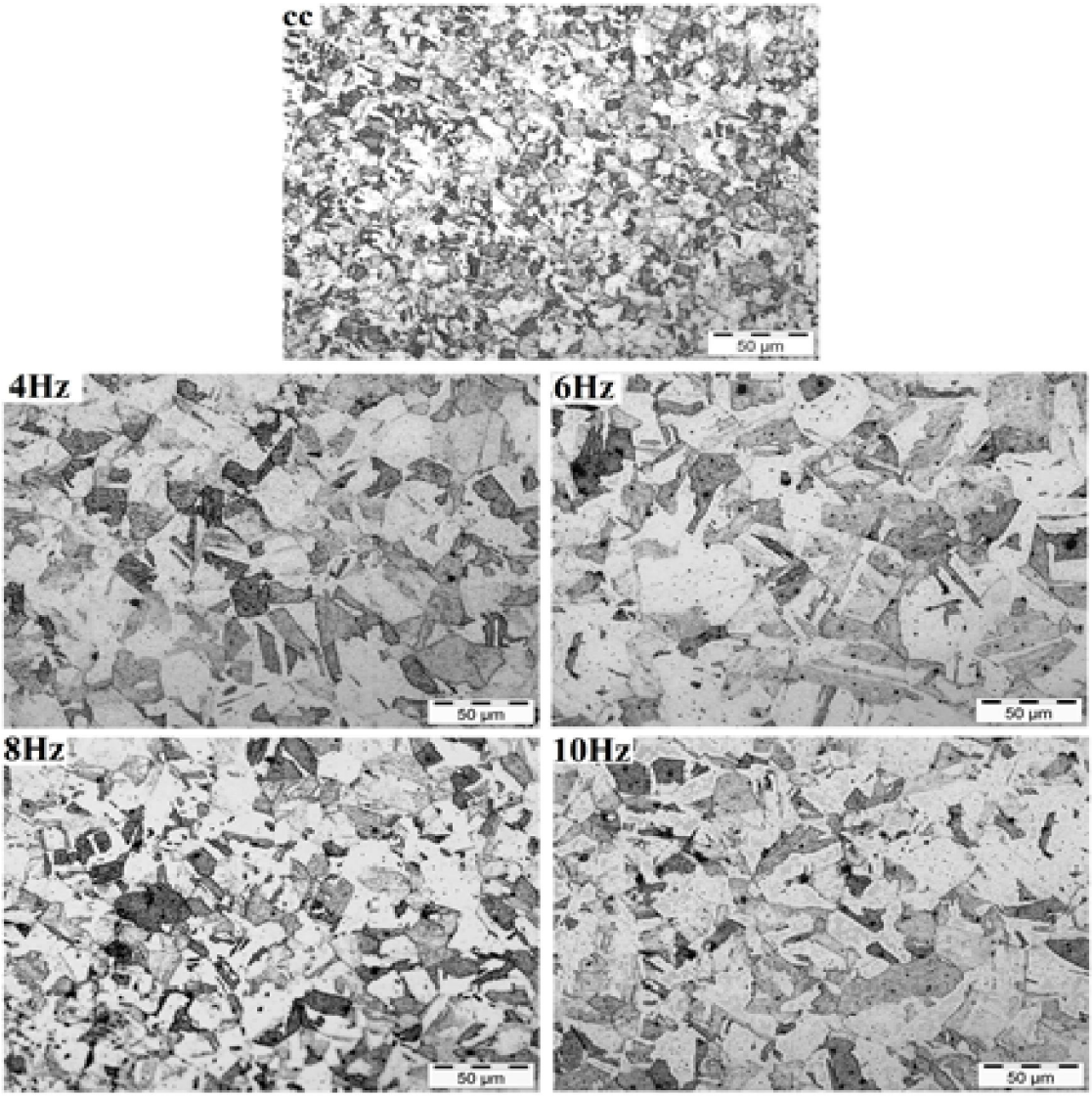

Fig. 4.19 Fine grain HAZ of the MDN250 side for various frequencies.

Weld microstructures of dissimilar welds at different frequencies and continuous welds is shown in Fig.4.20. Within weld bead, the grains consist of pools austenitic grain boundaries, the presence of austenite grain boundaries which softens the weld zone and its hardness also decreases. It is found that as the frequency increases the austenite at the grain boundaries is also increasing. The presence of Mo & Ti in the base material will prone to the formation of austenite in the material during welding. So if the same composition as base material consists of the filler wire, there is an increase in the percentage of austenite in the weld zone also. To reduce the austenite at the grain boundaries, a filler wire with the lower composition of Mo and Ti can be

used. As the frequency increases, the grain size is also increasing in the weld zone due to more heat absorption. In continuous (CC) weld, more austenite is formed at the grain boundaries compared to pulsed TIG weld at a lower frequency (i.e. 4HZ).

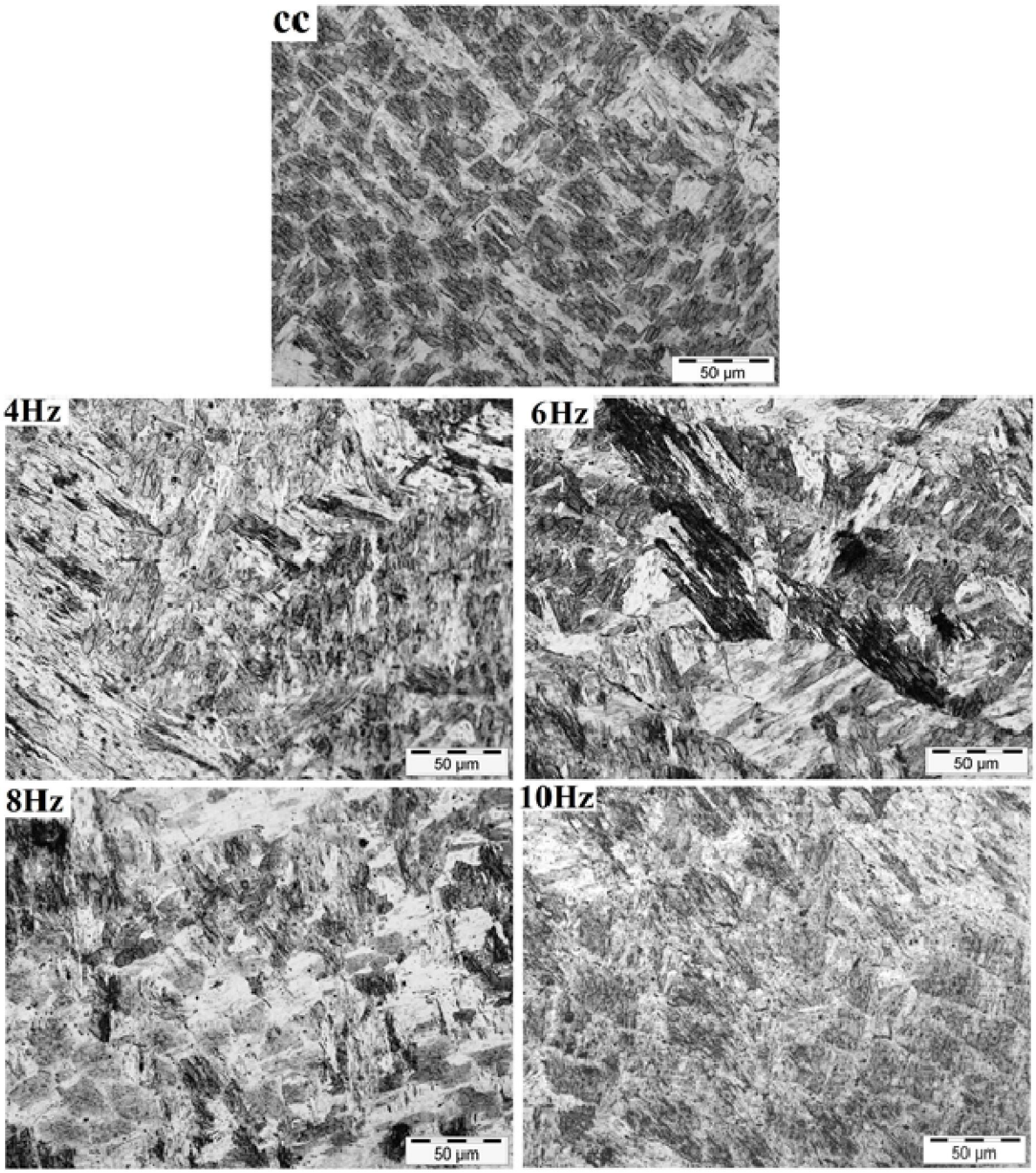

Fig. 4.20 Weld Zone for all frequencies at 500x magnification.

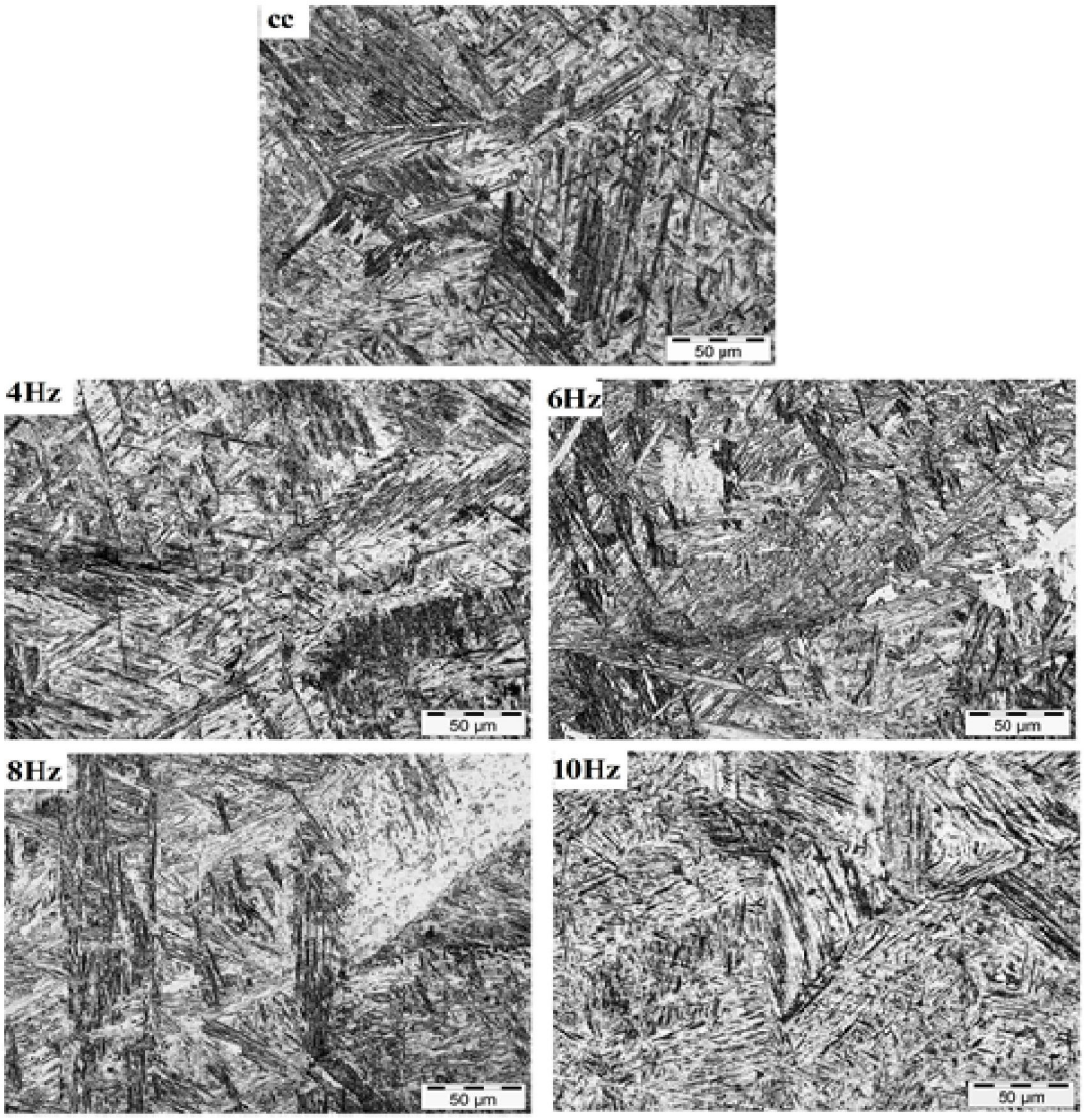

Fig. 4.21 Coarse HAZ of AISI 4130 for various frequencies.

Coarse HAZ and fine HAZ in AISI 4130 steel adjacent to the coarse HAZ at different frequencies are shown in Fig. 4.21 and 4.22. There the fine lathy martensite structure forms and therefore the hardness is moderate. This is very harder phase than the base metal. It can also observe that the lathe size is increasing as the frequency increases. The temperature just exceeds A3 line full austenite transformation, on cooling all grains will be normalized. The macrostructure and microstructure of ICHAZ in AISI 4130 steel at different frequencies are shown in Fig. 4.23 and 4.24 respectively. It is observed that as the frequency increases, increase in width of ICHAZ due to increase in heat input.

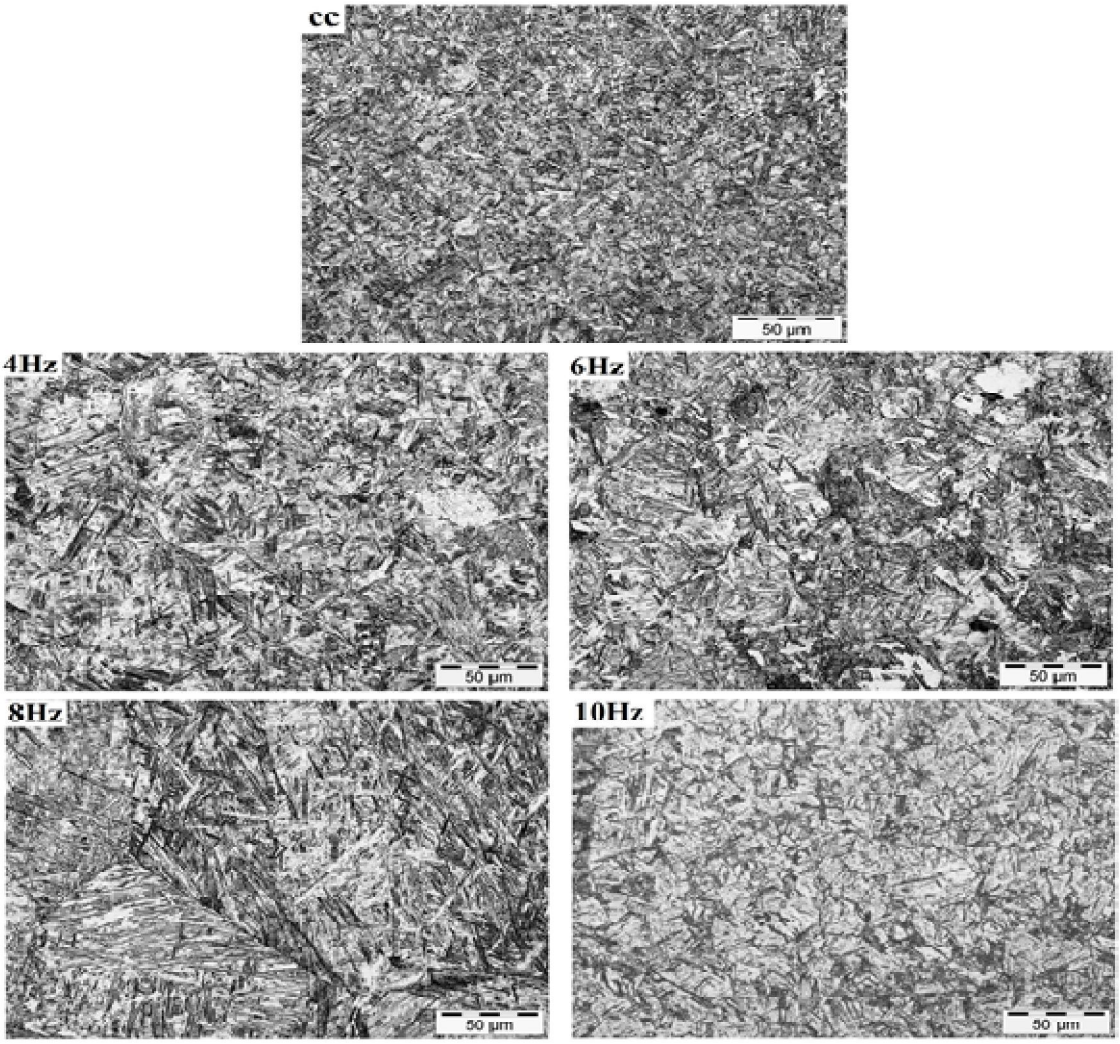

Fig.4.22 Fine HAZ of AISI 4130 for various frequencies.

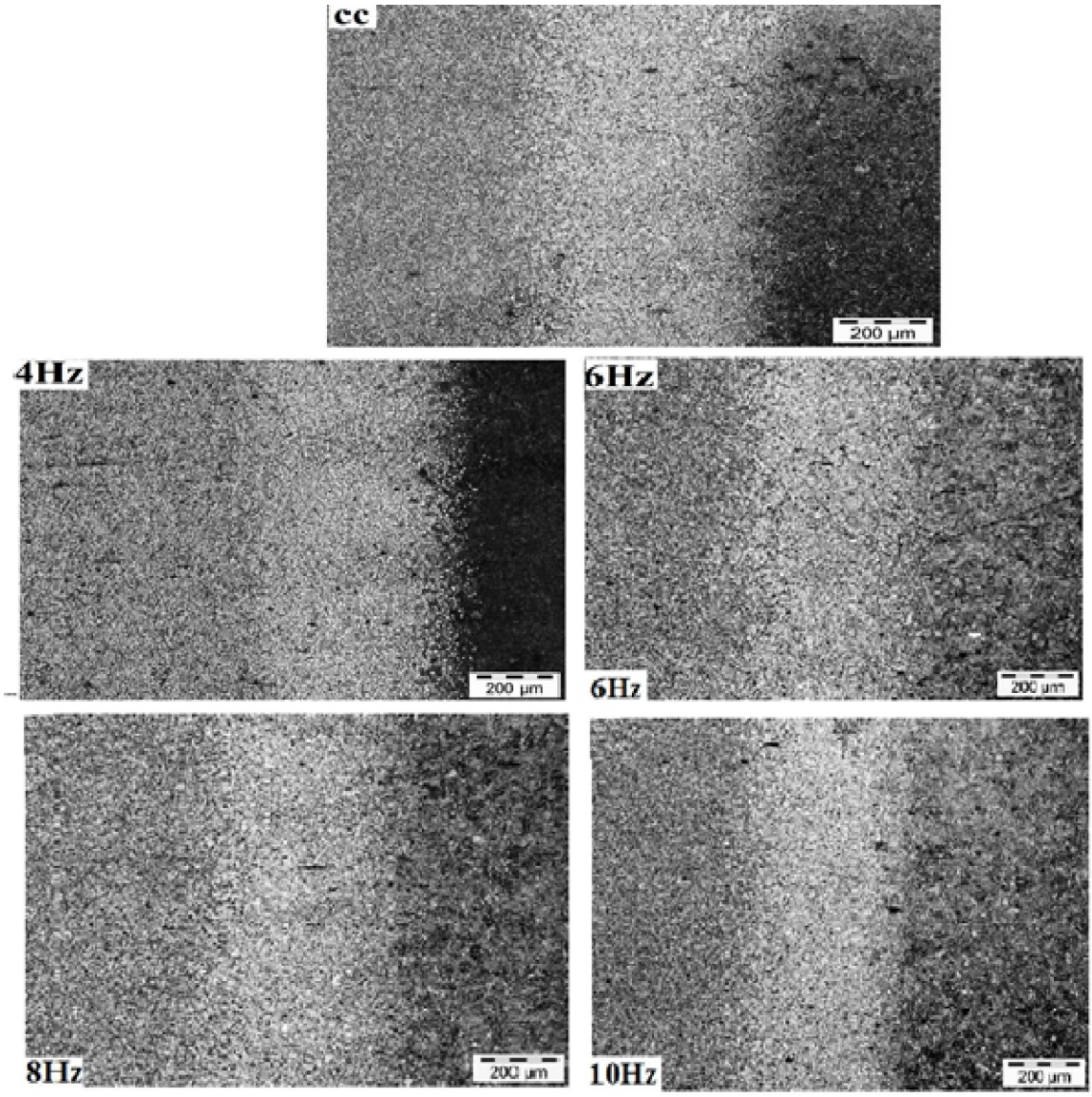

Fig. 4.23 White bands of AISI 4130 for all frequencies.

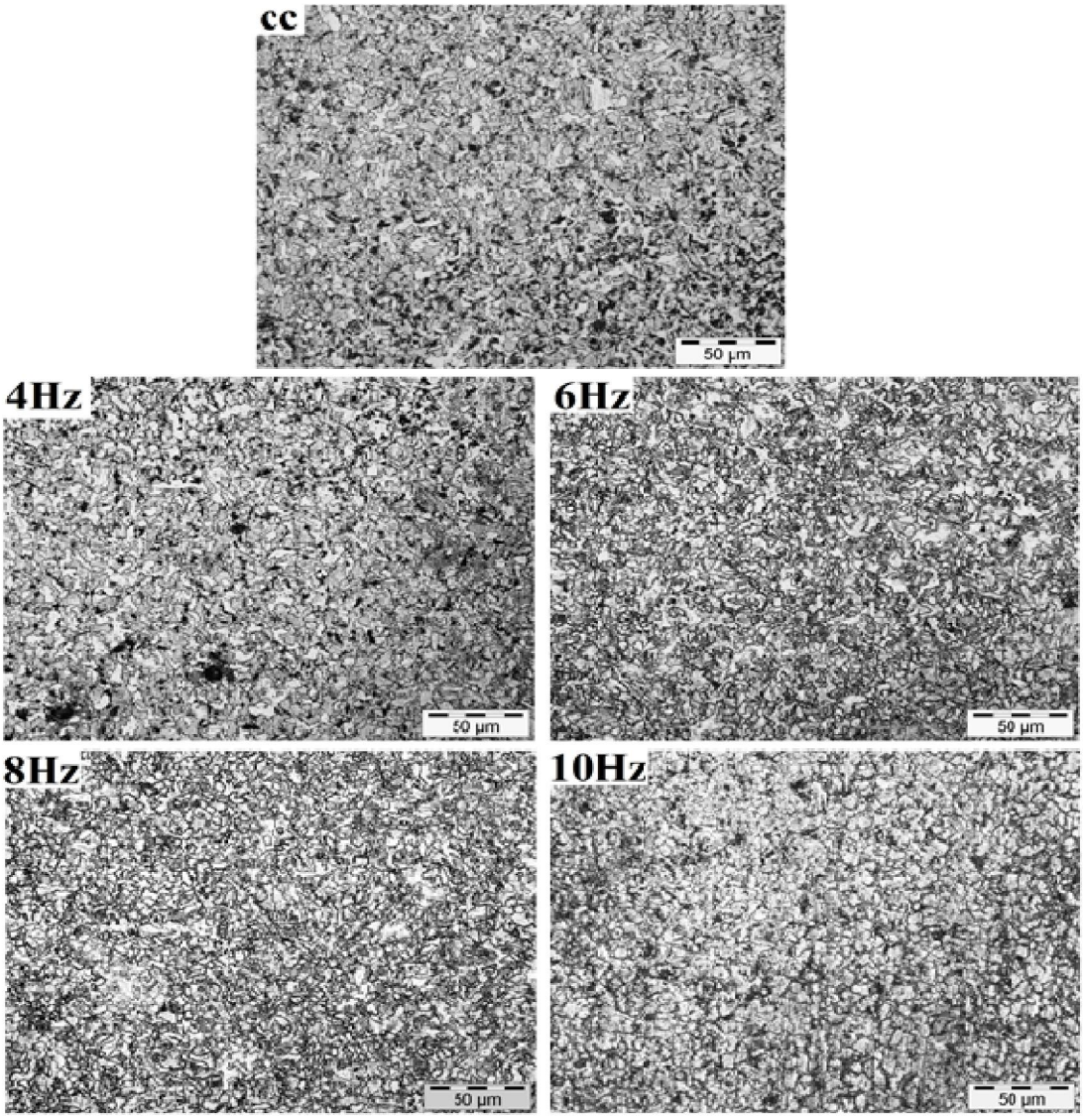

Fig. 4.24 White bands of AISI 4130 for all frequencies at 500x magnification.

The White band is the zone where the ferrite phase becomes stable. The zone where the white zone appears is adjacent to the fine HAZ in AISI 4130 as shown in Fig. 4.24.

From Fig. 4.24, it can be observed that the white band width increases as the frequency increases. This is due to the increase in heat causes ferrite to be stable. This is a soft phase where the hardness is low.

4.3.1.4 Microhardness

The microhardness distribution across the dissimilar metal weld of age hardened MDN 250 steel and quenched and tempered AISI 4130 steel with different pulse frequency is shown in Fig.4.25. The microhardness values on the HAZ of AISI 4340 side has tremendously increased and in the MDN 250 steel side, it has declined when compared to the values of its own parent metals. The parent metal MDN 250 steel adjacent to the weld experienced softening as a result of exposure to a temperature higher than the solution treatment temperature for MDN 250 steel. The microhardness gradient is opined to be due to composition gradient in the weld region, in that the weld on MDN 250 steel side would have lower carbon than that in the quenched and tempered steel. Due to carbon dilution, the quenched and tempered steel adjacent to the weld could not be hardened equal to that of the parent metal, in other words, the hardenability of the weld region on the quenched and tempered steel side is lower than the corresponding parent metal. The lowest hardness was found at 4 HZ frequency and highest value is observed at 10 HZ frequency.

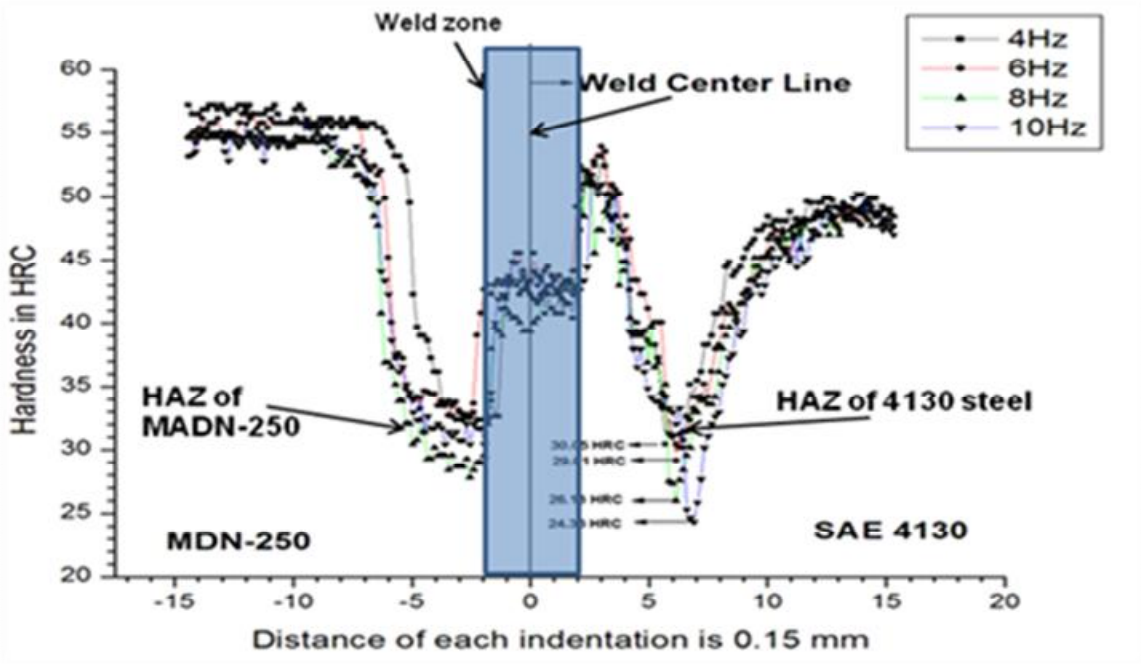

Fig. 4.25 Microhardness survey of dissimilar welded sample at 4 HZ,6 HZ, 8 HZ and 10 HZ.

From Fig.4.25, it can be observed that at all frequencies white band has the lower hardness value. At each frequency, the base metal acquired a hardness of 550-600 HV. In MDN 250 side HAZ zone is has a lower hardness value. Hardness in the HAZ of AISI 4130 is high due to the formation of lathy martensite structure there. In the white band, the hardness value is very less because of ferrite phase which is a very soft phase. As the frequency increases the hardness value in white band zone is decreasing and also the number of indentations are also increasing in the white band zone which says that width of the white band is increasing.

4.3.1.5 Tensile properties

The tensile testing was carried out on a universal testing machine with strain rate 3 mm/min and average results were presented in Table 4.6. In all the specimens, the tensile failure is observed in HAZ portion of AISI 4130 steel side which shows the weld strength is more than that of HAZ portion of AISI 4130 steel. The highest UTS, YS and percent elongation was observed at 4 HZ frequency compared to other frequencies.

Table 4.6 Mechanical properties of pulsed TIG welds with different frequencies.

Exp. No	Freq. (HZ)	YS (MPa)	UTS (MPa)	Percent Elongation
ID-1	4	1037	1068	1.24
ID-2	6	1064	1099	1.3
ID-3	8	985	1019	1.1
ID-4	10	963	1041	1.25

*Average of three results

4.3.1.6 Fractography

The macrographs of fractured transverse tensile specimens of dissimilar welds of different frequencies from 4Hz to 10Hz are shown in Fig 4.26. It is observed that the tensile test specimens corresponding to welds produced with pulse frequencies 6Hz and more have fractured at ICHAZ. But the specimens of welds made with pulse frequency of 4Hz have fractured in the base metal zone adjacent to ICHAZ. Though ICHAZ has reported lowest hardness, the base material reported lower hardness, the necking was concentrated at wider base material zone instead of narrower ICHAZ. The necking is clearly evident from figure 4.26 (a) as compared to the other fractured specimen metallographs.

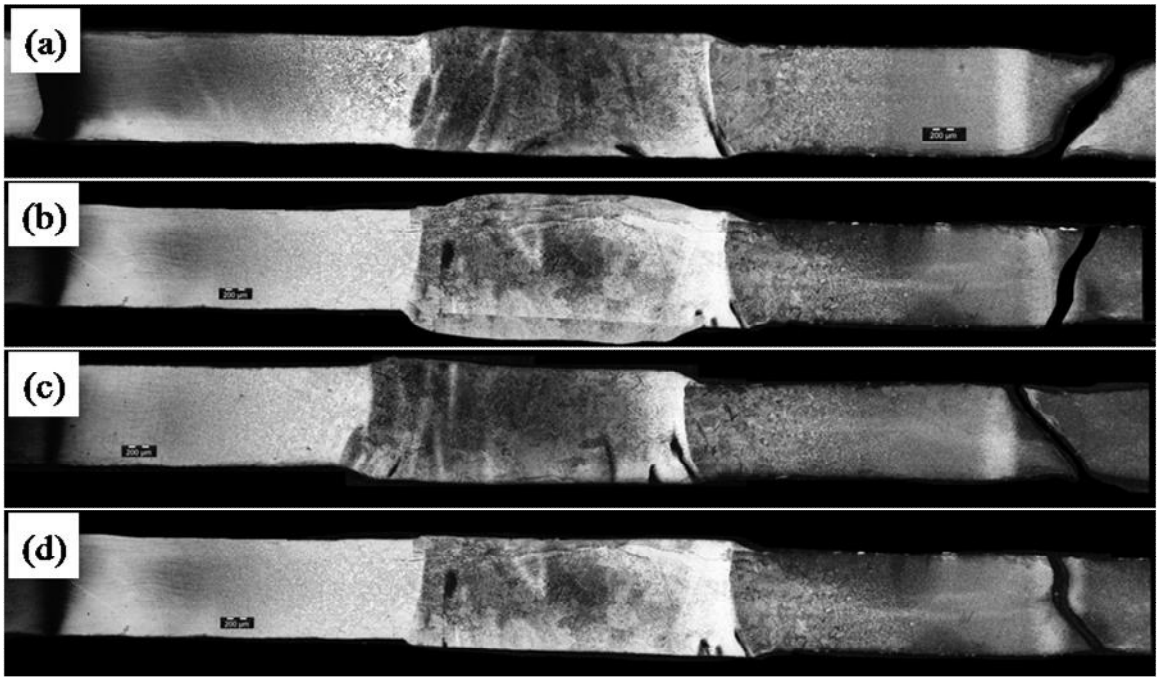

Fig.4.26 Macrographs of fractured tensile test specimens of dissimilar welds of pulsed TIG welds with different frequencies (a)4Hz (b) 6Hz (c) 8Hz (d) 10Hz.

4.4 Pulsed TIG welding (at 4HZ frequency) of Maraging steel to high strength low alloy steel (AISI 4130) without and with external cooling

4.4.1 Quality of weld joint

The appearance of the top surface of Pulsed current GTAW weld joint condition is shown in Fig.4.27 The ripples of weld bead are found to be uniform and the zone adjacent to weld joints is noticed to be darkened due to the exposure to the welding heat input. The extent of darkening indicates directly the width of heat affected zone. The X-ray radiographs of the respective weld joint are shown in Fig.4.27. The weld joint is found to be defect free as it is noticed from the radiograph.

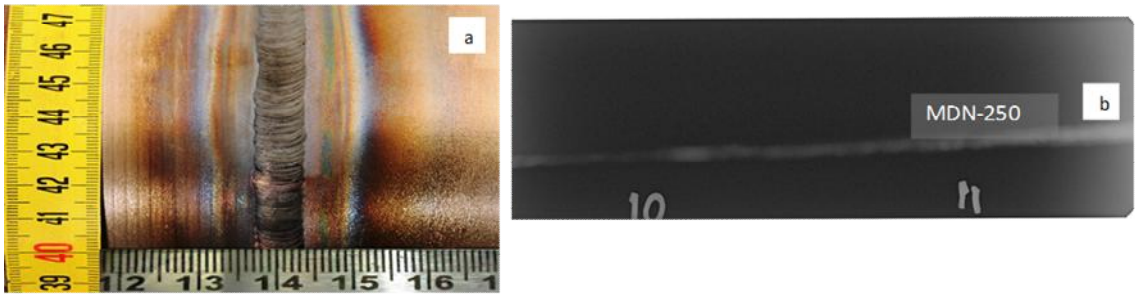

Fig. 4.27 (a) Macrograph (b) X-radiograph of pulsed current GTAW of the Dissimilar weld of Maraging steel and AISI 4130 steel.

4.4.2 Temperature profile

The peak temperatures measured during welding time at the locations adjacent to the weld joint such as CGHAZ and ICHAZ of AISI 4130 steel are presented in Table 4.7. The temperature versus time plots corresponding to CGHAZ and ICHAZ are shown in Fig 4.28 and Fig 4.30 respectively. The slope of the during heating is found to be higher than that of the cooling stage because of the fact that the sudden heating is experienced from the welding arc heat input. The slope of the plot is less while cooling because it takes more time for the welding heat to dissipate into the base material which generally acts as a heat sink in welding. The CGHAZ has experienced temperature maximum up to 1025^0C, much below the austenite finish

temperature. The peak temperature in ICHAZ was noticed to be much below the Ac1 temperature.

Table 4.7 Peak temperatures measured in CG HAZ and IC HAZ's of AISI 4130 steel.

Welding condition		**CGHAZ**	**ICHAZ**
without external cooling	Pulsed Current	1025^0C	595^0C
with external cooling	Pulsed Current	740^0C	355^0C

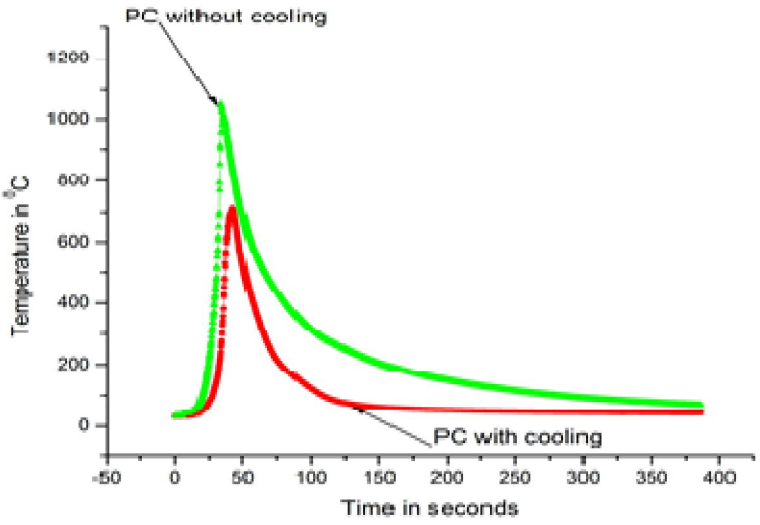

Fig 4.28 Pulsed TIG weld temperature profiles in CGHAZ of AISI 4130 steel with and without external cooling

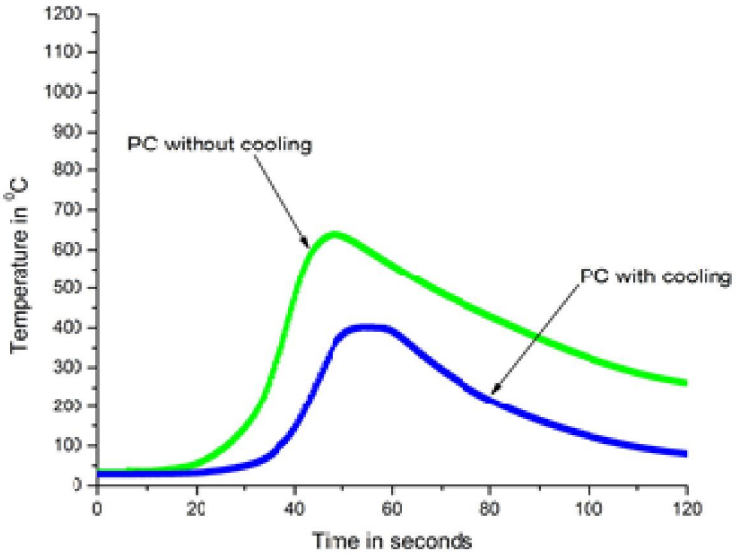

Fig 4.29 Pulsed TIG weld temperature profiles in ICHAZ of AISI 4130 steel with and without external cooling

4.4.3 Microstructure

The microstructure of ICHAZ of AISI 4130 steel with and without external cooling is shown in Fig. 4.30 and it is observed that It is clearly evident from these microstructures that, coarser ferrite surrounded coarser martensite is observed in the case of welds produced by the pulsed current with and without external cooling. More martensite is observed in without cooling compared to with cooling. It could be mainly because of higher peak temperatures (~595^{0}C) experienced by the region ICHAZ in case pulsed current welds made without external cooling. The macrostructures depicting varied widths of ICHAZ in weld joints made with and without cooling conditions are shown in Fig 4.31 Weld joints made with pulsed current without external cooling were noticed to have higher peak temperature and the HAZ of AISI 4130 steel is found to stay at relatively higher temperatures for longer time while cooling which might have contributed to increasing the width of ICHAZ shown in Table 4.8.

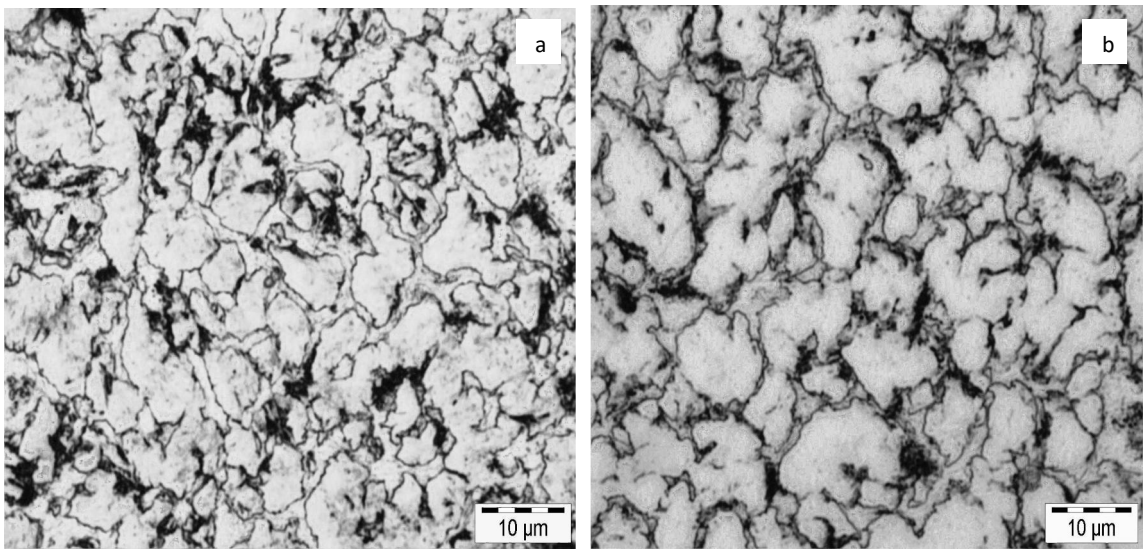

Fig.4.30 Microstructures of ICHAZ of welds produced with Pulsed current GTAW
a) without cooling b) with cooling

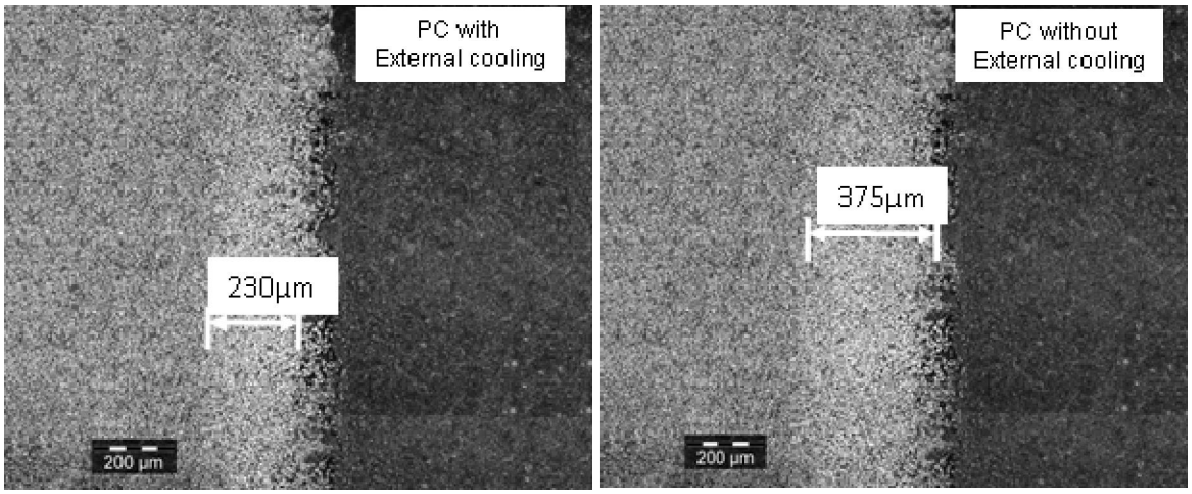

Fig.4.31 Widths of ICHAZ in dissimilar weld joints Pulsed current GTAW without external cooling.

Table 4.8 Width of the ICHAZ in AISI 4130 steel.

Welding condition		**Width of the ICHAZ (um)**
without external cooling	Pulsed Current	375
with external cooling	Pulsed Current	230

4.4.4 Microhardness

Influence of external cooling methods on microhardness distribution across the heat affected zone of AISI 4130 steel is shown in shown in Fig.4.32. The softening tendencies in heat affected zone of AISI 4130 steel due to the exposure of welding heat is presented in Fig 4.33. Location and width of soft zone, hardness in HAZ of AISI 4130 steel of dissimilar welds is shown in Table 4.9. The soft zone in HAZ of AISI 4130 steel can be characterized with respect to the width of the soft zone (considering any hardness less than 350Hv corresponds to soft zone) and distance of minimum hardness from the fusion line of weld towards AISI 4130 steel side. The weld joints produced with pulsed current without external cooling have a maximum width of the soft zone and a maximum distance of soft zone from fusion line.

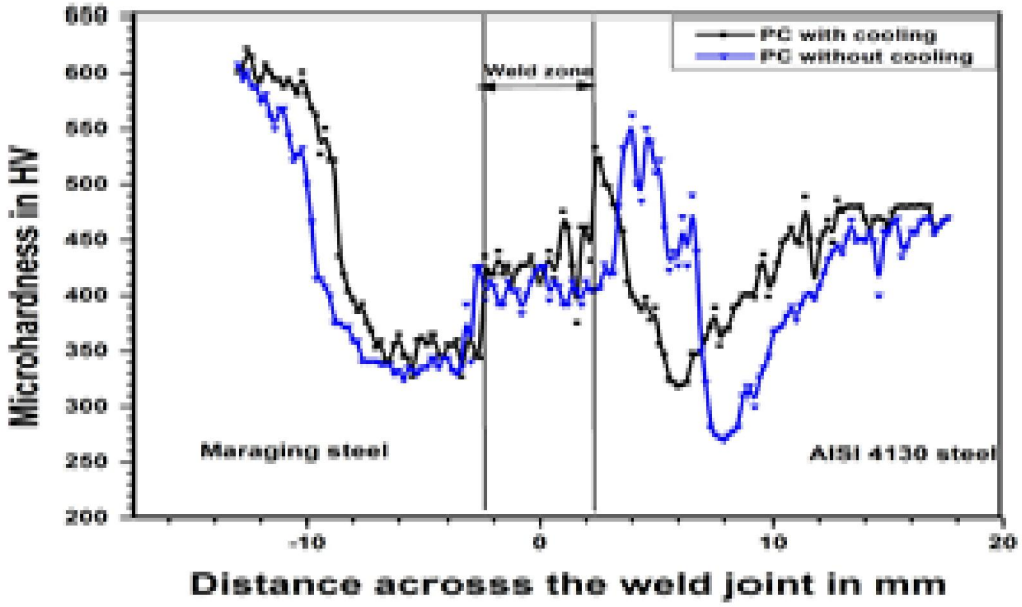

Fig 4.32 A typical microhardness distribution across the dissimilar weld of maraging steel and AISI 4130 steel produced by pulsed current TIG welds with and without external cooling.

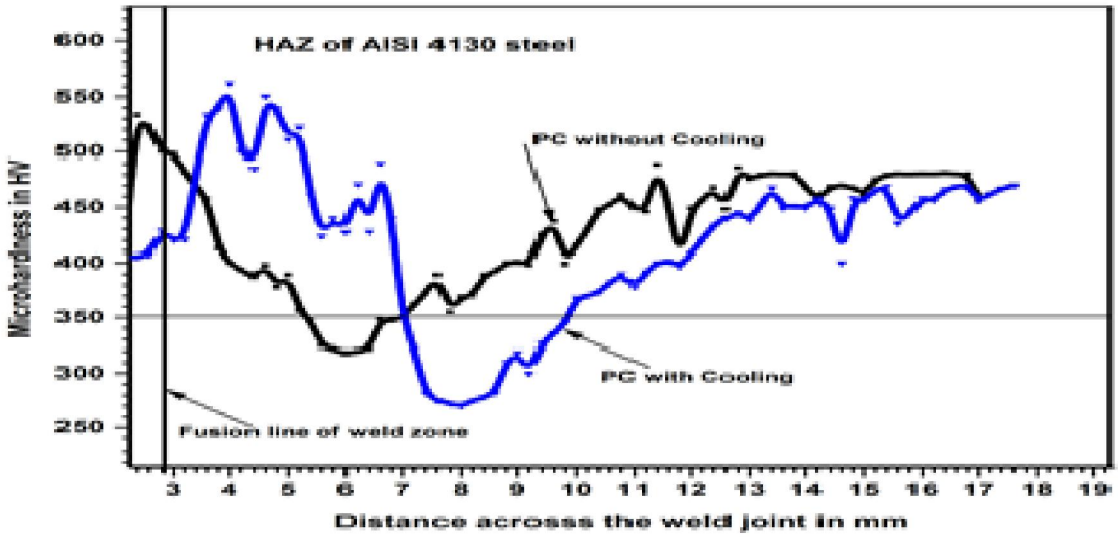

Fig 4.33 Comparison of microhardness distribution across the softened heat affected zone of AISI 4130 steel in weld joints produced by pulsed current TIG welds with and without external cooling.

Table.4.9 Location and width of the soft zone in HAZ of AISI 4130 steel of different dissimilar weld joints.

Welding condition	**Distance of soft zone from the fusion line (mm)**	**Width of soft zone (mm)**	**Minimum hardness in HAZ (Hv)**	**Maximum hardness in HAZ (Hv)**
Without external cooling				
Continuous current	7.0	5.8	259	556
Pulsed current	5.0	3.2	271	548
With external cooling				
Continuous current	4.4	2.4	300	537
Pulsed current	3.2	1.9	326	527

4.4.5 Degree of HAZ softening

The calculated degree of softening in HAZ of AISI 4130 steel in different welding conditions is presented in Table 4.10. The maximum softening has been observed in the case of weld joint produced with continuous current without external cooling compared to with cooling.

Table.4.10 Degree of softening in HAZ of AISI 4130 steel of different dissimilar weld joints

H_m	H_b	$\Delta H_{th}=H_m-H_b$(Hv)	$\Delta H_{expt}=H_{max}-H_{min}$ (Hv)				Degree of softening (%) in HAZ			
			Without external cooling		With external cooling		Without external cooling		With external cooling	
			CC	PC	CC	PC	CC	PC	CC	PC
572	261	311	297	277	237	201	95.49	89.06	76.21	64.63
CC –Continuous current, PC- Pulsed current										

4.4.6 Tensile properties

The tensile properties of weld joint made with different welding conditions are mentioned in Table 4.11. The comparison of tensile stress versus strain plots of different dissimilar weld joints is given in Fig 4.34. The macrographs of fractured transverse tensile specimens of all dissimilar welds are shown in Fig.4.35. The fracture location is observed in ICHAZ of AISI 4130 steel and also correlated to the minimum hardness zone on the microhardness profile of weld joint. The dissimilar weld joints made with pulsed current with external cooling have shown relatively higher tensile strength and yield strength compared to that of without external cooling, which could be due to the facts that the welding heat input was reduced by adapting the external cooling methods employed in the heat affected zones of AISI 4130 steel. Use of pulsed current with the external cooling method has enhanced the weld joint efficiency from 68 to 87%.

Table.4.11 Tensile properties of weld joint made with different welding conditions.

Welding condition	**0.2% YS in MPa**	**UTS in MPa**	**% Elongation**	**Weld joint efficiency based on 0.2% YS**
Without external cooling				
Continuous current	826	960	3.8	67.98
Pulsed current	885	995	3.4	72.84
With external cooling				
Continuous current	1014	1041	2.7	83.45
Pulsed current	1056	1115	3.0	86.91

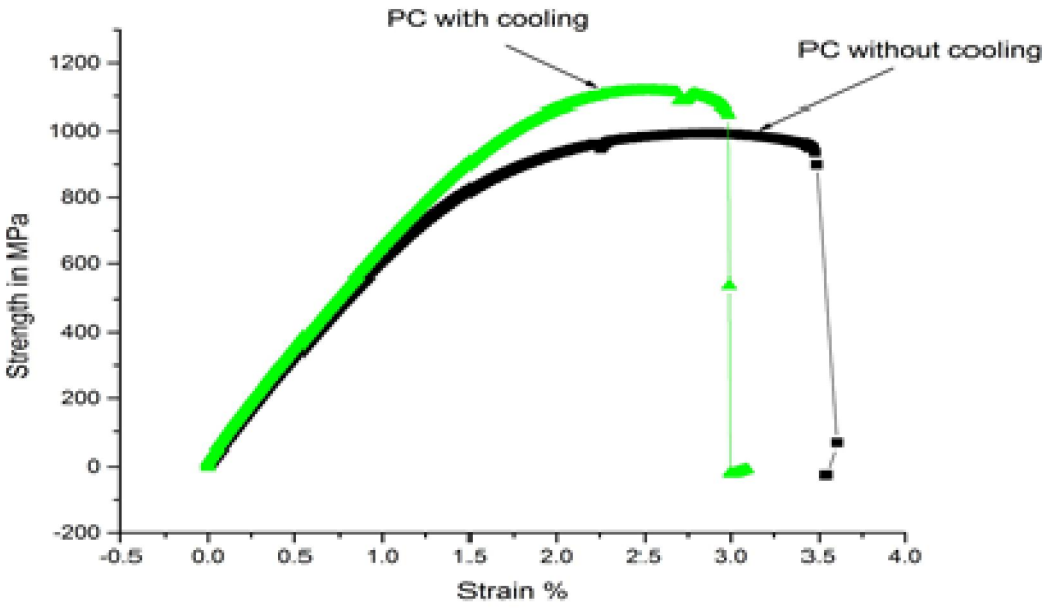

Fig 4.34 Comparison of strength versus strain plots of specimens pertaining to dissimilar welds of maraging steel AISI 4130 steel produced by pulsed current TIG welds with and without external cooling.

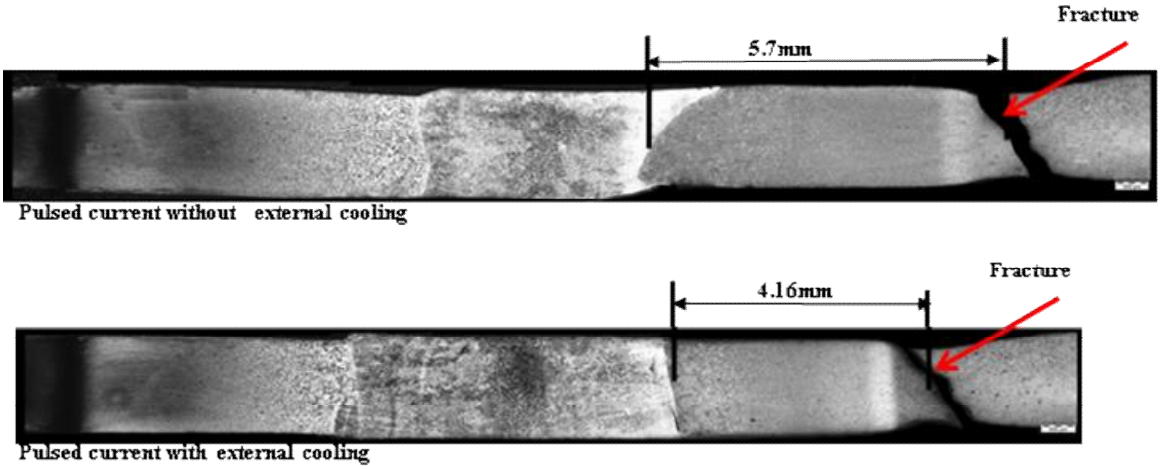

Fig 4.35 Macrographs of fractured tensile test specimens of dissimilar welds of pulsed current TIG welds current with and without external cooling.

4.4.7 Fractography

Scanning electron micrographs of fracture surfaces of tensile test specimens of dissimilar metal welds produced with different welding conditions are shown in Fig 4.36 It is observed that the fracture surfaces of tensile specimens corresponding to joints made with pulsed current without external cooling have revealed shallow dimpled features while those of pulsed current with external cooling has shown deep and finer dimples.

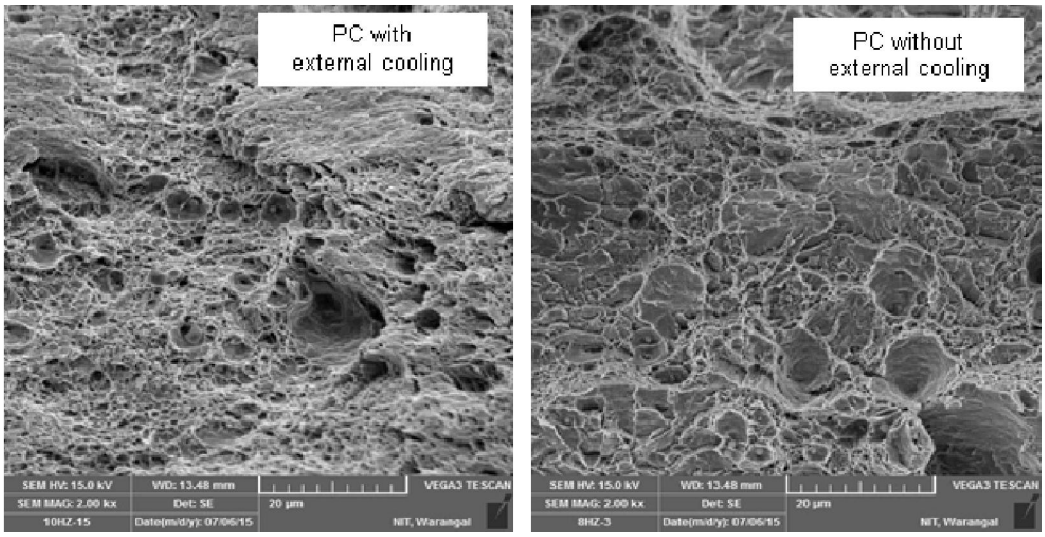

Fig 4.36 Scanning electron micrographs of fracture surfaces of tensile test specimens of dissimilar welds of pulsed current with and without external cooling.

4.5 Impact of contamination on quality and mechanical properties of dissimilar pulsed gas tungsten arc welds of 18% Ni maraging steel and AISI 4130 steel

4.5.1 Appearance weld joints

The appearance of all weld joints at the reinforcement side is shown in Fig. 4.37. It is observed from the joints that the width of discoloration zone due to welding heat is relatively more towards 4130 steel side compared to that on maraging steel side. This could be due to the fact that the AISI 4130 steel has higher thermal conductivity (43 W/m/K) compared to maraging steel (21 W/m/K). The extent of discoloration was noticed to less in the case of joint contaminated with heat extraction paste compared to the other welding joints. This might because of the reason that the heat extraction paste absorbs excess heat from the heat affected zones.

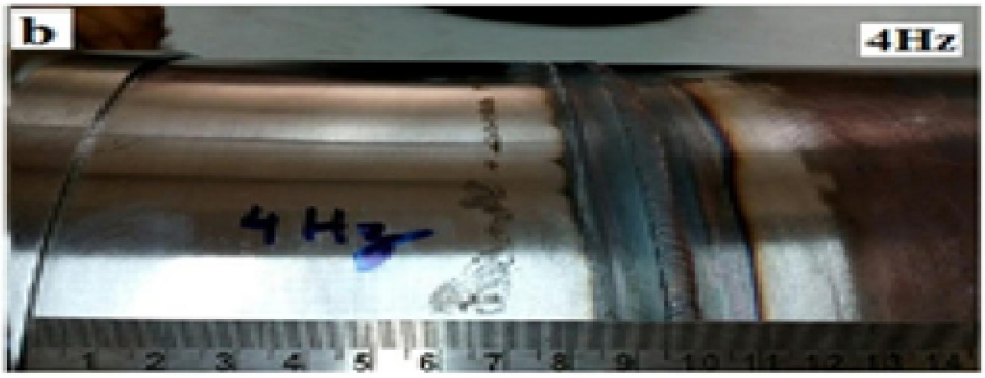

Fig.4.37. Macrograph (top surface) of welded joint

4.5.2 Quality of weld joints

The dye penetrant test was carried out on all the welded joints and observed that there is no any indications or discontinuities of the surfaces of weld and adjacent zones. X-ray radiography was also carried out on all the welded joints and the radiographic films are presented in Fig.4.38 revealed that, the presence of a number of gas pores varying from minimum 0.1mm

to maximum 1.5 mm in length. The gas porosity levels and their quantification for each weld joint are mentioned in Table 4.12. The acceptable limit of the isolated gas porosity as per ASME Section VIII Boiler and Pressure vessel code is (t/3) mm and random porosity is (t/4) mm. But in the case of all the dissimilar weld joints, the gas porosity was noticed to be far higher than these acceptable limits. The clustered and aligned porosity with maximum sizes was noticed in the joint contaminated with heat extraction paste. Relatively the joints contaminated with water and cutting oil contain a lesser amount of porosity both in numbers and cumulative area as compared to those of joints contaminated with heat extraction paste. This could be due to the fact that the paste contains moisture and also it releases more hydrogen during exposure to welding heat which in turn entrapped in the weld zone and formed severe porosities.

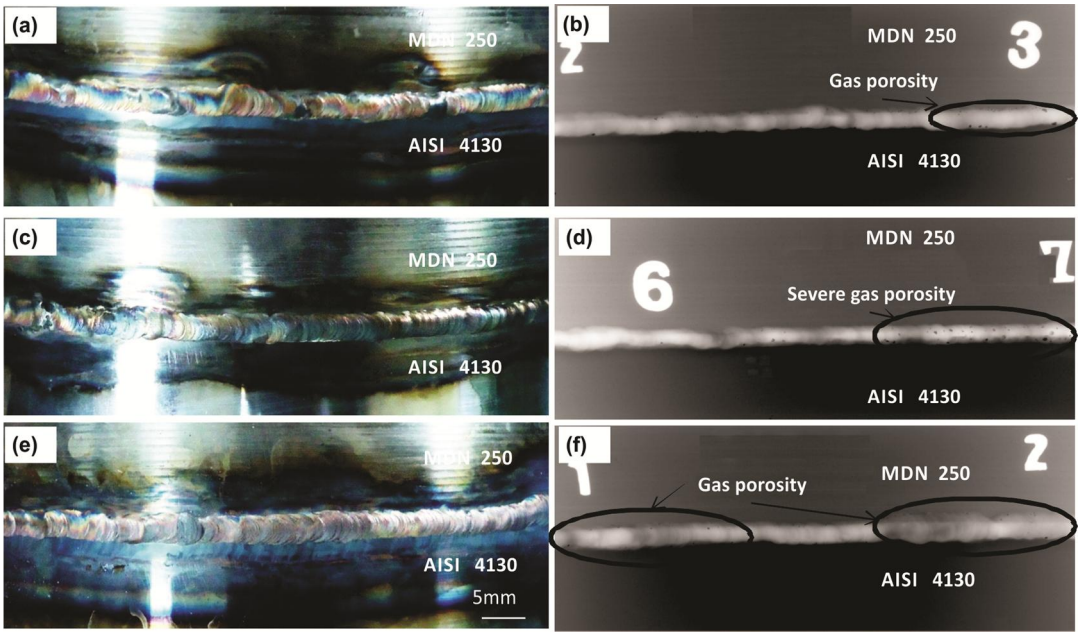

Fig.4.38 Appearance of weld joints and X-ray radiographs. (a and b) Joint contaminated with water (c and d) Joint contaminated with heat extraction paste (e and f) Joint contaminated with cutting oil.

4.5.3 Microstructures

The microstructure of maraging steel exhibits very fine lath martensite features elongated along flow forming lines. The AISI 4130 steel base material contains fine tempered martensite which was formed during the low-temperature tempering process.

The optical macrostructure of full joint and microstructures of various zones of dissimilar weld joint contaminated with cutting oil are shown in Fig. 4.39. The whole dissimilar weld joint may divide into four zones namely, fusion zone, heat affected zone (HAZ) of maraging steel, heat affected zone of AISI 4130 steel and unaffected base material zone. The HAZ of maraging steel comprises further three zones such as dark band zone, fine grained HAZ and coarse grained HAZ. The dark band zone contains predominantly pools of reverted austenite surrounded by soft iron nickel martensite [10].

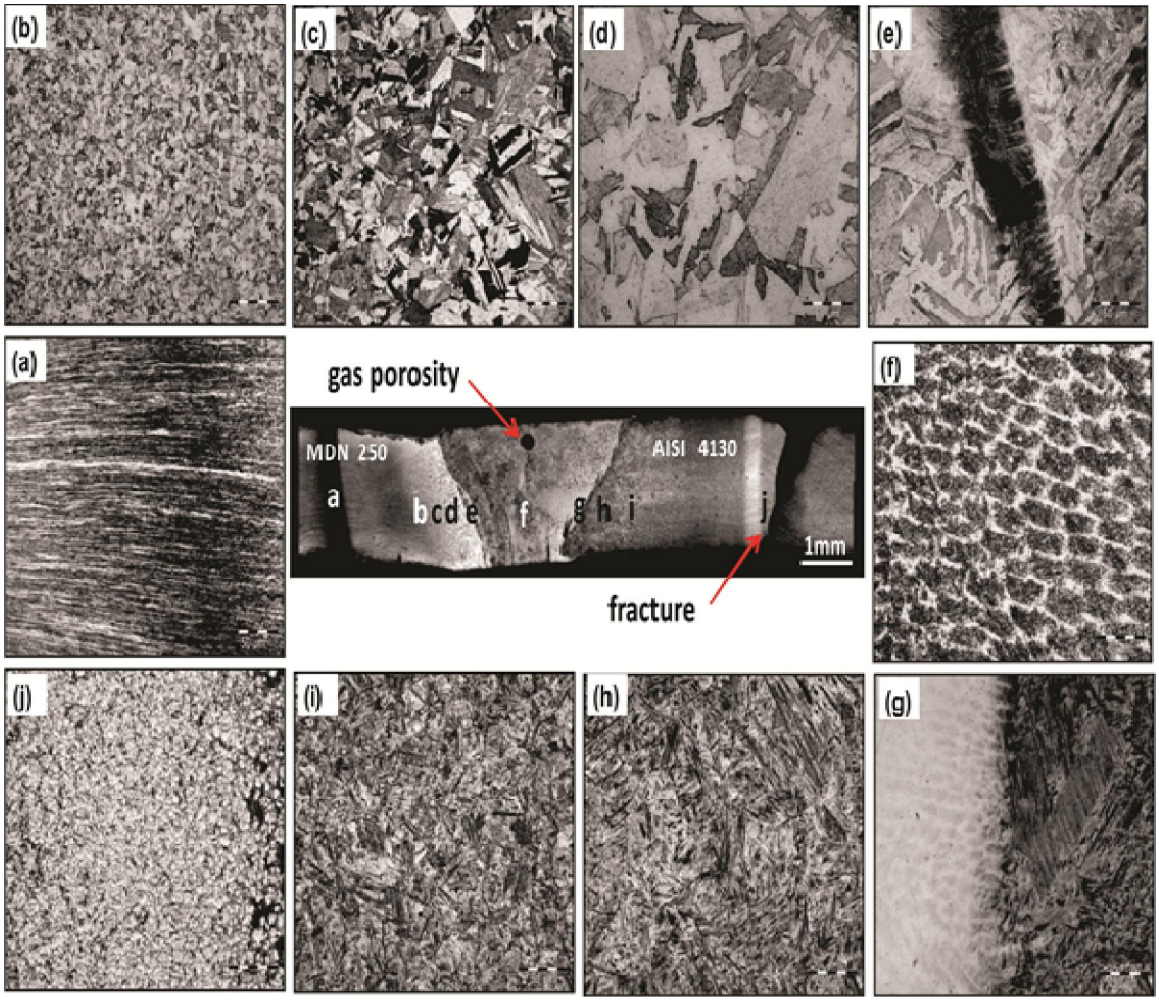

Fig. 4.39 Macrostructure of the dissimilar weld joint with gas porosity after tensile test and microstructures of various zones of the dissimilar weld joint. (a) dark band zone of HAZ in maraging steel side, (b) and (c) fine grained HAZ in maraging steel side, (d) Coarse grained HAZ in maraging steel side, (e) fusion interface towards maraging steel side, (f) fusion zone (g) fusion interface towards AISI 4130 steel side, (g) Coarse grained HAZ in AISI 4130 steel side,

(h) fine grained HAZ in AISI 4130 steel side, (j) white band zone of HAZ in AISI 4130 steel side.

The coarse grained HAZ is formed due to the phenomenon that during welding, the zone adjacent to weld fusion interface is heated to a high temperature in the austenite region, where a considerable amount of grain growth occurs. Upon cooling the austenite transforms to martensite inheriting prior coarse grain size of austenite. The microstructure of fusion zone of dissimilar weld shows re-solidified equiaxed grains look like a cell structure. On the other hand, the HAZ of AISI 4130 steel comprises further three zones such as fine HAZ Fig. 4.39 (h), coarse HAZ Fig.4.39 (i) and white band Fig. 4.39 (j). The fine grained HAZ of AISI 4130containing fine grain martensite containing a solid solution of α-fe. the HAZ of AISI 4130 adjoining to the weld interface shows coarse martensite and retained austenite which is formed during post weld cooling phase. Within the HAZ of AISI 4130 Steel, the grain size was noticed to be reduced while moving away from the fusion interface due to the varied cooling rates witnessed by different zone during post weld cooling. The structure of the transient region between the base metal and HAZ was a mixture of fine grain martensite which contains solid solution of α-fe and retained ferrite. The similar results reported by C.C.Huang et al [11].

4.5.4 Microhardness

A typical microhardness variation across the dissimilar weld joint contaminated with cutting oil is presented in Fig.4.40. Close to fusion boundary on the maraging side and 4130 steel side exhibited higher hardness than the weld region. Immediately away from the interface region, hardness has a drooping trend, probably due to the softening of these regions by the high temperatures generated during welding. Softest zone in HAZ of maraging steel side is called as dark band region. This region exhibited the lowest hardness due to the presence of fine dispersions of retained austenite in martensite [10]. The hardness along the HAZ of AISI 4130 side has shown greater hardness values near to the fusion zone and decline trend away from the fusion boundary. The region of the HAZ near to the fusion zone experiences a high peak temperature exceeding AC3 line and also subjected to fast cooling rates. The microstructure of this part of HAZ was characterized by being predominantly martensite (refer Fig 4.39(h)). Regions away from the fusion zone experienced lower peak temperature and probably these

regions are heated to within the inter-critical zones, exhibited lower hardness due to the presence of high-temperature transformation products in addition to martensite.

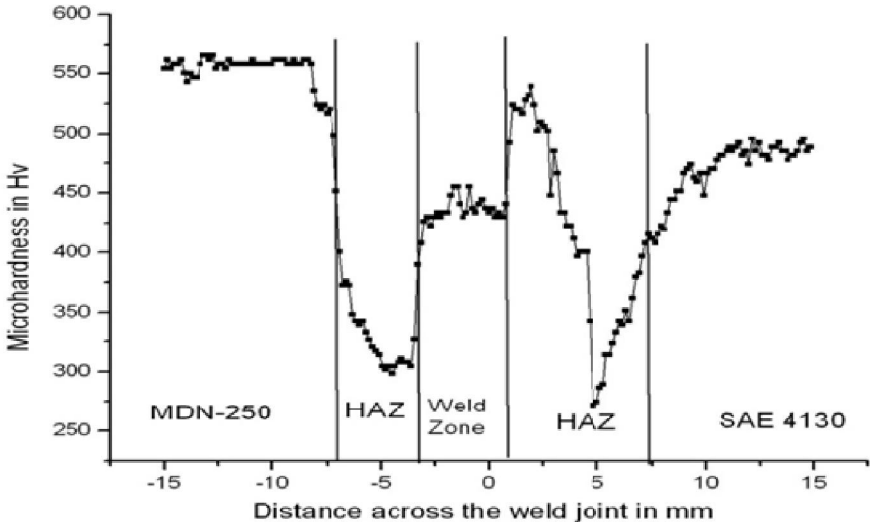

Fig.4.40 Microhardness profile across the dissimilar weld joint contaminated with cutting oil.

4.5.5 Mechanical properties

The mechanical properties of both base materials in their respective heat-treated conditions are shown in Table 4.13. The tensile properties of various contaminated dissimilar weld joints are mentioned in Table. 4.14. The fractured transverse tensile specimens of all dissimilar welds are shown in Fig.4.41 clearly reveal the fracture location as the heat affected zone of AISI 4130 steel in spite of containing gas porosities in weld joints.

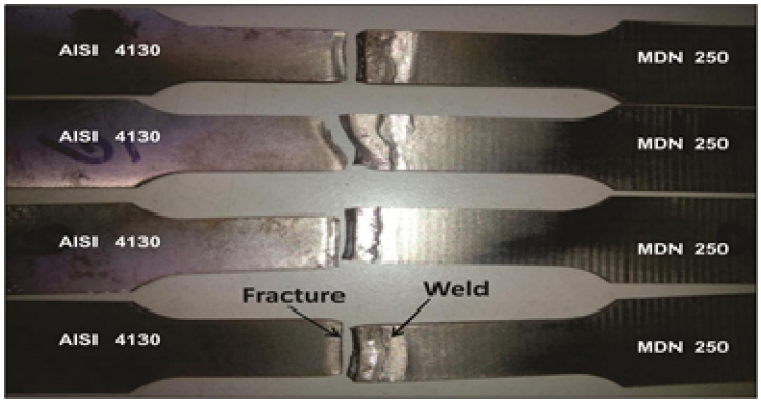

Fig.4.41 Photograph and X-ray radiograph of fractured tensile test specimens of dissimilar weld joints.

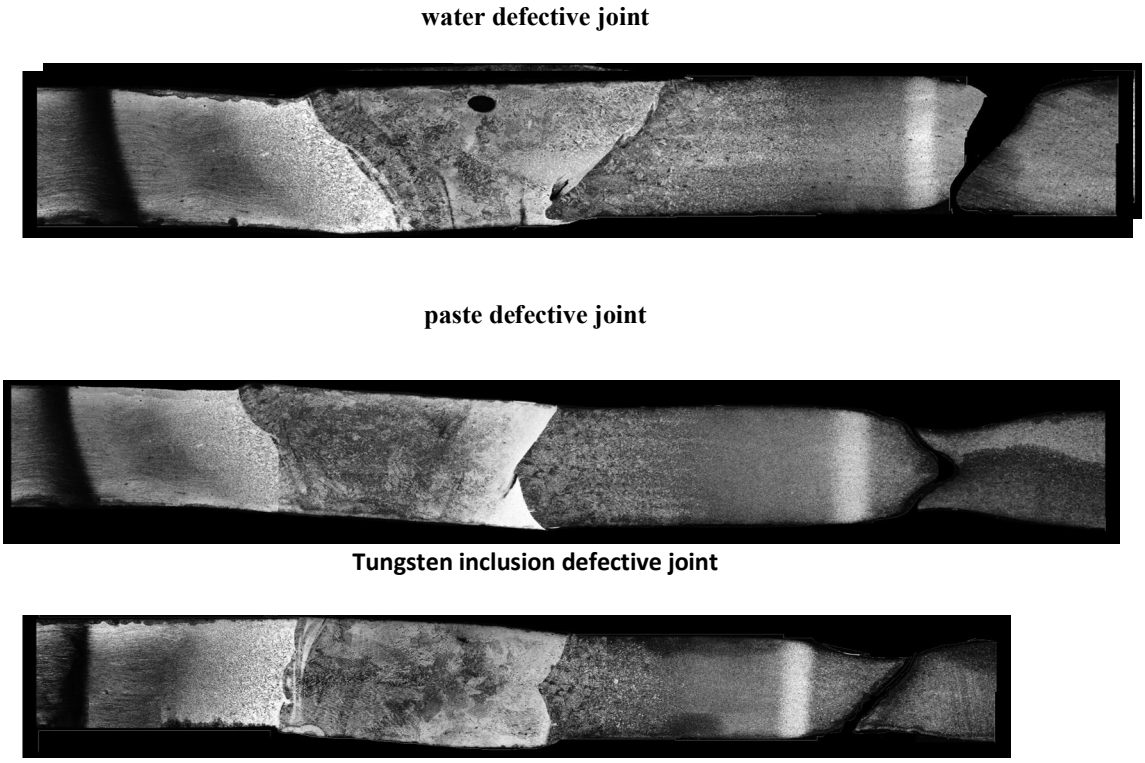

Fig. 4.42. Macrograph of fractured tensile test specimens of dissimilar welds of pulsed TIG welds at different contamination

The fracture location is correlated to the minimum hardness zone on the microhardness profile of weld joint. Though the dissimilar weld joints possess defects higher than the acceptable limits, weld joints demonstrated the yield strength more than 900 MPa which was a basic requirement for the designer. So it is possible to increase the acceptable size of porosities from the values that are specified by existing standard/code for this particular dissimilar weld joint.

Table 4.12 Gas porosity levels in the dissimilar weld joints.

Type of dissimilar weld joint	Weld bead width in mm	Length of the weld joint in mm	No of porosities along the length of the weld joint	Gas Porosity size in mm (numbers)
Joint contaminated with water	7	180	58	1.0 X 0.5 (8), 0.6 X 0.4 (5), 0.4 (10), 0.3 (12),0.2 (10), 0.1(13)
Joint contaminated with heat extraction paste	6	180	141	2 X 1(2), 1.0 (6), 0.6 (10),0.5 (18),0.4 (36) 0.21 (10),0.2 (26),0.1 (33)
Joint contaminated with cutting oil	7	180	60	1 X 0.6 (8), 0.5(7),0.4 (8) 0.3 (20),0.2 (17)

Table 4.13 The typical tensile properties of base materials in their respective heat-treated conditions.

Sr. No	Type of base material	UTS (MPa)	0.2%YS (MPa)	%Elongation
1	18% Ni Maraging steel	1839	1810	2.9
2	AISI 4130 steel	1530	1215	8.5

Table 4.14 Transverse tensile properties of dissimilar weld joints containing gas porosities

Sr. No	Type of weld joint	UTS (MPa)	0.2%YS (MPa)	%Elongation	Failure location	Gas Porosity size in specimen (mm)
1	Joint contaminated with water	1095	969	2.88	HAZ of 4130	1.5x0.5, 0.6x0.5
2	Joint contaminated with heat extraction paste	1122	1008	2.80	HAZ of 4130	0.8x0.5, Ø 0.5, Ø 0.4, Ø 0.3 (Clustered porosity)
3	Joint contaminated with cutting oil	1058	952	3.22	HAZ of 4130	0.5x0.4, 0.4x0.3

The dissimilar weld joint contaminated with heat extraction paste has shown relatively higher tensile strength compared to the other joints, which could be due to the fact that the excessive welding heat might have been effectively absorbed by the paste from the zones of HAZ of 4130 steel. The tensile properties of the dissimilar weld joint are less than the strength of the AISI 4130 steel base material due to the softening that occurs in the HAZ of AISI 4130 steel.

The fracture location of all welded samples are in the AISI 4130 side and the fracture location matches with minimum hardness region. Fractography of the transverse tensile specimen welds with contamination of water, oil and heat extraction paste are presented in Fig. 4.42.

4.6 Comparison of continuous and pulsed (4Hz) GTAW on Microstructure and Mechanical properties of Dissimilar welds of Maraging steel and AISI 4130 steel

4.6.1 Quality of weld joints

The appearance of the top surface of weld joints of different conditions is shown in Fig.4.43. The ripples of weld bead are found to be uniform and the zone adjacent to weld joints is noticed to be darkened due to the exposure to the welding heat input. The extent of darkening indicates directly the width of heat affected zone. It is observed from the Fig.4.43 that the zone of darkening in the case of pulsed current welds was less than that of continuous current welds and the external cooling in HAZ has tremendously reduced the width of darkened zone.

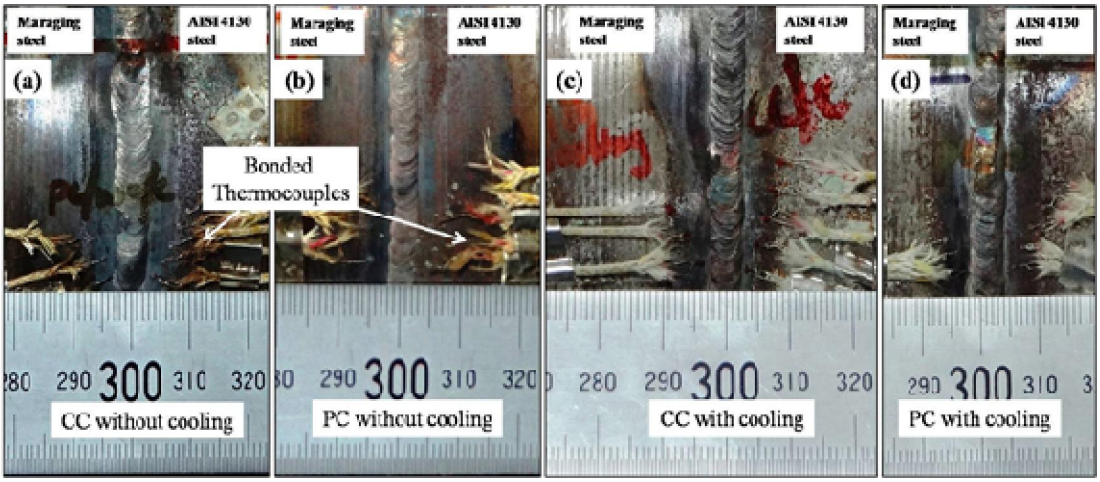

Fig 4.43 Top surface appearances of weld joints produced (a) continuous current without external cooling (b) pulsed current without external cooling (c) continuous current with external cooling (d) pulsed current without external cooling.

4.6.2 Temperature profiles during welding

The peak temperatures measured during welding time at the locations adjacent to the weld joint such as CGHAZ and ICHAZ of AISI 4130 steel are presented in Table 4.15. The temperature versus time plots corresponding to CGHAZ and ICHAZ are shown in Fig 4.44 and Fig 4.45 respectively. The slope of the during heating is found to be higher than that of the

cooling stage because of the fact that the sudden heating is experienced from the welding arc heat input. The slope of the plot is less while cooling because it takes more time for the welding heat to dissipate into the base material which generally acts as a heat sink in welding. The CGHAZ has experienced temperature maximum up to 1200^0C, just below the austenite finish temperature. The peak temperature in SCHAZ was noticed to be just below the Ac1 temperature. Use of pulsed current and external cooling has dramatically reduced the peak temperatures seen by both the zones.

Table 4.15 Peak temperatures measured in CG and IC HAZ's of AISI 4130 steel.

Welding condition		**CGHAZ**	**ICHAZ**
without external cooling	Continuous Current	1200^0C	650^0C
with external cooling	Continuous Current	900^0C	500^0C
without external cooling	Pulsed Current	1025^0C	595^0C
with external cooling	Pulsed Current	740^0C	355^0C

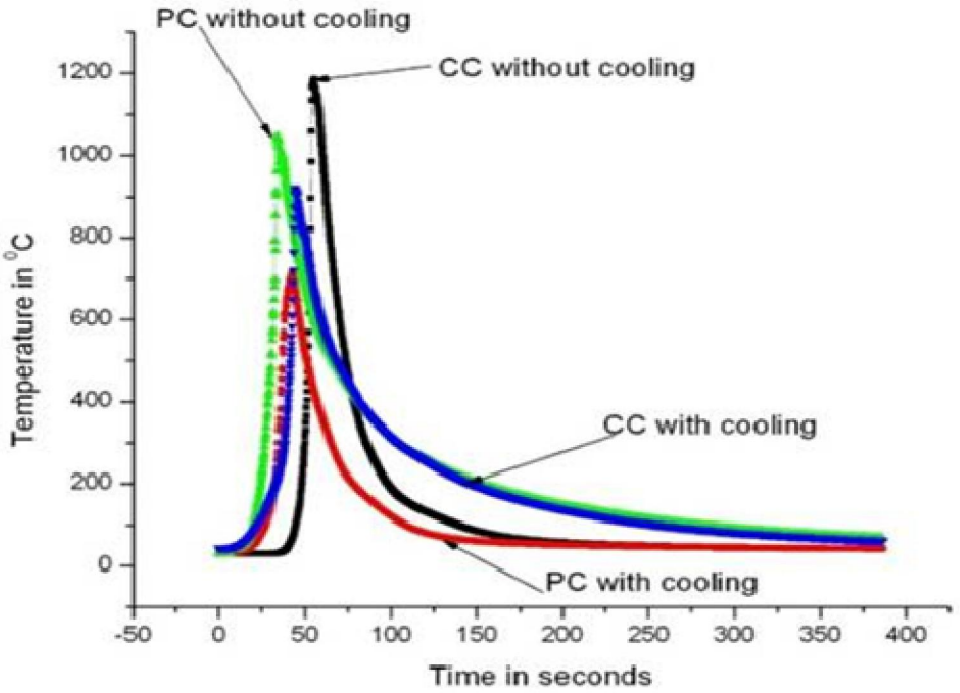

Fig 4.44 Comparison of temperature profiles in CGHAZ of AISI 4130 steel for different weld joints.

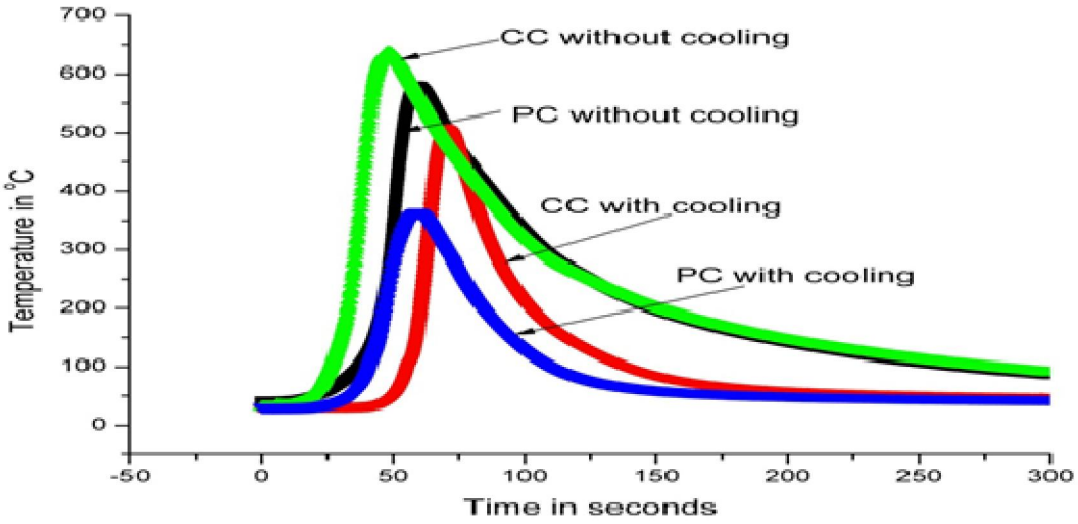

Fig 4.45 Comparison of temperature profiles in ICHAZ of AISI 4130 steel for different weld joints.

4.6.3 Metallography

A high magnification microstructures of ICHAZ regions pertaining to two extreme heat input conditions such as (a) continuous current without external cooling (b) pulsed current with external cooling are shown in Fig.4.46. It is clearly evident from these microstructures that coarser ferrite surrounded coarser martensite is observed in the case of welds produced by continuous current without external cooling as compared to those of pulsed current with external cooling. It could be mainly because of higher peak temperatures (~650^0C) experienced by the region ICHAZ in case continuous current welds made without external cooling.

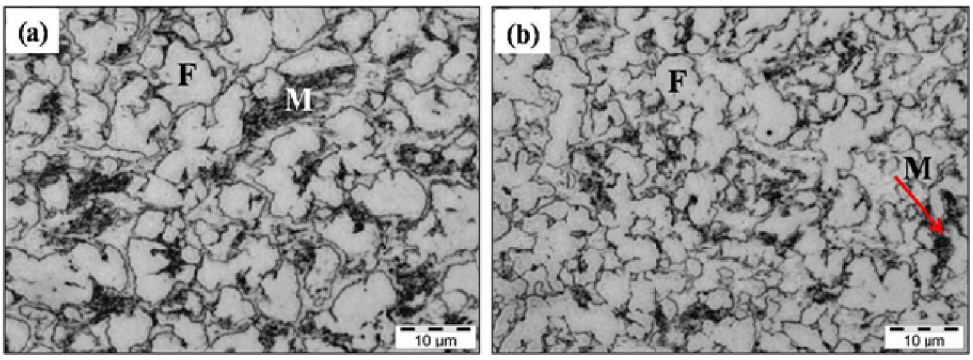

Fig.4.46 Microstructures of ICHAZ of welds produced with (a) continuous current without external cooling (b) pulsed current with external cooling.

The macrostructures depicting varied widths of ICHAZ in weld joints made with different welding and cooling conditions are shown in Fig 4.47 and the values are tabulated in Table 4.16. The width of ICHAZ was noticed to be increasing with increasing welding heat input conditions. The continuous current welding conditions have produced wider and brighter ICHAZ as compared to that of welds made with a pulsed current. Use of external cooling has reduced the width of ICHAZ. Use of pulsed current coupled with external cooling has drastically reduced the width of ICHAZ as compared to welds made with continuous current without any external cooling. Weld joints made with continuous current without external cooling were noticed to have higher peak temperature and the HAZ of AISI 4130 steel is found to stay at relatively higher temperatures for a longer time while cooling which might have contributed to increasing the width of ICHAZ.

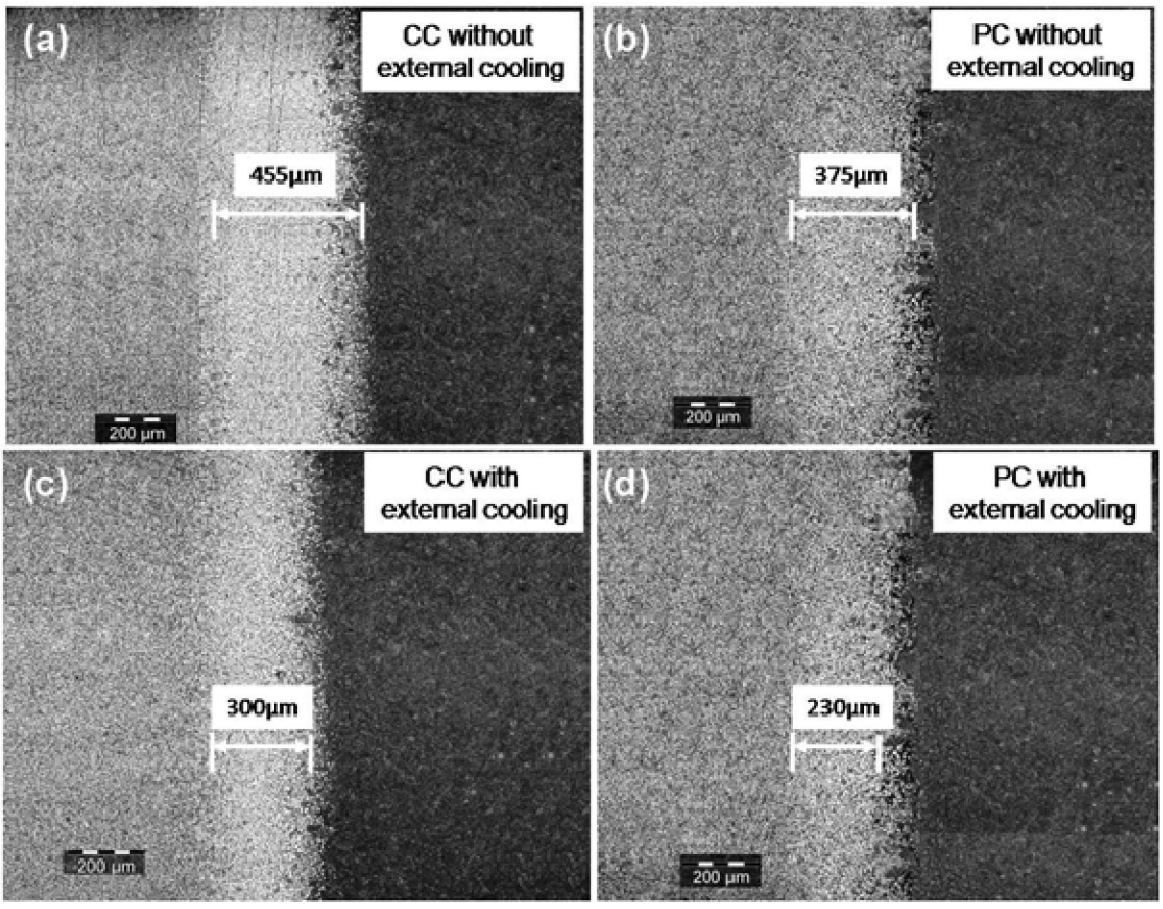

Fig.4.47 Varying widths of ICHAZ in dissimilar weld joints (a) continuous current without external cooling (b) pulsed current without external cooling (c) continuous current with external cooling(d) pulsed current with external cooling.

Table 4.16 Width of the ICHAZ in AISI 4130 steel.

Welding condition		Width of the ICHAZ (um)
without external cooling	Continuous Current	455
with external cooling	Continuous Current	300
without external cooling	Pulsed Current	375
with external cooling	Pulsed Current	230

4.6.4 Microhardness

The influence of welding technique and external cooling methods on microhardness distribution across the heat affected zone of AISI 4130 steel is shown in shown in Fig.4.48. The softening tendencies in heat affected zone of AISI 4130 steel due to the exposure of welding heat are presented in Fig 4.49 and Table 4.17. the line of weld towards AISI 4130 steel side. The soft zone in HAZ of AISI 4130 steel can be characterized with respect to width of soft zone (considering any hardness less than 350Hv corresponds to soft zone) and distance of minimum hardness from the fusion The weld joints produced with continuous current without external cooling have maximum width of soft zone and maximum distance of soft zone from fusion line while the joints made using pulsed current with external cooling has demonstrated minimum width of soft zone and minimum distance from the fusion line.

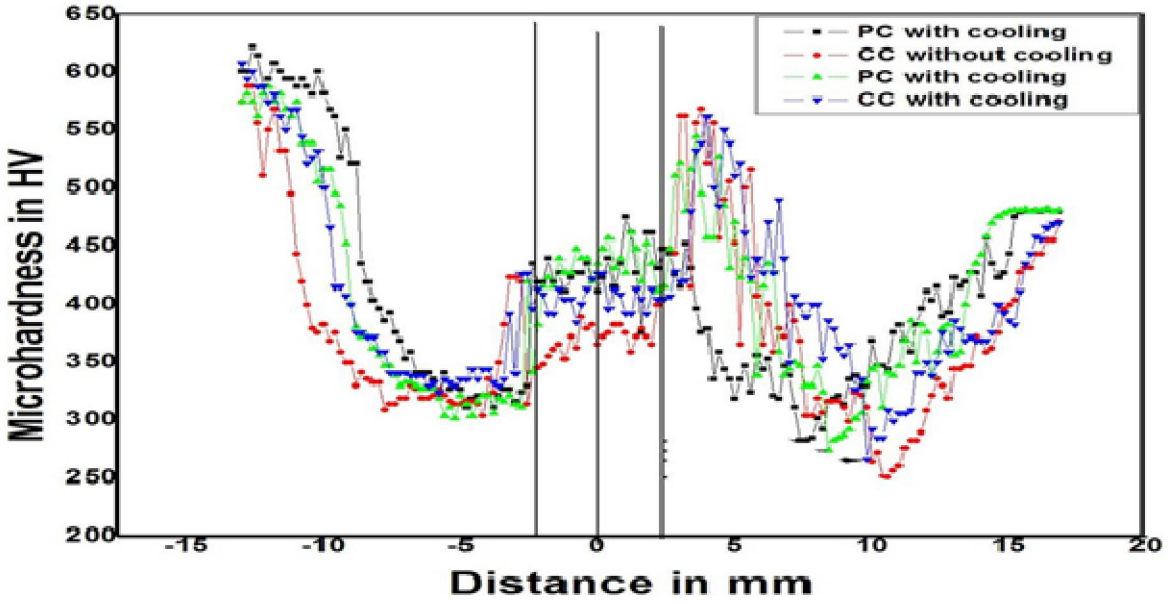

Fig 4.48 Comparison of microhardness distribution across the weld joints in all conditions.

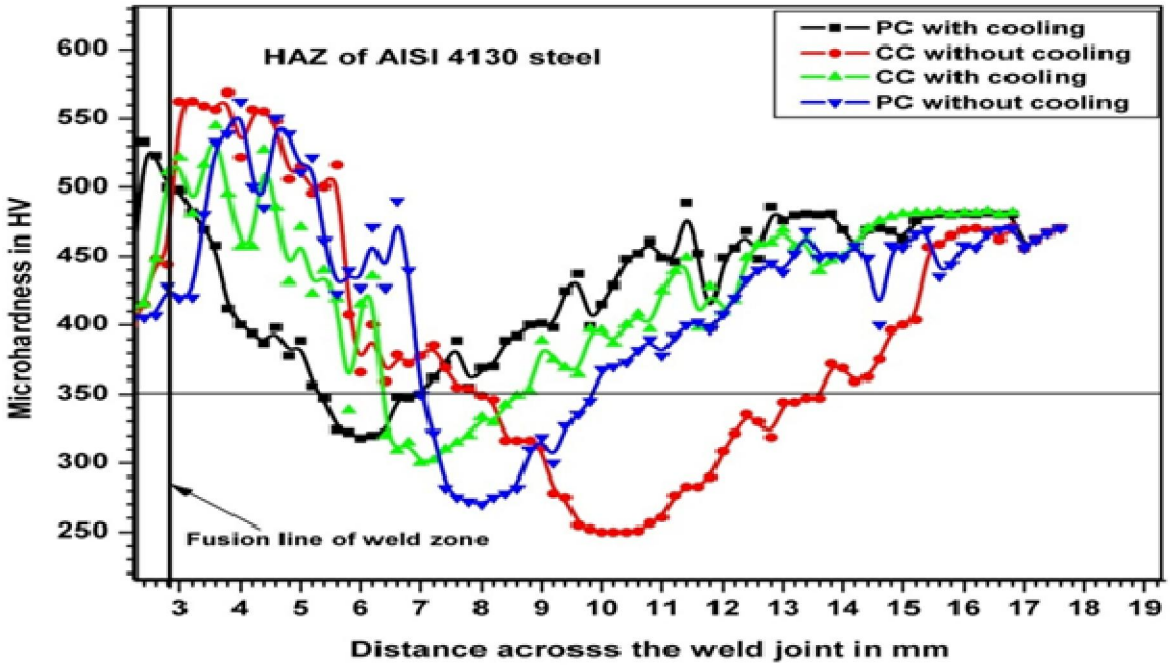

Fig 4.49 Comparison of microhardness distribution across the softened heat affected zone of AISI 4130 steel in weld joints corresponding to different welding conditions.

Table.4.17 Location and width of the soft zone in HAZ of AISI 4130 steel of different dissimilar weld joints.

Welding condition	Distance of soft zone from the fusion line (mm)	Width of soft zone (mm)	Minimum hardness in HAZ (Hv)	Maximum hardness in HAZ (Hv)
Without external cooling				
Continuous current	7.0	5.8	259	556
Pulsed current	5.0	3.2	271	548
With external cooling				
Continuous current	4.4	2.4	300	537
Pulsed current	3.2	1.9	326	527

4.6.5 Degree of HAZ softening

The calculated degree of softening in HAZ of AISI 4130 steel in different welding conditions are presented in Table 4.18 The maximum softening has been observed in the case of weld joint produced with continuous current without external cooling while the joints made using pulsed current with external cooling has demonstrated a lowest degree of softening.

Table.4.18 Degree of softening in HAZ of AISI 4130 steel of different dissimilar weld joints.

H_m	H_b	$\Delta H_{th}=H_m-H_b$(Hv)	$\Delta H_{expt}=H_{max}-H_{min}$ (Hv)				Degree of softening (%) in HAZ			
			Without external cooling		With external cooling		Without external cooling		With external cooling	
			CC	PC	CC	PC	CC	PC	CC	PC
572	261	311	297	277	237	201	95.49	89.06	76.21	64.63
CC –Continuous current, PC- Pulsed current										

4.6.6 Tensile properties

The tensile properties of weld joint made with different welding conditions are mentioned in Table 4.19. The comparison of tensile stress versus strain plots of different dissimilar weld joints is given in Fig 4.50. The macrographs of fractured transverse tensile specimens of all dissimilar welds are shown in Fig.4.51 clearly reveal the fracture location as the sub critical heat affected zone (ICHAZ) of AISI 4130 steel. The fracture location is correlated to the minimum hardness zone on the microhardness profile of weld joint. The dissimilar weld joints made with pulsed current with external cooling have shown relatively higher tensile strength and yield strength compared to all the other joints, which could be due to the facts that the welding heat input was reduced by adapting pulsed current instead of continuous current and excessive welding heat might have been effectively absorbed by the external cooling methods employed in the heat affected zones of AISI 4130 steel. Use of pulsed current with the external cooling method has enhanced the weld joint efficiency from 68 to 87%.

Table.4.19 Tensile properties of weld joint made with different welding conditions.

Welding condition	0.2% YS in MPa	UTS in MPa	% Elongation	Weld joint efficiency based on 0.2% YS
Without external cooling				
Continuous current	826	960	3.8	67.98
Pulsed current	885	995	3.4	72.84
With external cooling				
Continuous current	1014	1041	2.7	83.45
Pulsed current	1056	1115	3.0	86.91

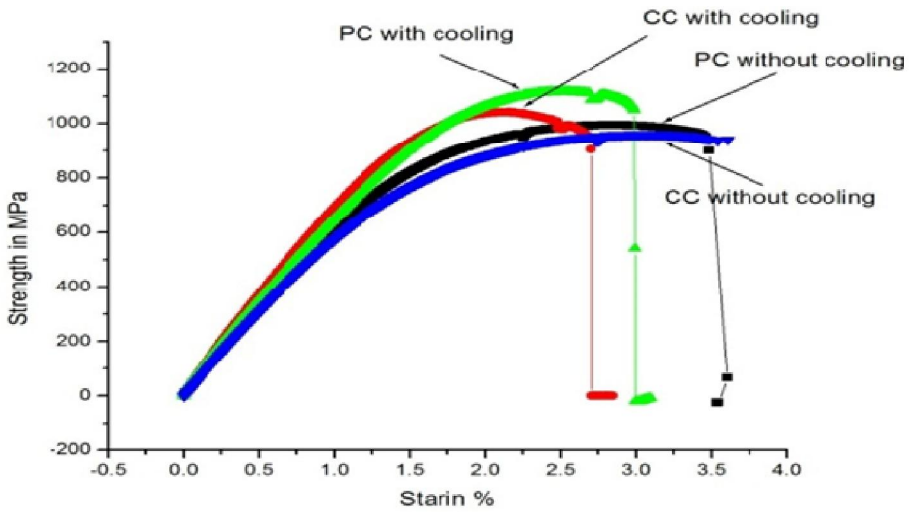

Fig 4.50 Comparison of strength versus strain plots of specimens pertaining to dissimilar welds of maraging steel AISI 4130 steel produced by continuous current and pulsed current TIG welds with and without external cooling.

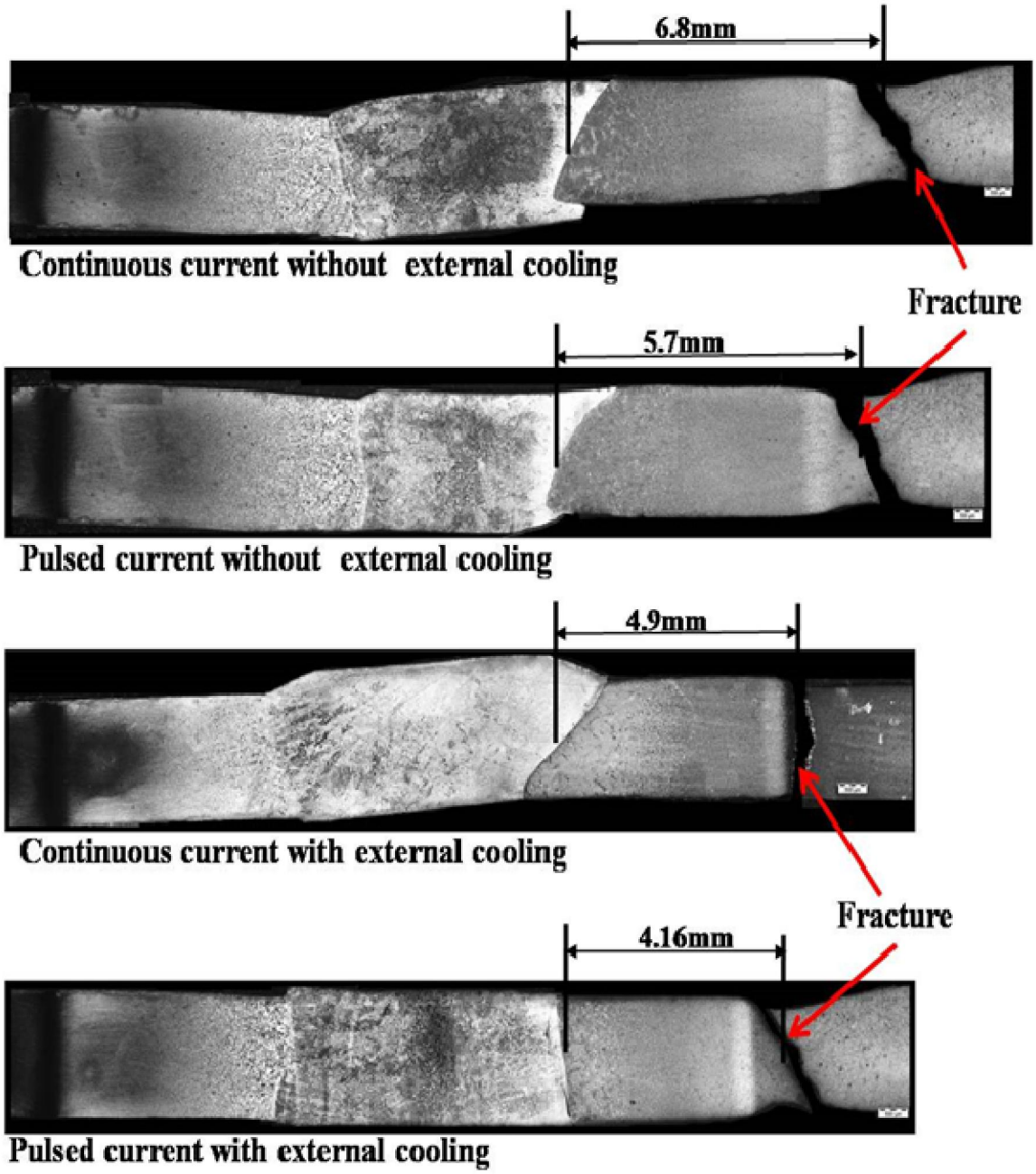

Fig 4.51 Macrographs of fractured tensile test specimens of dissimilar welds of continuous current and pulsed current TIG welds with and without external cooling.

4.6.7 Fractography

Scanning electron micrographs of fracture surfaces of tensile test specimens of dissimilar metal welds produced with different welding conditions are shown in Fig 4.52 It is observed that the fracture surfaces of tensile specimens corresponding to joints made with continuous current without external cooling have revealed shallow dimpled features while those of continuous and pulsed current with external cooling has shown deep and finer dimples.

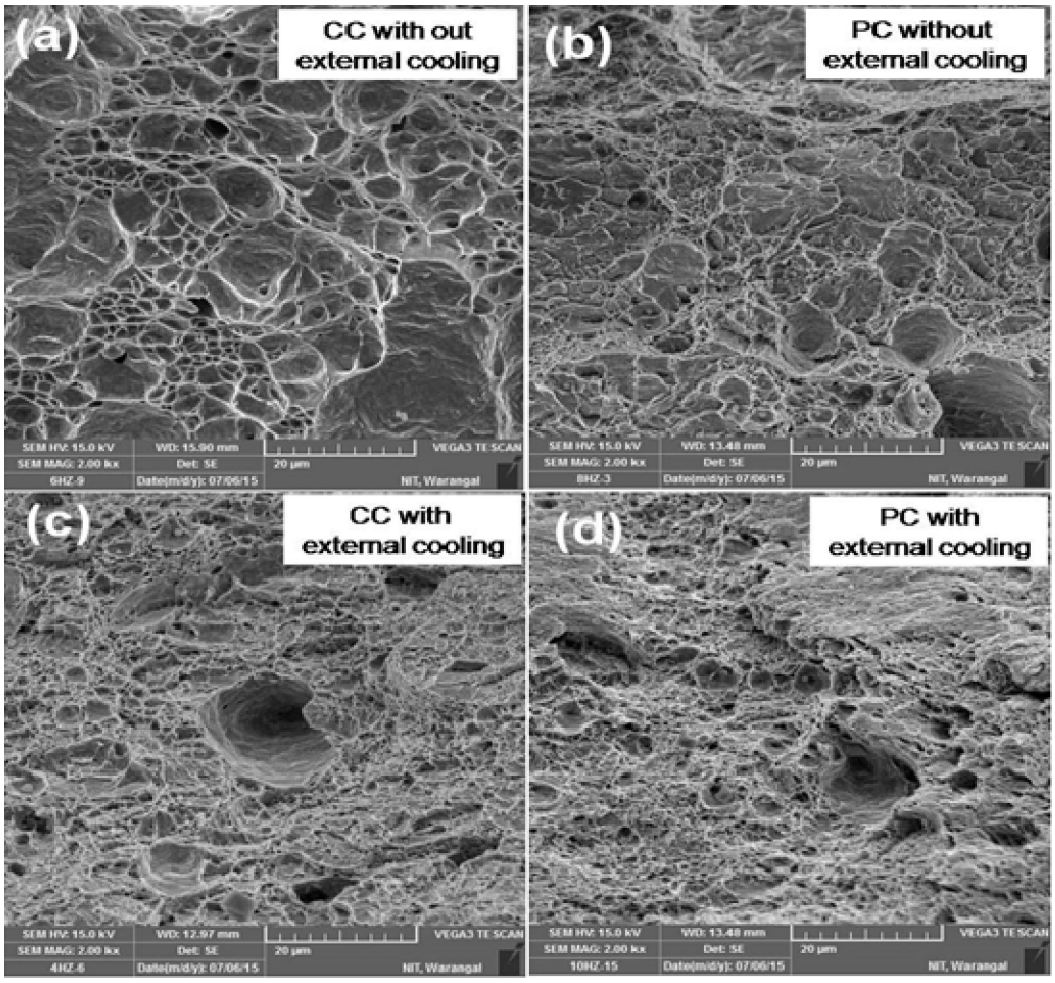

Fig 4.52 Scanning electron micrographs of fracture surfaces of tensile test specimens of dissimilar weld joints (a)continuous current without external cooling (b) pulsed current without external cooling (c) continuous current with external cooling(d) pulsed current with external cooling.

4.7 Laser welding of Dissimilar Steels i.e. Maraging steel to high strength low alloy steel (AISI 4130)

4.7.1 Quality of weld joints

The appearance of the top surface of X-ray radiography of Laser weld joint condition is shown in Fig. 4.53 (a, b). The ripples of the weld bead are found to be uniform and the zone adjacent to the weld joint is noticed to be less darkened due to the exposure of the welding heat input is low compared to continuous current welding. The width of the weld bead and reinforcement is observed to be less compared to continuous and pulsed welds.

Fig 4.53 (a) Macrograph (top surface) and (b) X-radiograph of Laser beam welding of the Dissimilar steel i.e. Maraging steel to AISI 4130 steel.

4.7.2 Microstructure

Various regions of heat affected zone of maraging steel side of the dissimilar metal weld (LASER welding) are shown in Fig 4.54. Broadly the heat affected zone of maraging steel can be divided into three zones, coarse grained (CG) HAZ, fine grained (FG) HAZ and inter critical (IC) HAZ depending upon the peak temperature that each zone experiences during.

Various regions of heat affected zone of high strength low alloy steel (AISI 4130) of the dissimilar metal weld (LASER welding) are shown in Fig 4.55. Broadly the heat affected zone of AISI 4130 steel can be divided into three zones, coarse grained (CG) HAZ, fine grained (FG) HAZ and inter critical(IC) HAZ depending upon the peak temperature that each zone experiences during exposure to weld thermal cycle. The CGHAZ (shown in Fig 4.55(a)) exists very next to the fusion interface and the temperature in this zone reaches peak temperatures of

austenitic transformation region and the grain growth occurs. Upon sudden cooling effects caused during weld cooling phase, the zone exhibits coarse martensite inheriting the prior austenite grain size. The FGHAZ (shown in Fig 4.55(b)) experiences the temperatures close to the AC3 point and the finer austenite grains are formed during the heating cycle. This finer prior austenite grain size leads to the formation of the fine grained heat affected zone upon cooling.

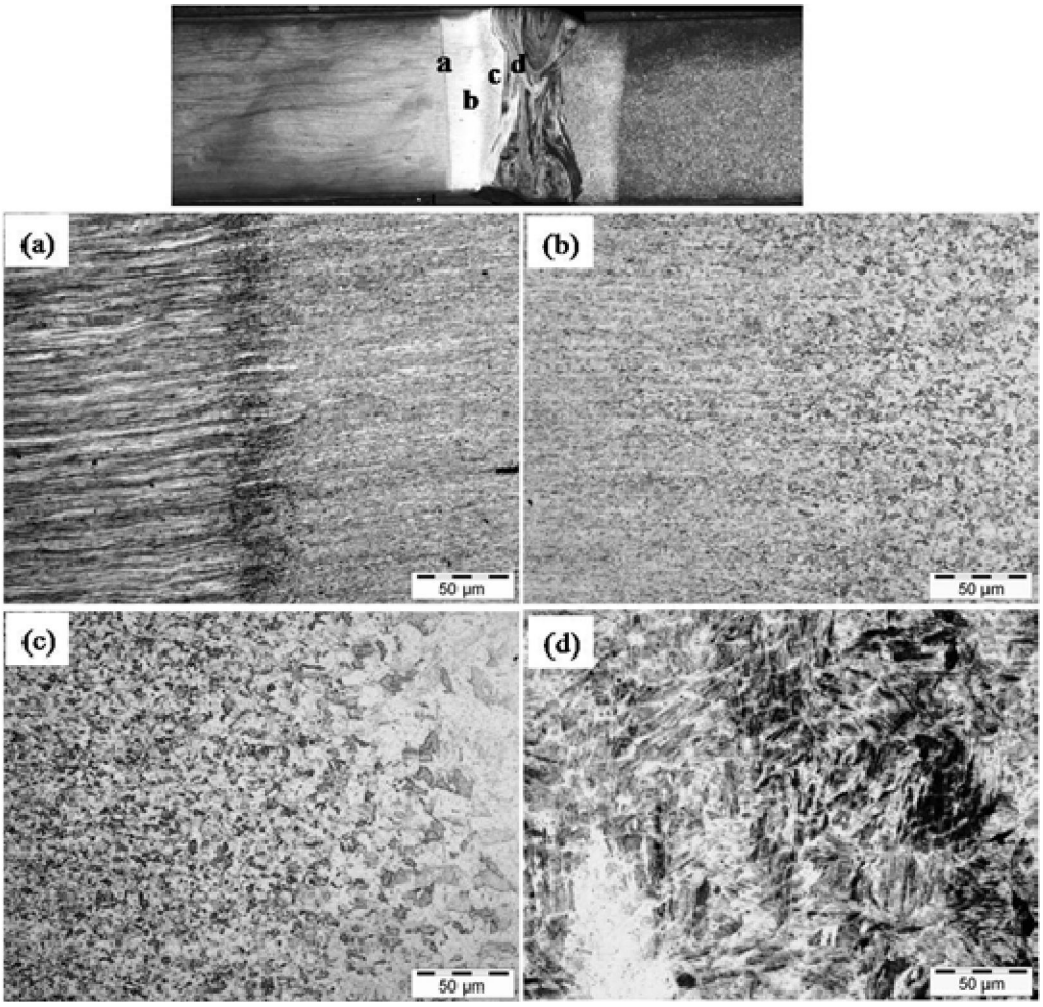

Fig.4.54 The microstructures of various zones of the heat affected zone on maraging steel side of weld produced with LASER welding (a) dark band region (b) fine grained HAZ (c) coarse grained HAZ (d) fusion zone.

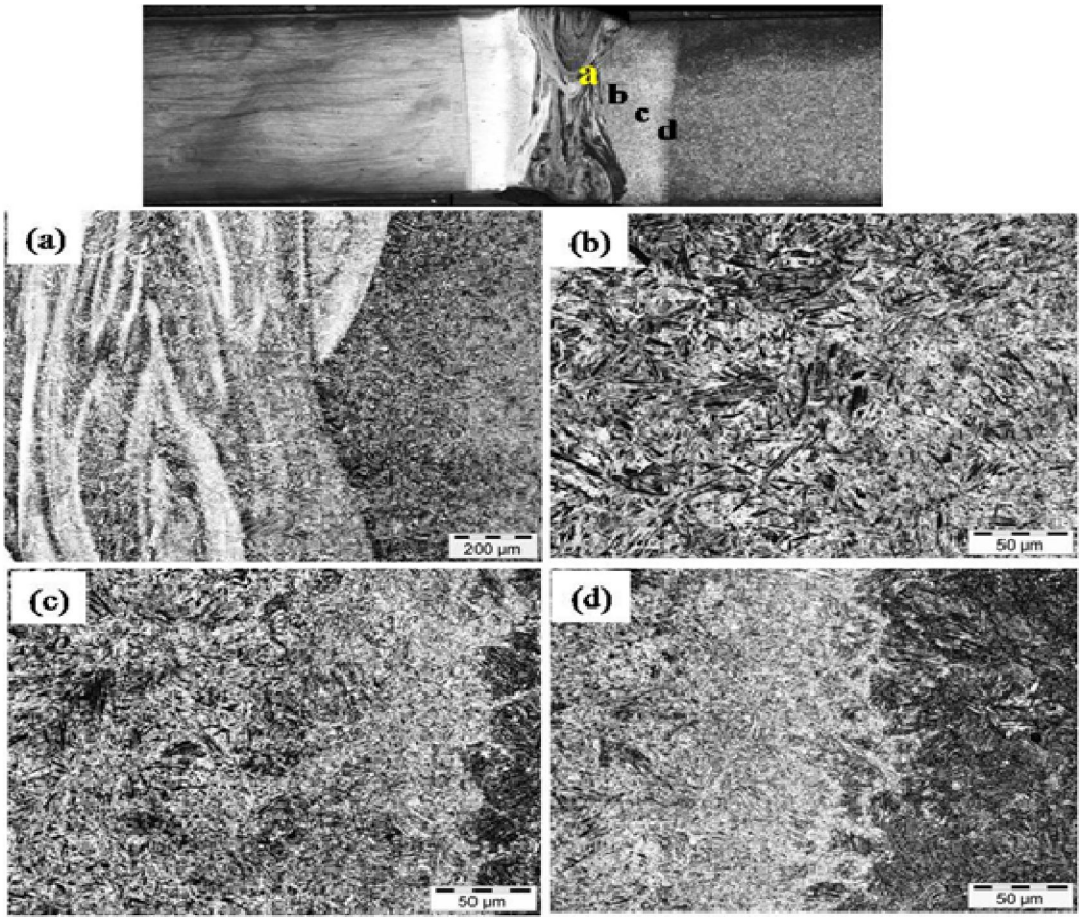

Fig.4.55 The microstructures of various zones of the heat affected zone on AISI 4130 steel side of weld produced with LASER welding (a) fusion zone (b) coarse grained HAZ (c) fine grained HAZ (d) ICHAZ

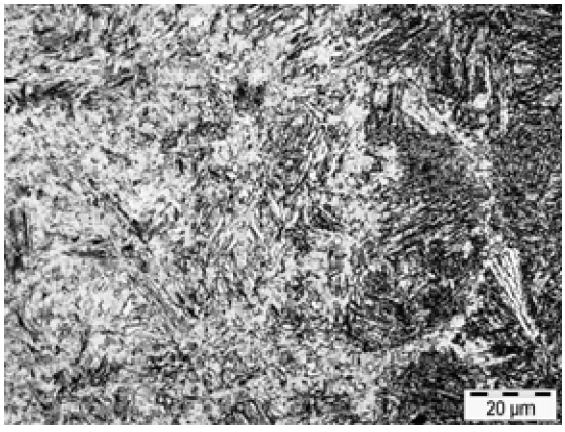

Fig.4.56 The microstructures of ICHAZ of welds produced with a laser weld.

Regions away from the fusion zone on AISI 4130 side experiences lower peak temperatures and probably these regions are heated to within the inter critical zone (temperature between A_{C1} and A_{C3}). The microstructure can be a mixture of ferrite and high carbon austenite which transforms to martensite on cooling. A high magnification microstructures of ICHAZ regions pertaining to two extreme heat input conditions are shown in Fig.4.56. It is clearly evident from these microstructures that coarser ferrite surrounded coarser martensite is observed in the case of welds produced by rapid heating and rapid cooling compared to other of welding processes. It could be mainly because of higher peak temperatures (~650^0C) experienced by the region ICHAZ in case rapid cooling. The macrostructures depicting varied widths of ICHAZ in weld joints made with different welding and cooling conditions.

4.8 Comparison of different welding processes and techniques on dissimilar welds of Maraging steel and AISI 4130 steel (CC welds, PC welds, and Laser welds)

4.8.1 Quality of weld joints

The dissimilar weld joints are visually examined and it is observed that the laser beam welds have very less bead geometry as compared to that of both continuous and pulsed TIG welds. The extent of darkening in HAZ of dissimilar weld joints also was very much minimal in the case of laser beam welds as compared to TIG welds. This could be due to the fact that the laser beam welding process imposes high power density and extremely low welding heat input compared to those of TIG welding process. All the welds are found to be defect free as investigated through X-ray radiography and dye penetrant tests.

4.8.2 Temperature profile during welding Dissimilar weld of Maraging steel and AISI 4130 steel

The peak temperatures measured during welding time at the locations adjacent to the weld in ICHAZ of AISI 4130 steel are presented in Fig. 4.57. The slope of the plot during heating is found to be lower than that of post weld cooling time. The laser beam welds have resulted in lowest peak temperature in ICHAZ as compared to that of both continuous and pulsed TIG welds.

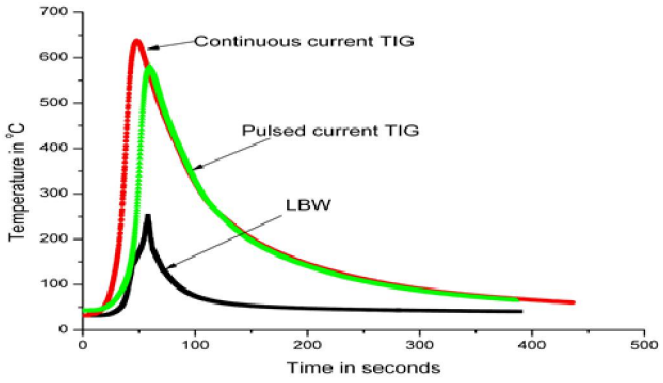

Fig.4.57. Variation of peak temperatures in ICHAZ of AISI 4130 steel side during various welding processes.

4.8.3 Microstructure

A high magnification microstructures of ICHAZ regions pertaining to TIG welds (both continuous current and pulsed current) and laser beam weld are shown in Fig. 4.58. It is clearly evident from these microstructures that higher amount of ferrite surrounded by martensite is observed in the case of welds produced by the continuous current as compared to that of pulsed current TIG welding. It could be mainly because of higher peak temperatures (~650^0C) experienced by the region ICHAZ in the case of TIG welds. But in ICHAZ of laser beam weld, the presence of ferrite is seen very less compared to that of TIG welds which could be due to the fact that the prevailing temperature in ICHAZ of laser beam weld is recorded to be around of 250^0C that too for a very short period as compare to TIG welds.

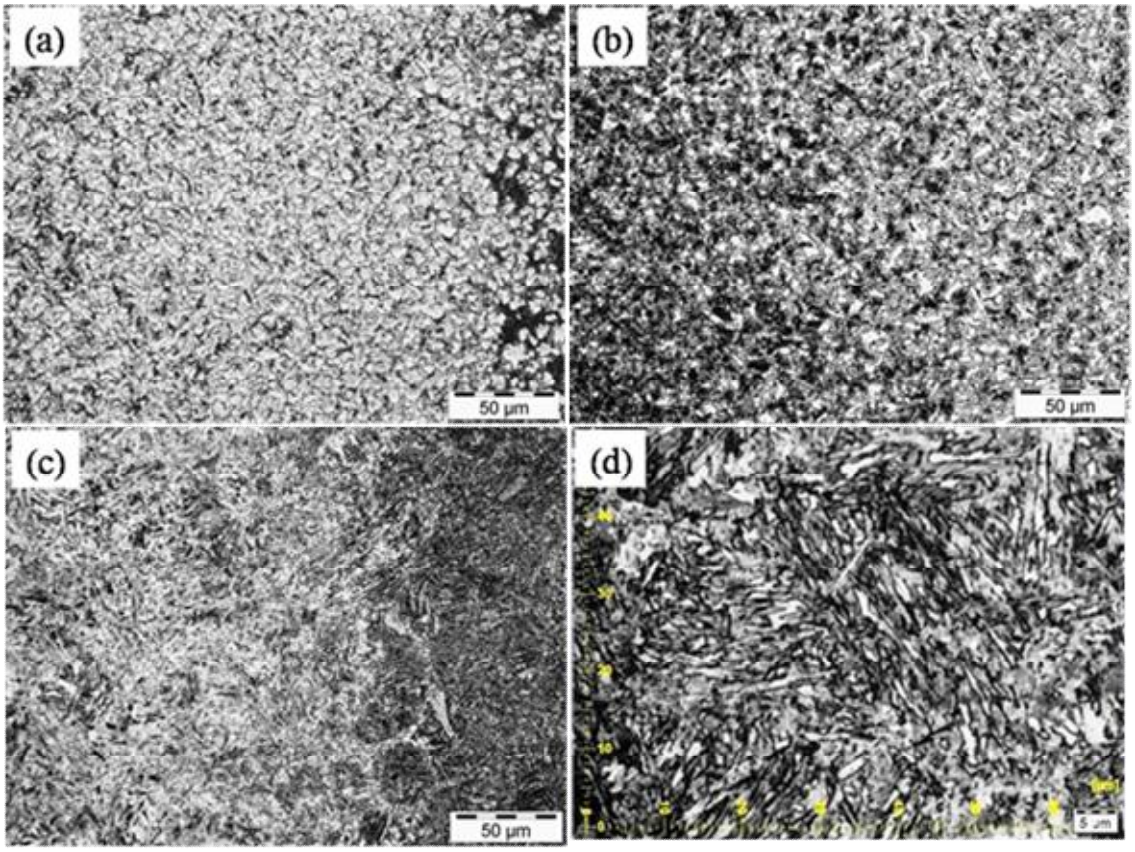

Fig.4.58 The microstructures of ICHAZ in AISI 4130 steel side (a) continuous current TIG weld (b) pulsed current TIG weld (c) laser beam weld (d) laser beam weld at high magnification.

4.8.4 Microhardness

A comparative microhardness survey across the weldment of dissimilar metal TIG and laser beam welds is shown in Fig.4.59. The hardness in the fusion zone is observed to have an increasing trend from maraging steel to high strength low alloy steel side. It is observed that the hardness of the weld is low compared to that of parent metals. The low hardness of the fusion zone can be attributed to the presence of low carbon soft BCC martensite and the material being in the as-cast condition which is similar to the solutionized condition of maraging steel. Increase in hardness within the fusion zone towards high strength low alloy steel side could be due to dilution fusion zone with low alloy steel. The reason low hardness of heat affected zone of maraging steel close to fusion boundary compared to that unaffected parent metal (maraging steel) can be explained as follows : though the parent metal is in flow formed condition, the region adjacent to the fusion zone during weld thermal cycle, is subjected to temperatures higher than the solutionizing temperature of maraging steel resulting in dissolution strengthening precipitates. This makes the hardness of the heat affected zone close to the fusion boundary lower than that of age hardened maraging steel. A dip in the magnitude of the hardness is observed in the far heat affected zones of maraging steel. This is known as the dark band or dark etched region and this is due to the martensitic phase experiencing a temperature of 590^0C to 730^0C resulting in the formation of reverted austenite in the martensitic phase. The presence of this dual phase structure resulted in lowest hardness in the HAZ of maraging steel.

The hardness along the HAZ of AISI 4130 steel side adjacent to the weld interface has shown high hardness. This can be explained as follows: the region of the HAZ near to the fusion zone experiences a high peak temperature exceeding A_{C3} line and also subjected to fast cooling rates similar to quenching and tempering treatment for the steel. The microstructure of this part of HAZ was characterized predominantly as martensite. Regions away from the fusion zone experienced lower peak temperatures which are close to A_{C1} and probably these regions are heated to within the inter-critical zones, exhibited lower hardness due to the presence of high-temperature transformation products in addition to martensite. This soft region is similar to that reported in quench and tempered steels [22,23].

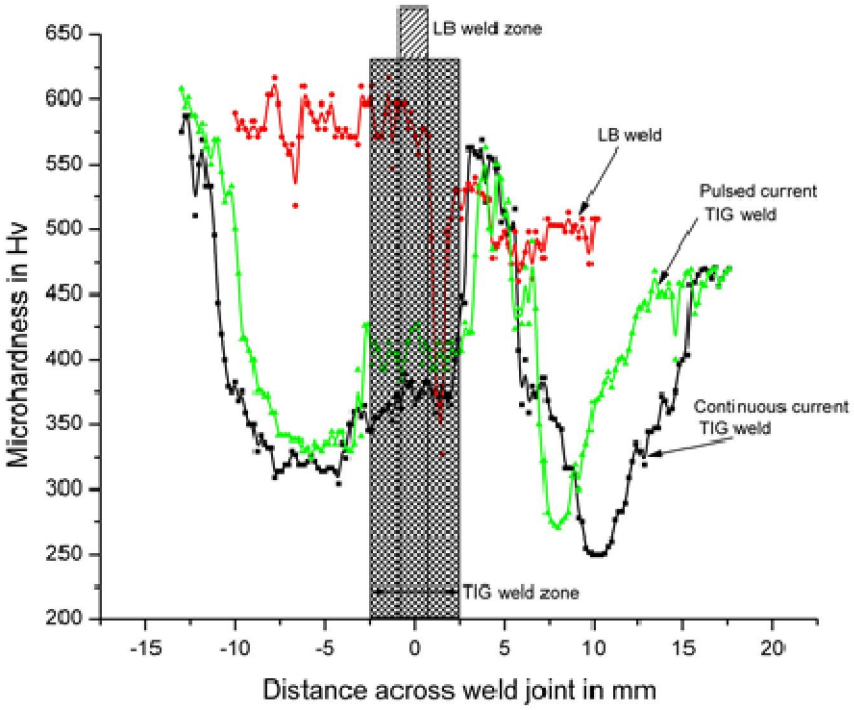

Fig 4.59 A comparative microhardness survey across the dissimilar weld joint produced through TIG and laser beam welding processes.

The softening tendencies in heat affected zone of AISI 4130 steel due to the exposure of welding heat are presented in Table 4.20. The soft zone in HAZ of AISI 4130 steel can be characterized with respect to the width of the soft zone (considering any hardness less than 400Hv corresponds to soft zone) and distance of minimum hardness from the fusion line of weld towards AISI 4130 steel side. The TIG weld joints produced with continuous current have a maximum width of the soft zone and a maximum distance of soft zone from fusion line while the joints made using laser beam welding process has demonstrated minimum width of the soft zone and minimum distance from the fusion line.

Table.4.20. Location and width of the soft zone in HAZ of AISI 4130 steel of different dissimilar weld joints.

Type of welding process/technique	Distance of soft zone from the fusion line in mm	Width of soft zone in mm	Minimum hardness in HAZ, Hv	Maximum hardness in HAZ, Hv
Continuous current TIG weld	7.0	10.0	259	556
Pulsed current TIG weld	5.0	4.5	271	548
Laser beam weld	1.0	0.25	350	545

4.8.5 Tensile properties

The mechanical properties of both the base materials in their respective heat-treated conditions are shown in Table 3.3. The tensile properties of weld joint made with different welding conditions and processes are mentioned in Table 4.21.The macrographs of fractured transverse tensile specimens of all dissimilar welds are shown in Fig.4.60. clearly, reveal the fracture location as the sub critical heat affected zone (ICHAZ) of AISI 4130 steel. The fracture location is correlated to the minimum hardness zone on the microhardness profile of weld joint. The dissimilar laser beam weld joints have shown relatively higher tensile strength and yield strength compared to the other joints, which could be due to the facts that the welding heat input was drastically reduced during the laser beam welding process. Use of laser beam welding has enhanced the weld joint efficiency from 62 to 97.6%.

Table 4.21. Tensile properties of different dissimilar weld joints.

	UTS in MPa	0.2% YS in MPa	El%	Weld joint efficiency based on UTS	Distance from fracture location from fusion zone on AISI 4130 steel side in mm
Continuous current TIG weld	960	826	3.8	62.74	4.16
Pulsed current TIG weld	995	885	3.4	65.03	4.90
Fiber laser beam weld	1494	1215	2.2	97.6	1.0

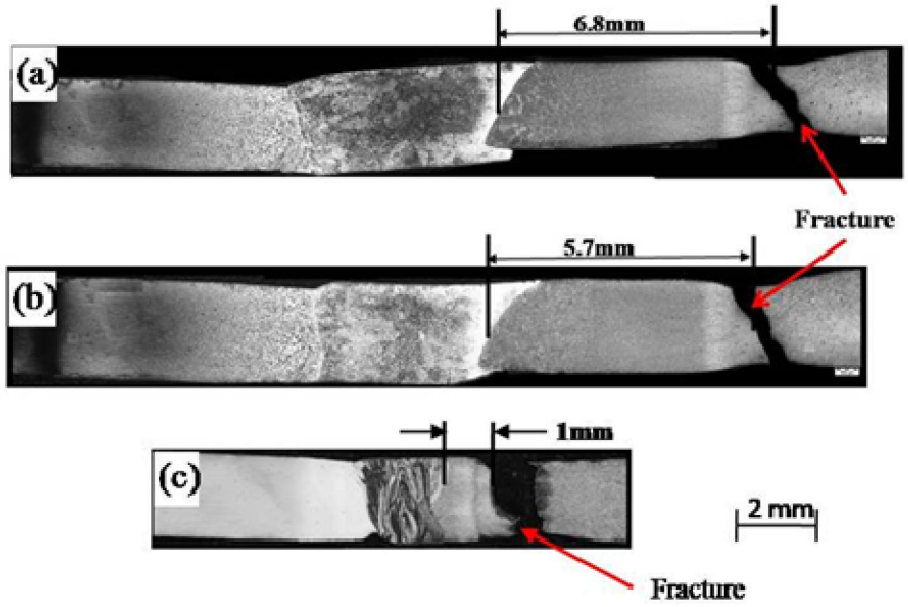

Fig 4.60. Macrographs of fractured tensile test specimens depicting varied widths of heat affected zone on AISI 4130 steel side (a) continuous current TIG weld (b) pulsed current TIG weld (c) fiber laser beam weld (arrow indicates fracture location).

4.8.6 Fractography

Scanning electron micrographs of fracture surfaces of tensile test specimens of dissimilar metal welds produced with different welding conditions are shown in Fig 4.61. It is observed that the fracture surfaces of tensile specimens corresponding to joints made with continuous current TIG have revealed shallow dimpled features while those of laser beam welding has shown deep and finer dimples.

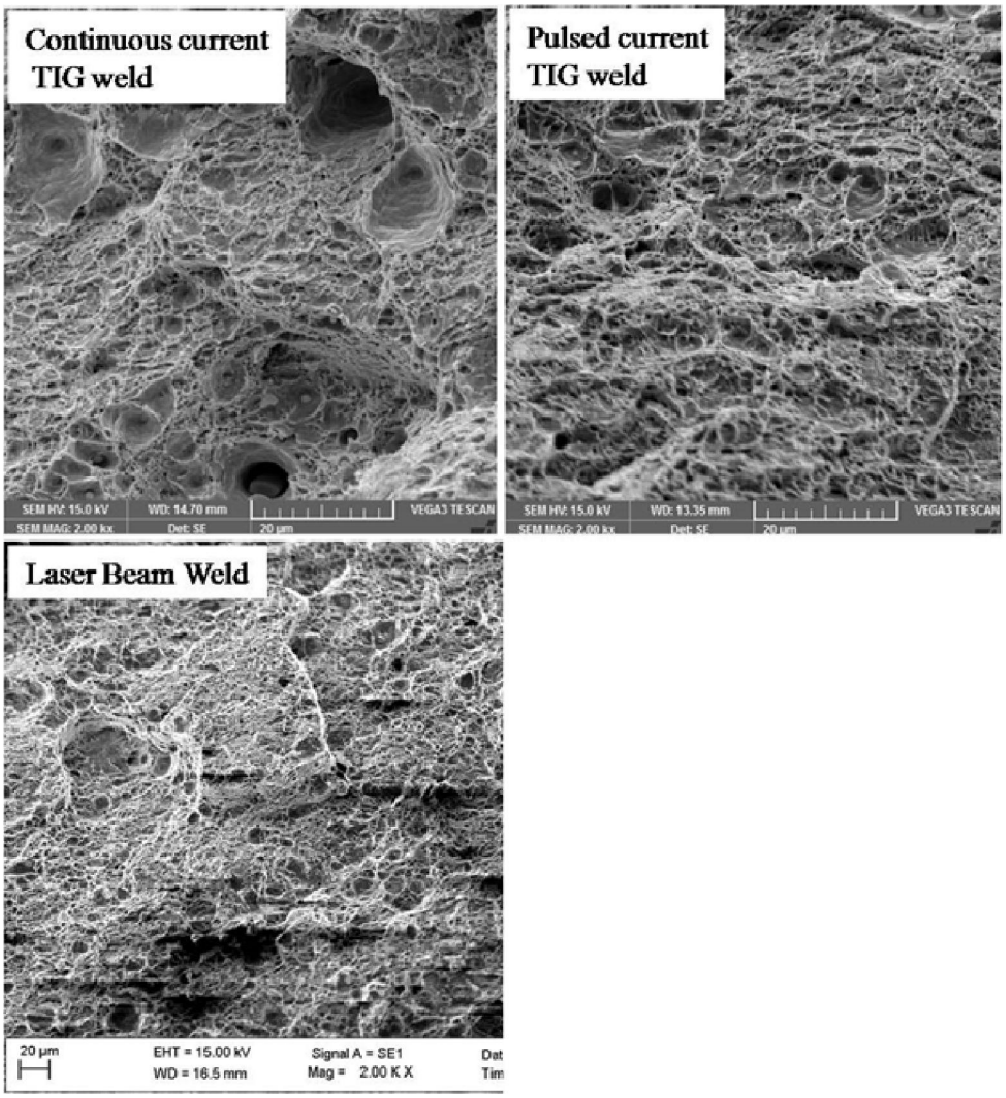

Fig 4.61. Scanning electron micrographs of fracture surfaces of tensile test specimens of dissimilar weld joints.

CHAPTER - V

CONCLUSIONS AND FUTURE SCOPE

Chapter 5 summarizes the investigation on the basis of experimental results and their analysis of Dissimilar welding of ultra-high strength steels: Maraging steel and high strength low alloy steel (AISI 4130) with different welding processes and conditions.

5.1 Continuous TIG welding of Maraging steel to high strength low alloy steel (AISI 4130) without and with external cooling

The effect of gas tungsten arc welding techniques using the external cooling method on microstructure, hardness, HAZ softening and tensile properties of the dissimilar metal weld of maraging steel and AISI 4130 steel weldments have been investigated and the salient features are as follows:

- The external cooling can efficiently lessen the degree softening in HAZ of AISI 4130 steel since it reduces the high-temperature tempering of tempered martensite. The utmost softening has been observed in the case of welds without external cooling.
- The size of the softened HAZ can be reduced by approximately 67% while the lowest hardness location in HAZ was shifted by 54% towards the fusion line of the dissimilar weld joint.
- More amount of ferrite is observed in without external cooling.
- Less hardness (259 HV) is found in CC welds without external cooling
- Ultimate tensile strength of welds made with external cooling is more (1041 Mpa) than that of without cooling (960 MPa).
- Distance of Fracture location (i.e from the fusion line to fracture) is more (6.8 mm) in the case of CC welds without external cooling compared to that of external cooling (4.9 mm).

5.2 Pulsed TIG welding of Maraging steel to high strength low alloy steel (AISI 4130)

The influence of pulse frequency of TIG welding on Microstructure and mechanical properties such as ultimate tensile strength (UTS), yield strength, percent elongation and hardness of dissimilar welds of Maraging steel and AISI 4130 steel have been analyzed in detail and the following conclusions have been obtained.

- Macrostructures show as frequency increases white band width and the width of weld fusion line to white band end line is also increasing.
- From microstructures it is observed that as frequency increases the grain size is also increasing in weld zone and HAZ's of MDN-250 side and AISI 4130 side.
- From all the frequencies of weld joints, it is found that 4Hz frequency has demonstrated highest 0.2% YS (961.566 MPa).
- Hardness graphs show that the there is a decrease in hardness adjacent to the white band where the temperature reaches to 650-750^{0}C and so there forms the coarse tempered martensite so there is a gradual decrease in hardness as compared to the white band.
- The external cooling can efficiently decrease the degree softening in HAZ of AISI 4130 steel since it reduces the high-temperature tempering of tempered martensite. The maximum softening has been observed in the case of weld joint produced without external cooling.
- More amount of ferrite is observed in without external cooling.
- Ultimate tensile strength of welds made with external cooling is more (1041 Mpa) than that of without cooling (1014 MPa).
- Distance of Fracture location (i.e from the fusion line to fracture) is more (6.8 mm) in the case of CC welds without external cooling compared to that of external cooling (5.7 mm).

5.3 Impact of contamination on quality and mechanical properties of dissimilar weld joints of 18% Ni maraging steel and AISI 4130 steel

Influence of contamination such as water, cutting oil and heat extraction paste in the gas tungsten arc welds of 18% Ni maraging steel and AISI 4130 steel is studied, by examining the fusion zone microstructures, microhardness across the weldment and tensile properties. Following conclusions were drawn as:

- Varied levels of gas porosities are observed to be formed in pulsed gas tungsten arc welds of dissimilar materials, maraging steel, and AISI 4130 steel because of usage of heat extraction paste. Heat extraction paste has produced the highest degree of gas porosity with respect to both in numbers and maximum size.
- The width of discoloration zone due to welding heat is relatively more towards AISI 4130 steel side compared to that on maraging steel side due to the higher thermal conductivity of AISI 4130 steel.
- Heat affected zone softening has been observed in maraging steel and AISI 4130 steel. Softening in AISI 4130 can be attributed to heating of the base material in the inter-critical and sub critical regions, resulting in microstructures other than fully martensitic microstructures. Soft zone in HAZ of maraging steel side is due to the presence of reverted austenite in a soft martensitic matrix due to weld thermal cycle.
- The effect of gas porosities on the mechanical properties of dissimilar weld joint was studied. The contamination due to water, heat extraction paste and cutting oil up to a certain level of porosity does not affect the mechanical properties of dissimilar welds.
- The amount reduction of strength of heat affected zone of AISI 4130 steel looks to be more than that of the corresponding reduction that may occur due to the presence of gas porosities in the weld joint.
- These particular dissimilar weld joints can tolerate a higher amount of defect level as compared to the limits specified by the standard procedures.

5.4 Comparison of continuous and pulsed GTAW on Microstructure and Mechanical properties of Dissimilar welds of Maraging steel and AISI 4130 steel

The influence of gas tungsten arc welding techniques using the external cooling method on microstructure, hardness, HAZ softening and tensile properties of the dissimilar metal weld of 18% Ni maraging steel and AISI 4130 steel weldments have been investigated and the salient observations are as follows:

- The external cooling can effectively reduce the degree softening in heat affected zone of AISI 4130 steel since it reduces the high-temperature tampering of tempered martensite. The maximum softening has been observed in the case of weld joint produced with continuous current without external cooling while the joints made using pulsed current with external cooling has demonstrated a lowest degree of softening.
- The size (width) of the softened HAZ can be reduced by approximately 67% while the lowest hardness location in HAZ was shifted by 54% towards the fusion line of the dissimilar weld joint.
- Use of pulsed current with the external cooling method has enhanced the weld joint efficiency from 68 to 87%.

5.5 Laser welding of Maraging steel to high strength low alloy steel (AISI 4130)

Effect of welding process on microstructural and mechanical properties of dissimilar welds joints of maraging steel and high strength low alloy steel has been evaluated and following are the conclusions:

- Laser beam weld joints have shown higher weld joint efficiencies as compared to both continuous current and pulsed current TIG weld joints.
- The rapid heating and cooling experienced by the heat affected zone of AISI 4130 steel during laser beam welding process can drastically lessen the amount of softening in HAZ of AISI 4130 steel because it reduces the high-temperature tempering of tempered martensite. The maximum softened HAZ is observed in CCTIG welds without external cooling.
- Use of laser beam welding process has enhanced the weld joint efficiency from 62 to 97% on ultimate tensile strength.

5.6 Comparison of different welding processes and techniques on dissimilar welds of Maraging steel and AISI 4130 steel (CC welds, PC welds, and Laser welds)

Effect of welding process on the microstructural and mechanical behavior of dissimilar metal weld joints of maraging steel and high strength low alloy steel has been investigated and the salient observations are as follows:

- Laser beam weld joints have shown higher weld joint efficiencies as compared to both continuous current and pulsed current TIG weld joints.
- The rapid heating and cooling experienced by the HAZ of AISI 4130 steel during laser beam welding process can drastically reduce the degree softening in heat affected zone of AISI 4130 steel since it reduces the high-temperature tampering of tempered martensite. The highest softened HAZ has been observed in the case of weld joint produced with continuous current TIG welds without external cooling.
- Use of laser beam welding process has enhanced the weld joint efficiency from 62 to 97% on ultimate tensile strength.

5.7 Future scope of work

Although the present study has helped in improving the joint efficiency of dissimilar ultra high strength steels by using different welding processes and techniques; a few areas emerged during the course of the present study, which needs further investigations as suggested below:-

1. Effect of aging on dissimilar welds of ultra-high strength steels.
2. Corrosion behavior of dissimilar welds of ultra high strength steels.
3. Fatigue behavior of dissimilar welds of ultra high strength steels.

BIBLIOGRAPHY

1. Lang F H, Kenyon N, Welding of Maraging steels, *WRC Bulletin*, (**1959),**1-41.
2. Olson D L, Siewert T A, Liu S, *ASM Handbook Volume 1: Properties and Selection: Irons, Steels, and High-Performance Alloys,* , ASM International (**1990)**.
3. Hamada M, Control of strength and toughness at the heat affected zone, *Weld Intl* 17(4),(2003) 265.
4. Kon Lee, Yi Cheng Chien, A Study of Microstructure and Mechanical Properties of Thick Welded Joints of a Cr – Mo Steel, Metal Science and Heat Treatment 57 (2015) 175.
5. Honggang D, XiaohuHao, Dewei D, Effect of Welding Heat Input on Microstructure and Mechanical Properties of HSLA Steel Joint, Metallography, Microstructure, and Analysis. (2014) 138.
6. Hochhauser F, Ernst W, Rauch R, Vallant R, Enzinger N, Influence of the Soft Zone on The Strength of Welded Modern HSLA Steels, *Weld in the World* 56 (2012)77.
7. Sun Z, Karppi R. The application of electron beam welding for the joining of dissimilar metals: an overview. J Mater Process Technol 1996;59:257–67.
8. Venkata Ramana P, Madhusudhan Reddy G, Mohandas T, Gupta AVKS. Microstructure and residual stress distribution of similar and dissimilar electron beam welds – maraging steel to medium alloy medium carbon steel. Mater Des 2010;31:749–60.
9. Meshram SD, Madhusudhan Reddy G, Pandey S. Friction stir welding of maraging steel (Grade-250). Mater Des 2013;49:58–64.
10. Fawad Tariq, Rasheed Ahmed Baloch, Bilal Ahmed Nausheen Naz. Investigation into microstructures of maraging steel 250 weldments and effect of post-weld heat treatments. J Mater Eng Perform 2010;19:264–73.
11. Nagarajan K.V. Welding aspects of maraging steels. In: Proceedings of the conference on steels for engineering industries-trends in weldability, Indian Institute of Metals, Tiruchirapalli, India; 1998. p. 43–53.

12. Radhakrishnan VM. Welding technology and design. New Age Intl (P) Ltd.; 2005
13. Mohandas T, Madhusudhan Reddy G, A comparison of continuous and pulse current gas tungsten arc welds of an ultra high strength steel, Journal of Materials Processing Technology, 68 (1997) 222.
14. Mohandas T, Madhusudhan Reddy G, Venkata Ramana VSN. Welding of dissimilar ultra-high strength steels", National Welding Seminar; January 2001.
15. Mohandas T, Madhusudhan Reddy G, " Characterization of dissimilar GTA welds of high stremgth steels", International welding conference on advances in welding and cutting, 15–17 February 2001, New Delhi, p. 219–32.
16. Madhusudhan Reddy G, Venkata Ramana P. Role of nickel as an interlayer in dissimilar metal friction welding of maraging steel to low alloy steel. J Mater Process Technol 2012;212:66–77.
17. Muthupandi V, Bala Srinivasan P, Seshadri SK, Sundaresan S. Effect of weld metal chemistry and heat input on the structure and properties of duplex stainless steel welds. Mater Sci Eng A 2003;358:9–16.
18. Rohrbach Kurt, and Michal Schmidt, "Maraging steels", Carpenter Technology Corporation ASM.
19. R.F. Decker, J.T.Eash and A.J. Goldman, "Source book on maraging steels", Transactions of ASM , Vol.55(1962),pp.1-19.
20. Thoni. V.Philip, TVP Inc; and Thomos J. Mc Caffrey, "Ultrahigh strength steels", Carpenter steel division Technology Corporation.- Metal Hand Book, ASM ed.
21. N.Kenyon, Effect of austenite on the toughness of maraging steel welds Weld.Journal, 53(3) (1969), pp.105s-109s.
22. Aborn, R.H," Low Carbon Martensite", Transactions of ASM, p51-85,1956.
23. Boniszewski, T., Brown,E.D., and Baker, R.G., " Metallography and Hardness of the Heat affected zones on Ausformining and Maraging Steels". Iron and steel Inst. spec.Rpt, vol.76(1962),pp.100-105.
24. T. Bonsizewski and D.M Kenyon; Examination of electron beam welds in 18%Ni/Co/Mo maraging steel sheet, British .Welding Journal, vol.50(1966), 415-435.

25. D.A.Canonico; Gas Metal arc welding of 18% Ni Maraging steel, Welding Research Supplement, vol.48(1964), pp.433s-442s.
26. C.M.Adams, jr, and R.E.Travis, Welding of 18% Ni-Co-Mo maraging alloys weld.J.,vol48(5)(1964), pp.193s-198s.
27. P.H.Salmon cox, A.J.Birkle , B.G.Reisdorf, and G.E.Pellissier; The Origin and Significance of Banding in 18Ni (250) Maraging Steel , ASM Trans.Q;60(1967), pp. 125-143.
28. Boniszewski, T., "Hydrogern induced delayed cracking in maraging steels",. Br.weldingJ.,vol.49(1965),pp.557-566.
29. Wakkinson,F., Baker, R.G., and Tremlett,HF., " Hydrogen Embrittlement in relation to the Heat Affected Zone". weld.J,Vol.47(1963),pp.54-62,.
30. Farell,.K., and Quarrell, A.G., " Hydrogen Embrittlement of ultra high strength steel". Jnl.Iron steel Inst, vol.202(1964), pp.1002-1011.
31. J.J.Pepe and W.F.Savage, The Weld Heat-Affected Zone of the 18Ni Maraging Steels Welding journal, vol.51(1967), pp.411s-422s.
32. Knoth and Lang, Source book on maraging steels, American society of metals (source metals engineering quarterly may 1966).
33. C.Lundin, J Henning, and M. Richey, 1983, ' Transformation metallurgical response and behavior of the weld fusion zone and HAZ in Cr-Mo-steel for fossil energy applications ' Progress report' 1983.
34. K. Sree Kumar, A. Natarajan, P. P. Sinha, K. V. Nagarajan, " Microstructural aspects of weld repair in 18 nickel 1800 MPA maraging steel", Journal of Materials ScienceJanuary 1992, Volume 27, Issue 14, pp 3817–3820
35. P. P. Sinha, K. T. Tharian, K. Sreekumar, K. V. Nagarajan , D. S. Sarma, "Effect of aging on microstructure and mechanical properties of cobalt free 18%Ni (250 grade) maraging steel", Materials Science and Technology , Volume 14, 1998 - Issue 1.
36. T.Mohandas and G.Madhusudhan Reddy, Characterization of dissimilar GTA welds of high stremgth steels , International welding conference on advance in welding and cutting 15-17 feb.2001 New Delhi pp.219-232.
37. YMD Randall, R.E.Monroe, and P.J.Rieppel, weld.J, vol.46 (1962), pp.193-206.

38. G. Madhusudhan reddy,and T.Mohandas , international journal for joining of materials, vol 8(3), pp. 231-228.
39. G. Madhusudhan reddy, T. Mohandas and GRN Tagore, Journal of material processing technology, 49 (1995),pp.231-228.
40. T. Mohandas et al. Welding of ultra high strength steels (unpublished work)
41. T. Mohandas and G.Madhusudhan Reddy, Heat-affected zone softening in high-strength low-alloy steels, journal of material processing Technology, Volume 74, Issues 1–3, February 1998, Pages 27-35
42. T.Mohadas and G.Madusudhan Reddy,Effect of welding process on the ballistic performance of high-strength low-alloy steel weldments, journal of material processing Technology, vol.69(1998),pp.222-226.
43. R.E.Travis, V.P.Ardito and C.M Adams jr, Welding journak, vol.47(1963),pp.9s-17s.
44. Kenneth Easterling; 1983, 'Introduction to the physical metallurgy of welding'. 2nd ed. Butterworth-Heinemann, p.126.
45. H. G. Pisarski and R. E. Dolby, 'The Significance of Softened HAZs in High Strength Structural Steels' Welding in the World, May 2003, Volume 47, Issue 5–6, pp 32–40
46. Wei Meng, Zhuguo Li, Jian Huang, Yixiong Wu, and Seiji Katayama,'Microstructure and Softening of Laser-Welded 960 MPa Grade High Strength Steel Joints', Journal of Materials Engineering and Performance, Feb 2014, DOI: 10.1007/s11665-013-0795-5.
47. Reisuke Ito, Chiaki Shiga, Yoshiaki Kawaguchi, Shiro Torizuka. 'Controlling of the Softened Region in Weld Heat Affected Zone of Ultra Fine Grained Steels', January 2000,
48. Franz Hochhauser, Wolfgang Ernst, Rudolf Rauch, Norbert Enzinger, Influence of the Soft Zone on The Strength of Welded Modern HSLA Steels,May 2013, Welding in the World, Vol. 56.
49. L. Zhang, A. Pittner, T. Michael, M. Rhode & T. Kannengiesser, Effect of cooling rate on microstructure and properties of microalloyed HSLA steel weld metals, May 2015, Science and Technology of Welding and Joining , Volume 20, 2015 - Issue 5, 371-377.
50. J.F. Lancaster 1980; ' Metallurgy of Welding'. 4th ed, Chapman & Hall p.167.
51. J. M. B. Bosz, and K.D.Challanger; 1990, 'HAZ Microstructures in HSLA steel weldments'. advanced in welding metallurgy, p.207.

52. C.D.Lundin 1986, ' structure and properties of weldments', advances in welding metallurgy 1990, p.51
53. C.Lundin, Richey, M., and J. Henning, 1984, ' Transformation, Metallurgical response and behavior of the weld fusion zone and Heat- affected zone in Cr-Mo-steels for fossil energy applications', Final technical report 1984.
54. J.G.Youn, H.J.Kim, 1987, ' characteristics of TMCP steel and its softening', Proc.Int.Sym. on welding metallurgy of structural steels, Denever, colorado, metallurgical soc. Inc, p.157.
55. N. Yurioka 199., weldability of modern high strength steels', Advances in welding metallurgy 1990, p.51. 25. F.ADE, 1991, ' Armour steel weldments'. welding journal sept 1991.
56. W.F.Hess, L.L.Merril, E.F.Nippes and A.P.Bunk 1943,' Measurement of cooling associated with Arc welding & Their application to selection of optimum welding condition ' welding journal 1943, 22(a).s
57. G.E.Doan, R.D.Stout, S.S.Tor and J.H.Fgye, ' A tentative system for preserving ductility in weldments '. Ibid, 22(17).
58. C.E.Jackson; 1987, ' Metallurgy and weldability', weldability of steels, 3rd ed. welding research council, new York, p.79.
59. C.D.Lundin, T.P.S.Gill, C.Y.Qiao, 1989, ' Heat-affected zones in low carbon microalloyed steels', recent trends in welding science and technology-1989, ASM international, p.249.
60. George E. Linneert, 1965, ' Welding Metallurgy' vol.2, American welding society.
61. P Venkata Ramana , G.M. Reddy, and T Mohandas , Microstructure, hardness and residual stress distribution in maraging steel gas tungsten arc weldments, Science and Technology of welding and joining, 2008, vol.13, No.4, 388-394
62. D.Siva Kumar, P.P.sinha, N.Prabhu, and G.V.prabhugaunkar, Influence of post -weld solution treatment on mechanical properties and microstructure of fusion zone of cobalt free maraging steel weldments, Science and Technolgy of welding and joining, 2005, vol.10, No.2, 169-175.

63. Jian An, Fanyan Meng,Xiaoxia LV,Haiyuan Liu,Xiaoxi Gao,Yuanbo Wang,You Lu, Improvement of Mechnaical Properties of stainless maraging steel laser weldments by post weld ageing treatment , Materials and Design 40(2012) 276-284
64. C.R. Shamantha, R. Narayanan, K.J.L. Iyer, V.M. Radhakrishnan, Microstructure Changes During Welding and Subsequent Heat Treatment of 18ni (250-Grade) Maraging Steel, Materilas Science and Engineering A287 (2000)43-51.
65. I.K. Lee, C.L.Chowdary, Y.T.Lee, Y.T Cheen, Effect of thermal refining on mechanical properties of annealed SAE4130 by multilayer GTAW, Journal of Iron and Steel , Research International, 2012,19(7),71-78.
66. F.Souza Nel, D.Neves, O.M.Silva, M.S.F.Lima, A.J.Aballa, An analysis of the mechanical behavior of AISI 4130 steel after TIG and laser welding process, Procedia Engineering,114 (2015) 181-188
67. Mohammad W et. al, Effect of post-weld heat treatment and electrolytic plasma processing on tungsten inert gas welded AISI 4140 alloy steel, Materials and Design 54 (2014) 6-13.
68. P Venkata Ramana , G.M. Reddy, and T Mohandas and AVSS KS Gupta, Microstructure and residual stress distribution of similar and dissimilar Electron Beam Welds-maraging steel to medium alloy medium carbon steel, Materials and Design 31(2010) 749-769.
69. G.Madhusudhan Reddy And P.Venkata Ramana, Influence of Filler Material Compositio Non Residual Stress Distribution of Dissimilar Gas Tungsten Arc Weldments of Ultrahigh Strength Steels, Journal of Materials Processing Technology 212(2012)66 -77.
70. G.Madhusudhan Reddy, P.Venkat Ramana., Influence of Filler Material Compositio Non Residual Stress Distribution of Dissimilar Gas Tungsten Arc Weldments of Ultrahigh Strentgth Steels, Sueuce And Technology Of Welding And Joining 2011 Vol-16 No.3 273
71. A. Kumar, et.al, Optimiztion Of Pulsed Tig Welding Process Parameters on Mechanical Properties of A4 5456 Aluminum Alloy Weldments (2009),
72. Mingxuan Yang et.al. Effect of Pulse Frequency on Microstructure And Properties of Ti-6Al4V By Ultrahigh –Frequency Pulse Gas Tungsten Arc Welding.(2013).

73. S. Krishnan et.al, Pulsed Current Gas Metal Arc Welding Of P91 Steels Using Metal Cored Wires. (2016)
74. G. Lothongkum et.al. Study on The Effects of Pulsed Tig Welding Parameters on Delta – Ferrite Content, Shape Factor & Bead Quality In Orbital Welding of Aisi3611 Stainless Steel Plate. (2001).
75. K.Devendranath Ram Kumar et.al Development of Pulsed Current Gas Tungsten Arc Welding Technique For Dissimlar Joints of Marine Grade Alloys.(2016),
76. N.Arivazhagan ,V.Rajkumar, Role of Pulsed Current on Metallurgical and Mechanical Properties of Dissimilar Metal Gas Tungsten Arc Welding of Maraging Steel to Low Allloy Steel. Materials and Design 63(2014)69-82.
77. Huang CC, Pan YC, Chuang TH. Effects of post weld heat treatments on the residual stress and mechanical properties of electron beam welded SAE 4130 steel plates. J Mater Eng Perform 1997;6:61–8.
78. Chang Y, Wang C. Effect of post weld heat treatments on the fatigue crack growth rate of electron beam welded AISI 4130 steel. Metall Mater Trans A 1996;27A:3162–9.
79. Souza Neto F, Neves D, Silva OMM, Lima MSF, Abdalla AJ. An analysis of the mechanical behaviour of AISI 4130 steel after TIG and Laser welding process. Procedia Eng 2015;114:181–8.
80. Quintino L, Costa A, Miranda R, Yapp D, Kumar V, Knong CJ. Welding with high power fiber lasers – a preliminary study. Mater Des 2007;28(4):1231–7.
81. Madhusudhan Reddy G, Mohandas T, Ballistics performance of high strength low alloy steels ,J Mater Process Technol 57 (1996) 23.
82. Mohandas T, Madhusudhan Reddy G, and Satish Kumar B, Heat affetced zone softening in high strength low alloy steels, J Mater Process Technol 88 (1999) 284.

CURRICULUM VITAE

JAITEERTH R JOSHI
H. No. 3-10-93/1,
Gokhale Nagar, Ramanthapur,
Hyderabad – 13

Ph. No. +91 9440049272
Email : joshidrdl@gmail.com

Academic Qualification

Ph.D (Thesis submitted) (Mechanical Engg. Dept.), National Institute of Technology, Warangal – 2017.

Thesis : "**Influence of welding processes and techniques on welding of dissimilar ultra high strength steels**"

Masters of Management Science from Pune University - 1996

Bachelor of Engineering, Mechanical from Osmania University - 1991

Intermediate – Board of Intermediate Education - 1987

SSC Board of Secondary Education - 1985

Research Interest

- Missile Engineering
- Welding Technology
- Non Destructive Testing
- Technology Management
- R&D Management

International / National Publications

- **Jaiteerth R.Joshi** P.Mastanaiah, A.Kumar , G.Madhusudhan Reddy and K.Ramesh Kumar "Influence of welding techniques on heat affected zone softening of dissimilar metal maraging steel and high strength low alloy steel gas tungsten arc weldments" Trans Indian Inst Met (2016), doi:10.1007/s12666-016-0861-4**.(*Springer Publications*)**

- **Jaiteerth R.Joshi** P.Mastanaiah, A.Kumar , G.Madhusudhan Reddy and K.Ramesh Kumar "A comparative evaluation of microstructural and mechanical behavior of fiber laser beam and tungsten inert gas weld joints of dissimilar ultra high strength steels" Defence Technology(2016), doi: 10.1016/j.dt.2016.08.003 **(Elsevier publications)**

- **Jaiteerth R.Joshi** P.Mastanaiah, A.Kumar and K.Ramesh Kumar " Impact of Contamination on Quality and Mechanical Properties of dissimilar Gas Tungsten Arc Welds of 18% Ni Maraging Steel and AISI 4130 Steel" – **Proceedings of International Conference on Advances in Production and Industrial Engineering** INCAPIE-2015, NIT Trichy.

- Proceedings on **"Non Destructive Evaluation (NDE) for SME" – NDE-2006**.

- Proceedings on **"Role of Quality Assurance (NDT) in Aerospace Industry"-** NDE-2005.

- NDE Proceedings on **"Characterization of defects in Aerospace components using Infrared Pulse thermography".**

- Paper on Evaluation of "**Internal details in Rocket Motors using Computed Tomography"** Proceedings of NDE - 2009, Tiruchi, 10-12 December, 2009.

- Paper on Evaluation of "**Pyrogen Igniter Using Computed Tomography"** Proceedings of NDE 2010, Kolkata, 9-11 Dec. 2010.

Awards and Honors

- **Technology group award -2008** from DRDO for the development of dual propulsion system for long range surface to air missile.
- **Distinguished NDT'ian of the decade – 2012** by Indian Society for Non-Destructive Testing for the contribution in development of novel MPI techniques and ISNT training & certification activities.
- **Laboratory Scientist of the Year - 2013** by DRDL, Hyderabad for the development of Rocket Motor assemblies for critical missile projects.
- **National Technology Day Award – 2016** by Chairman, DRDO for Development of Innovative Technologies to Improve Production, Quality & Cost effectiveness of LRSAM Missile System.

Membership of Academic bodies

- Fellow, Institution of Engineers India (IEI)
- Fellow, Indian Institution of Production Engineers (IIPE)
- Fellow, Indian Society for Nondestructive Testing (ISNT)
- Fellow, Indian Society of Mechanical Engineers (ISME)
- Life Member of Society for Aerospace Quality and Reliability (SAQR)
- Life Member Indian Welding Society (IWS)
- Life Member of Indian Institute of Welding (IIW)
- Life Member, Indian Institute of Metals (IIM)
- Life Member, Administrative Staff College of India (ASCI) Association, Hyderabad
- Member, National Certification Board of ISNT
- Member, National Governing Council of ISNT
- Vice Chairman, ISNT, Hyderabad Chapter from 2014 onwards.

Employment Summary

Joined DRDO in the year 1997 as Scientist 'C' and presently working as **Scientist 'G' & Project Director, Indigenous Aircraft Carrier**.

Assistant Manager, Bharat Dynamic Limited, Hyderabad - 1994 – 1997

Sr. Engineer at Alfa Laval at Pune - 1993 -1994

Engineer at Aluminium Industries Limited, Hyderabad - 1992- 1993

Personal Information

Father's Name	:	Shri Raghavendra Joshi
Mother's Name	:	Late Smt. Shanta Joshi
Sex	:	Male
Date of Birth	:	30-12-1970
Languages Known	:	English, Hindi, Telugu & Kannada

References

Arjun Vedadri
Director, DP&TT
Defence R&D Laboratory
Hyderabad - 500058

Dr. Ramesh Kumar
Director, Technical, Brahmos
Defence R&D Laboratory
Hyderabad - 500058

LIST OF PUBLICATIONS

1. **Jaiteerth R. Joshi,** P.Mastanaiah, A.Kumar , G.Madhusudhan Reddy and K.Ramesh Kumar "Influence of welding techniques on heat affected zone softening of dissimilar metal maraging steel and high strength low alloy steel gas tungsten arc weldments"Trans Indian Inst Met (2016), doi:10.1007/s12666-016-0861-4**.(*Springer Publications*)**
2. **Jaiteerth. R.Joshi,** P.Mastanaiah, A.Kumar, G.Madhusudhan Reddy and K.Ramesh Kumar"A comparative evaluation of microstructural and mechanical behavior of fiber laser beam and tungsten inert gas weld joints of dissimilar ultra high strength steels"Defence Technology(2016),doi: 10.1016/j.dt.2016.08.003**(Elsevier publications)**
3. **Jaiteerth. R. Joshi,** P.Mastanaiah,A.Kumar and K.Ramesh Kumar " Impact of Contamination on Quality and Mechanical Properties of dissimilar Gas Tungsten Arc Welds of 18% Ni Maraging Steel and AISI 4130 Steel" – **Proceedings ofInternational Conference on Advances in Production and Industrial Engineering** INCAPIE-2015, NIT Trichy.
4. **Jaiteerth. R. Joshi,** P.Mastanaiah, A.Kumar, G.Madhusudhan Reddy and K.Ramesh Kumar "Influence of Pulse frequency on microstructure and mechanical properties of dissimilar Maraging steel and AISI 4130 steel TIG welds" **(Manuscript communicated to Materials and Manufacturing Processes).**